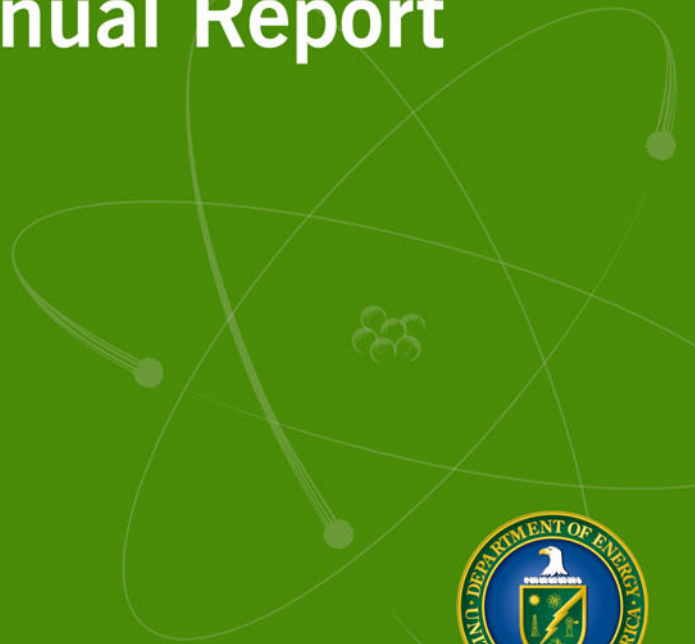


International Nuclear Energy Research Initiative



Annual Report



2010



Disclaimer

This document was prepared as an account of work sponsored by an agency of the United States Government. Neither the United States Government nor any of its employees makes any warranty, expressed or implied, or assumes any legal liability or responsibility for the accuracy, completeness, or usefulness of any information, apparatus, product, or process disclosed, or represents that its use would not infringe upon privately owned rights. Reference herein to any specific commercial product, process, or service by trade name, trademark, manufacturer, or otherwise, does not necessarily constitute or imply its endorsement, recommendations, or favoring by the United States Government. The views and opinions expressed by the authors herein do not necessarily state or reflect those of the United States Government, and shall not be used for advertising or product endorsement purposes.

Available to DOE, DOE contractors, and the public from the

U.S. Department of Energy
Office of Nuclear Energy
1000 Independence Avenue, S.W.
Washington, D.C. 20585

Foreword

The U.S. Department of Energy, Office of Nuclear Energy (DOE-NE), established the International Nuclear Energy Research Initiative (I-NERI) in fiscal year (FY) 2001 to conduct advanced nuclear energy systems research in collaboration with international partners. This annual report provides an update on research and development (R&D) accomplishments which the I-NERI program achieved during FY 2010.

I-NERI supports bilateral scientific and engineering collaboration in advanced reactor systems and the nuclear fuel cycle and is linked to two of DOE-NE's primary research programs: Reactor Concepts Research, Development and Demonstration and the Fuel Cycle Research and Development program. I-NERI is designed to foster international partnerships to address key issues affecting the future global use of nuclear energy. Through I-NERI collaborations, DOE can effectively leverage its economic resources, more readily expand the knowledge base of nuclear science and engineering, and establish valuable intellectual relationships with researchers from other countries. Forging these partnerships enhances the United States' participation in the global nuclear community and helps build an international consensus on critically important issues such as increasing the safety and expanding the benefits of nuclear power and helping design proliferation resistance into advanced nuclear systems.

Through I-NERI, the United States has signed collaborative nuclear research agreements with Brazil, Canada, the European Union, France, Japan, the Republic of Korea, and the Republic of South Africa. In FY 2010, DOE initiated ten new collaborative projects: six with Euratom and four with the Republic of Korea. FY 2010 also marked the completion of seven projects, six with the Republic of Korea and one with France. The *I-NERI 2010 Annual Report* provides descriptions of the new projects, final activities and findings of the completed projects, and comprehensive progress summaries of ongoing projects initiated since FY 2007.



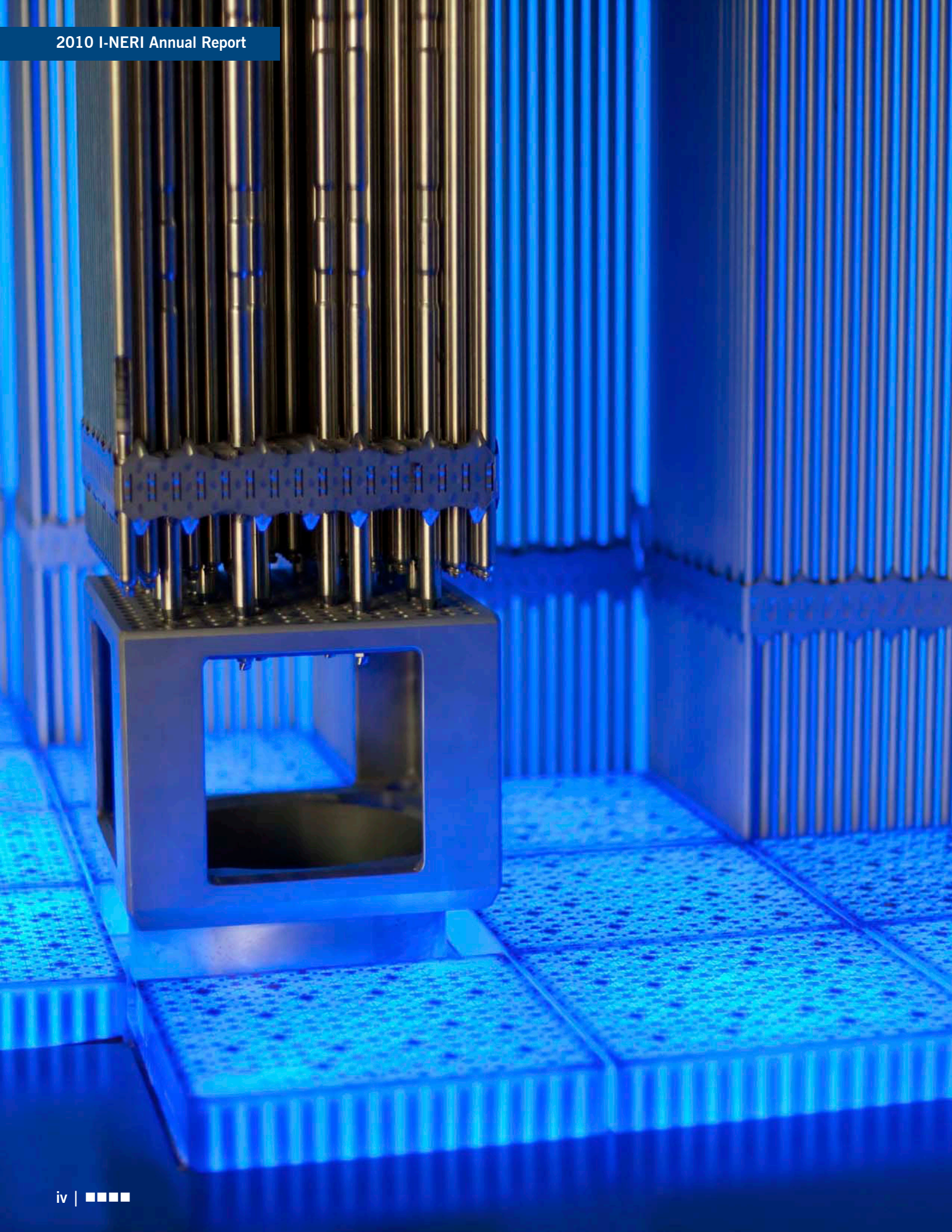
Dr. Peter B. Lyons

Assistant Secretary, Office of Nuclear Energy
U.S. Department of Energy



Contents

1. Introduction	1
1.1 Overview	2
1.2 Objectives.....	2
1.3 <i>I-NERI 2010 Annual Report</i>	2
2. Program Background	5
2.1 Foundation.....	6
2.2 International Agreements	6
2.3 Funding	7
2.4 Program Participants.....	10
3. Research Work Scope and Accomplishments.....	13
3.1 Reactor Concepts Research, Demonstration and Development	14
3.2 Fuel Cycle Research and Development	15
3.3 FY 2010 Research Accomplishments.....	16
3.4 FY 2010 Programmatic Accomplishments	17
4. Project Summaries and Abstracts.....	19
4.1 U.S.–Canada Collaboration	20
4.2 U.S.–European Union Collaboration	24
4.3 U.S.–France Collaboration	32
4.4 U.S.–Republic of Korea Collaboration	42
Appendix I: Index of I-NERI Projects	87
Appendix II: Acronyms and Initialisms	91



1. Introduction

1.1 Overview

The International Nuclear Energy Research Initiative (I-NERI) is a research-oriented collaborative program that supports the advancement of nuclear science and technology in the United States and the world. Innovative research performed under the I-NERI umbrella addresses key issues affecting the future use of nuclear energy and its global deployment. The *2010 Nuclear Energy Research and Development Roadmap* issued by the U.S. Department of Energy, Office of Nuclear Energy (DOE-NE), identifies these issues as high capital costs, safety, high-level nuclear waste management, and non-proliferation. Projects under the I-NERI program investigate ways to address these challenges and support future nuclear energy systems. To attain these objectives, I-NERI promotes bilateral scientific and engineering research and development (R&D) with other nations. U.S. researchers partner with international organizations, allowing for broader perspectives and faster results at reduced costs. A link to the program can be found on the NE website.¹

1.2 Objectives

I-NERI's mission is to sponsor innovative scientific and engineering R&D in cooperation with partnering international countries. The I-NERI program is designed to foster closer collaboration among international researchers, improve communications, and promote sharing of nuclear research information. The program has established the following overall objectives:

- To develop advanced concepts and scientific breakthroughs in nuclear energy and reactor technology in order to address and overcome the principal technical and scientific obstacles to expanding the global use of nuclear energy.
- To promote bilateral and multilateral collaboration with international agencies and research organizations to improve the development of nuclear energy.
- To promote a nuclear science and engineering infrastructure to meet future technical challenges.

Through the I-NERI program, DOE-NE has coordinated wide-ranging scientific discussions among governments, industry, academia, and the worldwide research community regarding the development of advanced reactor concepts and advanced fuel cycles. Figure 1 illustrates key features of the I-NERI program.

I-NERI is integrated into two of DOE-NE's principal research programs: Reactor Concepts Research, Development and Demonstration (RD&D) and Fuel Cycle Research and Development (FCR&D).

1.3 I-NERI 2010 Annual Report

The *I-NERI 2010 Annual Report* serves to inform interested parties about the program's progress on current collaborative nuclear energy research projects. Following is an overview of each section:

- Section 1 provides an overview of the I-NERI program and this annual report.
- Section 2 provides background information, describing the events that led to establishing I-NERI and the countries and organizations that have participated, through both research and funding, in the program.
- Section 3 provides an overview of research objectives and I-NERI's contribution to those objectives, along with a summary of recent accomplishments.
- Section 4 presents the R&D work scope for current I-NERI collaborative projects between the United States and four partners: Canada, the European Union, France, and the Republic of Korea. For these four partnerships, the report presents summary information for projects that were initiated, ongoing, or completed in FY 2010. This section addresses research started in or after FY 2007. Progress summaries of earlier research efforts can be found in previous annual reports, which can be found at the web address noted above.

¹ <http://www.nuclear.gov/INERI/neINERI1.html>

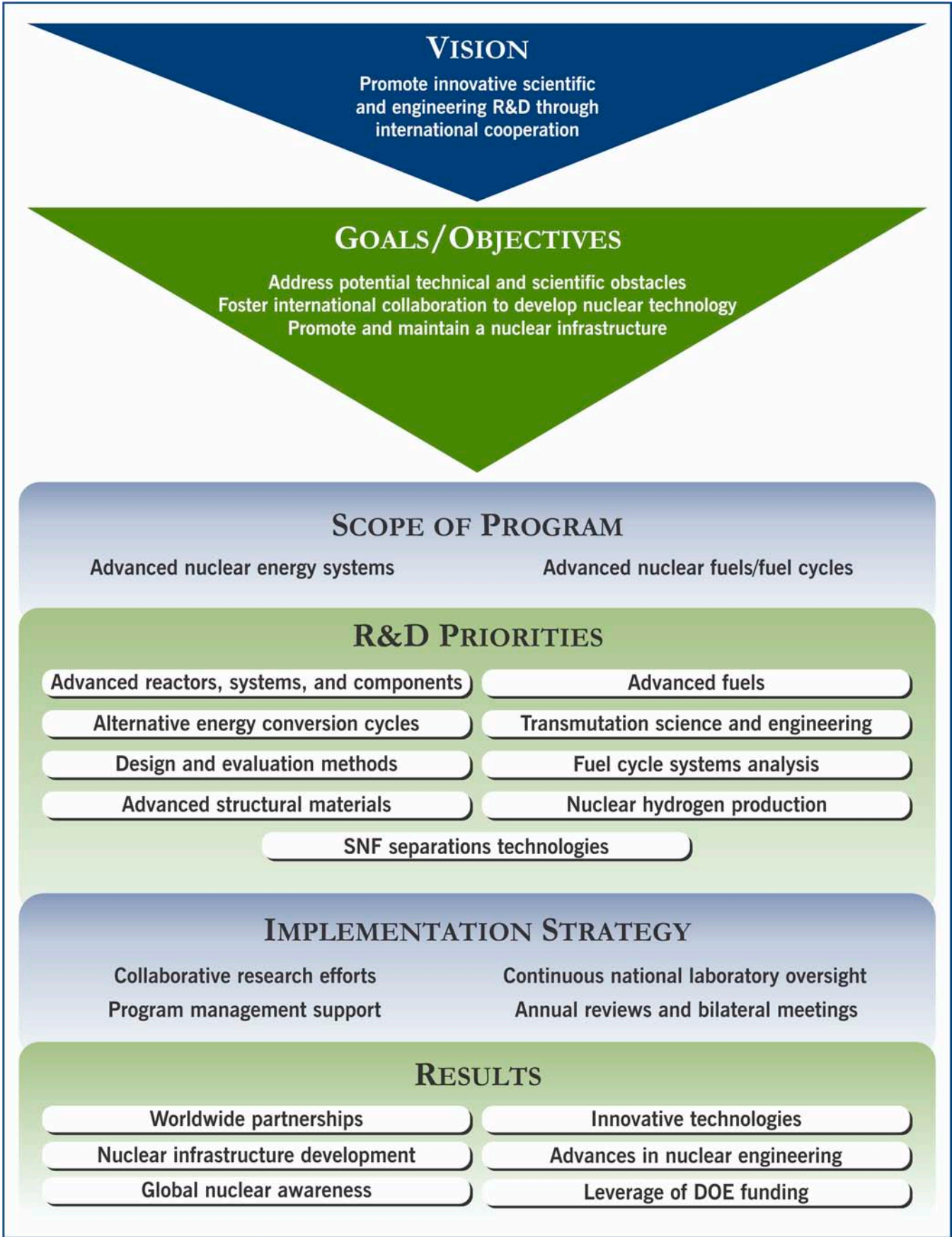
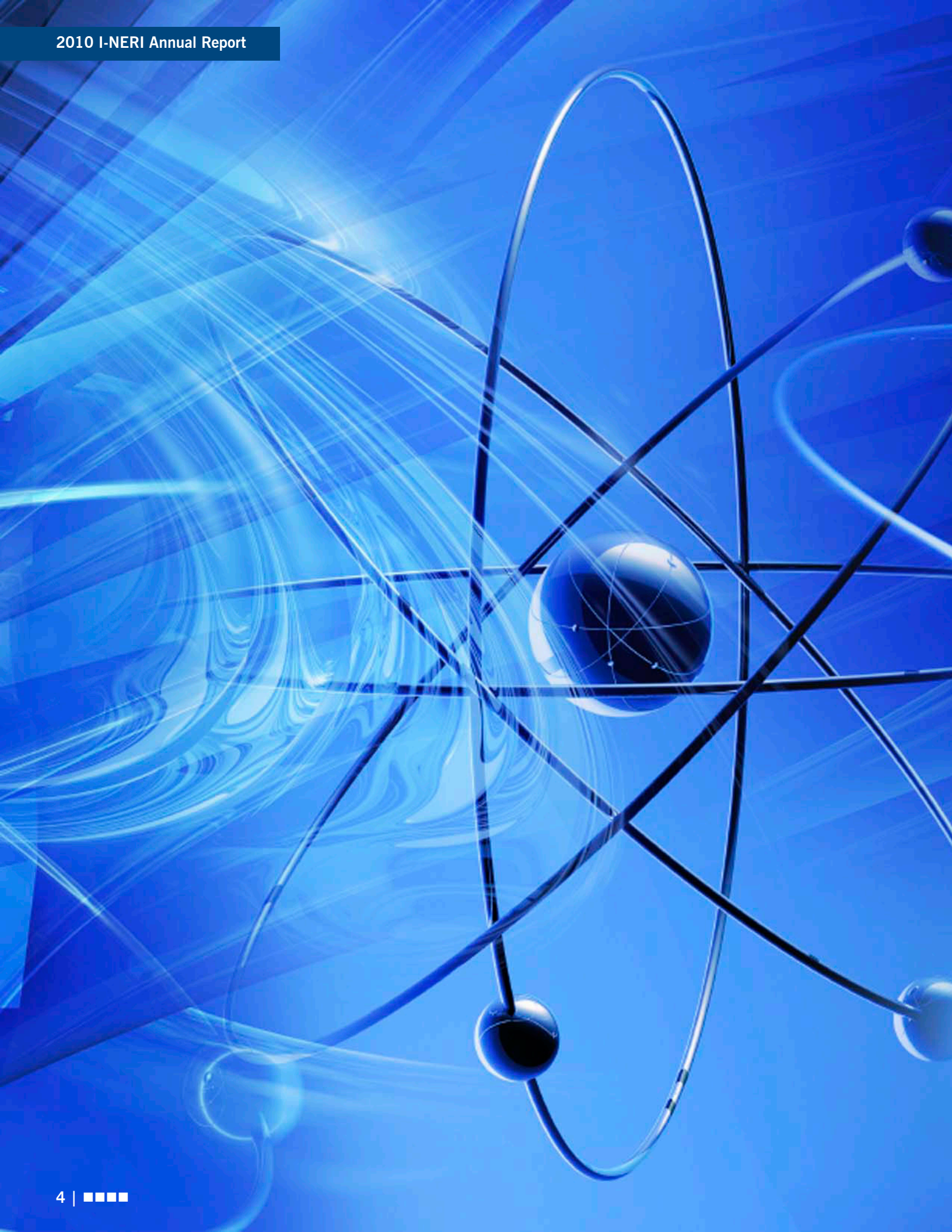


Figure 1. I-NERI program features.



2. Program Background

2.1 Foundation

DOE-NE created I-NERI in FY 2001 in response to recommendations provided by the President's Committee of Advisors on Science and Technology in a report entitled *Powerful Partnerships: The Federal Role in International Cooperation on Energy Innovation*.² This report promoted "bilateral and multilateral research focused on advanced technologies for improving the cost, safety, waste management, and proliferation resistance of nuclear fission energy systems." The report stated, "The costs of exploring new technological approaches that might deal effectively with the multiple challenges posed by conventional nuclear power are too great for the United States or any other single country to bear, so that a pooling of international resources is needed."

In an increasingly global society, the importance of international cooperation has escalated. The initial focus of the I-NERI program was on developing bilateral frameworks for international collaboration, program planning, and project procurements. As noted in the NE R&D Roadmap: "There is potential to leverage and amplify effective U.S. R&D through collaboration with other nations via multilateral and bilateral agreements." The United States can benefit from the resources in countries with mature nuclear systems and assist those countries with developing ones. The NE R&D roadmap also states: "International expansion of the use of nuclear energy raises concerns about the proliferation of nuclear weapons stemming from potential access to special nuclear materials and technologies." Bilateral and multilateral R&D collaborations are key to a common understanding, as well as an integrated approach to nuclear technologies that incorporates their technical development, including safeguards and security technologies and systems, and the maintenance and strengthening of non-proliferation frameworks and protocols.

I-NERI is helping to establish the U.S. role in this growing international nuclear community. Since the program's inception, 100 projects have been awarded, 67 of which have been completed. Both the number of awards and the consistency of project achievement demonstrate I-NERI's success in fostering international collaboration.

2.2 International Agreements

In order to initiate an international collaboration, a government-to-government agreement must first be in place. I-NERI bilateral agreements serve as the vehicles to conduct R&D under the various DOE programs, enabling U.S. researchers to establish international collaborations supporting development of next-generation nuclear energy systems and fuel cycle technologies.

To date, DOE has implemented agreements with six countries and two international organizations. Brief descriptions of and links to these agreements can be found on the I-NERI website.³ The agreements were signed by DOE and the international partners noted in the table below. The table also presents a breakdown, by fiscal year, of the number of projects undertaken with each partner.

The United States also collaborates with the international community via the Generation IV International Forum, the International Atomic Energy Agency (IAEA), and the International Framework for Nuclear Energy Cooperation (IFNEC), formerly the Global Nuclear Energy Partnership. Please visit their websites for more information.⁴

² <http://www.whitehouse.gov/administration/eop/ostp/pcast/docsreports/powerfulpartnerships>

³ http://www.nuclear.gov/INERI/neINERI_bilateralcollaborations.html

⁴ <http://www.gen-4.org>, <http://www.iaea.org/>, and <http://www.ifnec.org/>

Table 1. Number of I-NERI projects awarded.

Collaborator	Organization	FY 01	FY 02	FY 03	FY 04	FY 05	FY 06	FY 07	FY 08	FY 09	FY 10	Total
Brazil	Ministério da Ciência e Tecnologia (MST)					1	1					2
Canada	Department of Natural Resources Canada (NRCan) and Atomic Energy of Canada Limited (AECL)				7			2	3			12
The European Union	European Atomic Energy Community (Euratom)				8	2	5				6	21
France	Commissariat à l'énergie atomique (CEA)	4	1		11		3		2			21
Japan	Ministry of Education, Culture, Sports, Science, and Technology (MEXT)					1	1					2
Republic of Korea	Ministry of Education, Science and Technology (MEST) ⁵		6	5	6	4	4	7	3	2	4	41
Organization for Economic Co-operation and Development (OECD)	The Nuclear Energy Agency (NEA) of OECD		1									1
Republic of South Africa	The Government of the Republic of South Africa											
Total		4	8	5	32	8	14	9	8	2	10	100

2.3 Funding

I-NERI is an important vehicle for enabling international R&D in nuclear technology on a leveraged, cost-shared basis. Each country in an I-NERI collaboration provides funding for its respective project participants; funding provided by the United States may be spent only by U.S. participants. The United States funds I-NERI projects through its national laboratories, with the annual contribution based upon current-year budgets of DOE-NE R&D programs. I-NERI projects typically last three years, with the U.S. portion funded annually. Actual cost-share amounts are determined jointly for each selected project. The program's goal is to achieve approximately 50–50 matching contributions from each partnering country. This section provides approximate domestic and international funding numbers for FY 2010 and the I-NERI program to date.

In FY 2010, the United States provided \$4.9 million to support I-NERI projects: \$2.0 million toward ongoing projects and \$2.9 to launch new projects. International funding for FY 2010 was \$1.9 million toward ongoing projects and \$2.1 million for Year 1 of FY 2010 projects, for a total of \$4.0 million.

The total pledge for FY 2010 projects (i.e., the three-year sum) is \$9.9 million. The United States has committed just over \$5.5 million. The Republic of Korea will provide \$3.4 million to fund four new U.S.–ROK projects, and Euratom's commitment is \$1.0 million for six new U.S.–Euratom collaborations.

To date, I-NERI sponsors have committed a total R&D investment of \$240.3 million: \$129.6 million contributed by the United States and \$110.7 million by international collaborators (see Figure 2).

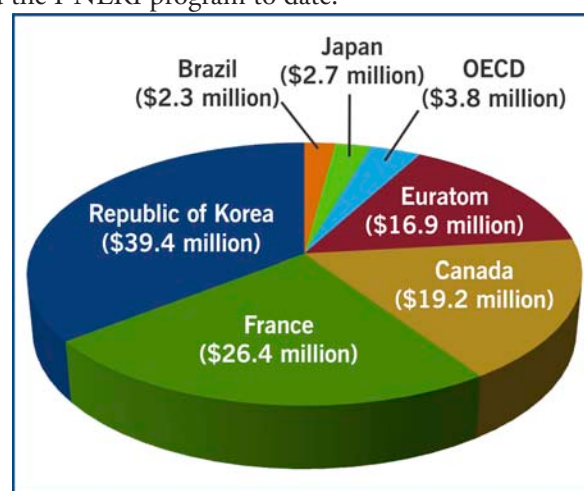


Figure 2. Breakdown of funding since I-NERI's inception by international collaborator (numbers are approximate).

⁵ Signatory agency was the Ministry of Science and Technology (MOST), superseded by MEST in March 2008.

Figure 3. Research institutions.



KEY
 * FY 2010 participant
 [G] Government agency
 [U] University
 [I] Industry



National Laboratories and Government Organizations

- Argonne National Laboratory (ANL) *
- Brookhaven National Laboratory (BNL)

- Idaho National Laboratory (INL) *
- Lawrence Livermore National Laboratory (LLNL)
- Los Alamos National Laboratory (LANL) *
- National Institute of Standards and Technology (NIST) *
- Oak Ridge National Laboratory (ORNL) *
- Pacific Northwest National Laboratory (PNNL)
- Sandia National Laboratories (SNL) *

Industry

- Gas Technology Institute
- General Atomics
- Westinghouse Electric

Universities

- Idaho State University *
- Iowa State University
- Massachusetts Institute of Technology
- Ohio University *
- The Ohio State University
- Pennsylvania State University
- Purdue University

- Rensselaer Polytechnic Institute
- Texas A&M University *
- University of California–Santa Barbara
- University of Florida
- University of Idaho *
- University of Illinois–Chicago
- University of Maryland
- University of Michigan
- University of Nevada–Las Vegas
- University of Notre Dame
- University of Wisconsin *
- Utah State University



Brazil

Eletronuclear [I]
 Instituto de Pesquisas Energéticas e Nucleares (IPEN) [G]
 Ministério da Ciência e Tecnologia (MST) [G]



Canada

Atomic Energy of Canada Limited (AECL) *[I]
 Chalk River Laboratories (CRL) *[G]
 CanmetENERGY [G]
 Ecole Polytechnique de Montréal [U]
 Gamma Engineering [I]
 Université Bordeaux [U]
 Université de Sherbrooke [U]
 University of Manchester [U]
 University of Manitoba [U]



Republic of Korea

Cheju National University [U]
 Chosun University [U]
 Chungnam National University [U]
 Hanyang University [U]
 Korea Advanced Institute of Science and Technology (KAIST) *[G]
 Korea Atomic Energy Research Institute (KAERI) *[G]
 Korea Electric Power Research Institute (KEPRI) [G]
 Korea Hydro and Nuclear Power Company (KHNP) [I]
 Korea Maritime University [U]
 Pusan National University [U]
 Seoul National University *[U]
 Ulsan National Institute of Science and Technology *[U]



Italy

Ente per le Nuove Tecnologie, l'Energia e l'Ambiente (ENEA) [G]
 Società Informazioni ed Esperienze Termoidrauliche (SIET) [I]



Belgium

Joint Research Centre–Institute for Energy (JRC-IE) *[G]
 Joint Research Centre–Institute for Reference Materials and Measurements (JRC-IRMM) *[G]

Joint Research Centre–Institute for Transuranium Elements (JRC-ITU) *[G]

SCK•CEN (Belgian Nuclear Research Centre) *[G]



France

Commissariat à l'énergie atomique (CEA) *[G]
 Electricité de France (EDF) [G]

Framatome ANP [I]

Laboratoire des Composites Thermostructuraux (LCTS) [G]

Organisation for Economic Co-operation and Development–Nuclear Energy Agency (OECD/NEA) [G]



Japan

Hitachi, LTD [I]
 Hitachi Works [I]
 Japan Atomic Energy Agency (JAEA) [G]

Japan Atomic Energy Research Institute (JAERI) [G]

Tohoku University [U]

Toshiba Corporation [I]

University of Tokyo [U]



UK

University of Ontario Institute of Technology [U]



Germany

Karlsruhe Institute of Technology *[U]



Switzerland

Paul Scherrer Institute (PSI) *[G]

2.4 Program Participants

I-NERI encourages global sharing of resources. The program crosses both institutional and geographical boundaries, soliciting projects from international proposal teams that comprise participants from universities, industry, and government organizations, including federal laboratories. Collaborative efforts between the public and private sectors in both the United States and partnering international entities have resulted in significant scientific and technological enhancements in the global nuclear power arena. I-NERI collaborative projects produce findings that would take the United States alone far more time and money to accomplish. The international infrastructure also brings multiple perspectives and priorities together to address shared obstacles. Figure 3 (on the previous page) shows the broad spectrum of participants in the I-NERI program since its inception.

Student Participation

One I-NERI program benefit is development of nuclear-related education and research opportunities. Encouraging young academics to participate in nuclear research promotes the nuclear science and engineering infrastructure, both in the United States and abroad. Support from the I-NERI program helps educational institutions remain at the forefront of science education and research, advance the important work of existing nuclear R&D programs, and create training for the next generation of nuclear scientists and engineers—those who will resolve future technical challenges. In FY 2010, five U.S. and three foreign academic institutions participated in I-NERI research projects. Approximately 25 U.S. students and 29 students from partner countries worked on active I-NERI research projects.

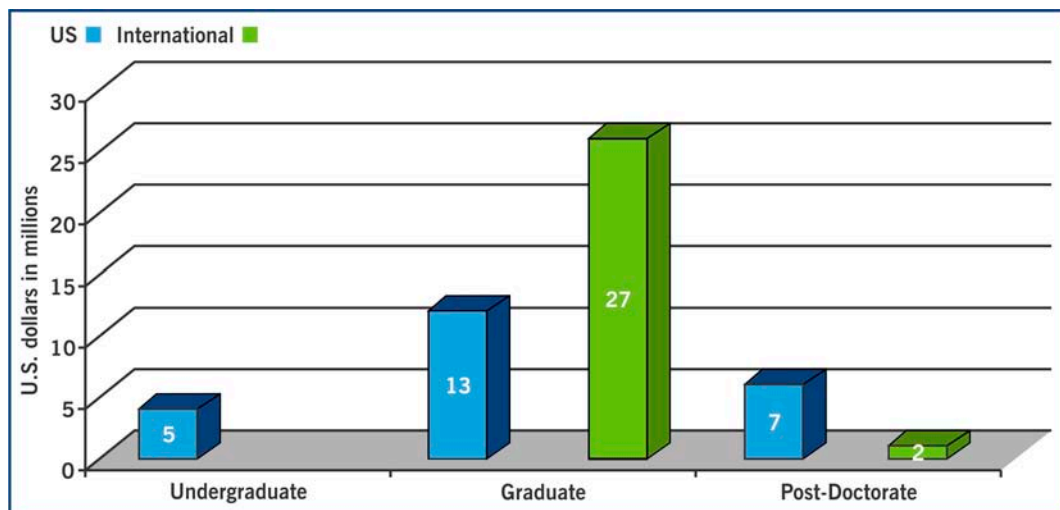


Figure 4. I-NERI student participation broken down by degree level (numbers are approximate).



3. Research Work Scope and Accomplishments



The work scope of all current I-NERI projects is directly linked to the scientific and engineering needs of DOE-NE R&D programs. These programs, in turn, support the four objectives specified in the NE R&D roadmap. U.S. research aims to develop:

- Technologies to improve the reliability, sustain the safety, and extend the life of current reactors
- Improvements in the affordability of new reactors to enable nuclear energy to help meet the Administration's energy security and climate change goals
- Sustainable nuclear fuel cycles
- Understanding and minimization of risks of nuclear proliferation and terrorism

I-NERI project work scopes are jointly developed by the United States and the collaborating country based on terms of the bilateral agreement and current common R&D needs.

Sections 3.1 through 3.3 provide an overview of the work scopes for the NE R&D programs directly supported through I-NERI. Section 3.4 summarizes I-NERI's contributions to these programs via FY 2010 research activities, and Section 3.5 summarizes I-NERI's FY 2010 programmatic accomplishments.

3.1 Reactor Concepts Research, Demonstration and Development

The mission of the Reactor Concepts Research, Development and Demonstration (RD&D) program is to develop new and advanced reactor designs and technologies with broader applicability and improved affordability and competitiveness. RD&D activities address technical, cost, safety, and security challenges associated with four program elements: the Next Generation Nuclear Plant (NGNP) gas-cooled reactor, Advanced Reactor Concepts (ARC), Small Modular Reactors (SMR), and aging of existing light water reactors (LWRs). The NGNP demonstrates the technical viability of gas-cooled reactor technology for hydrogen production and high-temperature process heat for industrial uses. The ARC program conducts research into advanced reactor concepts that improve the nuclear fuel cycle and nuclear waste management, while offering the potential of reduced capital and operating costs, better performance, enhanced safety, and reduced proliferation risk. SMRs can potentially improve the affordability of nuclear power with streamlined construction and simplified operation, along with design features that enhance safety and security.

At the end of FY 2010, the Reactor Concepts RD&D program incorporated and expanded upon the former Generation IV Nuclear Energy Systems Initiative (Generation IV) which, along with the FCR&D program, had formed the technical basis for I-NERI research. Additional international cooperation takes place through the Generation IV International Forum (GIF), established in 2001, which brings together 13 countries to conduct the R&D that will establish the feasibility and performance capabilities of the next generation nuclear energy systems. In December 2002, DOE's Nuclear Energy Research Advisory Committee (NERAC) and the GIF issued *A Technology Roadmap for Generation IV Nuclear Energy Systems*.⁶ This document identified six reactor concepts as the most promising for the next generation of nuclear systems: the molten salt reactor (MSR), lead-cooled fast reactor (LFR), gas-cooled fast reactor (GFR), supercritical water-cooled reactor (SCWR), sodium-cooled fast reactor (SFR), and very high-temperature reactor (VHTR). The roadmap defined needed R&D to develop each of these concepts. Research teams investigated the six reactor concepts and associated technologies. The following is a sampling of early project topics:

- Evaluation of the scientific basis for molten salt technology
- Design concepts, cladding materials, and an analysis database for the LFR
- Optimized design, fuel development, actinide recycling, and safety in the GFR

⁶ http://www.nuclear.gov/genIV/documents/gen_iv_roadmap.pdf

- Instability, heat transfer, and candidate materials for the SCWR
- Metal and oxide fuel core design, actinide processing, and safety optimization in the SFR
- Analysis codes for reactor design and safety, thermohydraulics, decay heat removal systems, and corrosion testing of nickel alloy materials for the VHTR

The results of these early I-NERI projects helped narrow the focus of U.S. nuclear research, which is directed towards the SFR and the VHTR. The former is conducted under the Advanced Reactor Concepts program, while the VHTR concept is being pursued under the NGNP Demonstration Project.

Completed I-NERI projects have investigated such topics as tristructural-isotropic (TRISO) fuel particles, nano-composited and oxide dispersion-strengthened (ODS) steels, silicon carbide composites, zirconium alloys, and development of a Generation IV materials handbook. Other I-NERI teams have conducted research in related technologies such as energy conversion through the Brayton cycle; advanced sensors, instrumentation, and controls; and proliferation resistance. I-NERI projects have also investigated hydrogen production through various thermochemical reactions and high-temperature electrolysis. Researchers have assessed production viability and efficiency, addressed safety issues, and analyzed distribution and storage methods.

The research scope of the Reactor Concepts RD&D program also includes the recently established Modeling and Simulation Hub, which will provide validated advanced modeling and simulation tools necessary to enable fundamental change in how the United States designs and manages nuclear facilities. Some of the first I-NERI project teams utilized modeling and simulation tools and roughly half the current projects explicitly state within their objectives the use, qualification, and/or improvement of such tools.

3.2 Fuel Cycle Research and Development

One of the four NE R&D objectives delineated in the *Nuclear Energy Research and Development Roadmap* is achievement of sustainable fuel cycle options, defined as those that improve uranium resource utilization, maximize energy generation, minimize waste generation, improve safety, and limit proliferation risk. Through a long-term, science-based approach the FCR&D program will develop a suite of technology options that will enable informed decisions about the management of nuclear waste and used reactor fuel. The program also supports roadmap objectives regarding current reactors, new reactors, and minimizing nuclear proliferation and terrorism risks.

Today's nuclear power plants run on a once-through fuel cycle, which utilizes only about five percent of the fuel's energy potential before the used fuel is placed in intermediate- or long-term storage. NE seeks to develop fuels to increase the efficient use of uranium resources, reduce the amount of used fuel requiring direct disposal, and evaluate the inclusion of non-uranium materials to reduce the long-lived radiotoxic elements in used fuel. NE is also investigating a modified open fuel cycle, which is supported through advanced fuels and processing techniques that allow more energy to be drawn from the same amount of nuclear material, as well as reducing the quantity of long-lived radiotoxic elements in the spent fuel. Relevant R&D investigates fuel processing and separations techniques to minimize proliferation risk. The FCR&D program ultimately aims to develop a cost-effective sustainable closed fuel cycle that eliminates much of the high-level waste, reclaiming the energy from used fuel by recycling the long-lived actinide elements. In a full recycle system, only waste products require disposal, not used fuel. The program is applying a methodical systems engineering analysis approach to identify suitable technologies.

Research under this initiative covers not only advanced nuclear fuels and recycling but also used fuel disposition, separations and waste forms, transmutation, and materials protection. FCR&D research has also supported the SFR, whose design is geared toward management of high-level wastes, specifically actinides. This topic area is now part of Advanced Reactor Concepts. Past I-NERI project teams have contributed to the knowledge base. Sample research topics include advanced transmutation fuels, inert matrix fuels, waste forms, separation of fission products from nuclear waste, and advanced head-end processes that condition spent fuel.

Figures 5 and 6 shows the distribution of projects by each of the three major program areas since the program's inception.

3.3 FY 2010 Research Accomplishments

This year marked the completion of seven I-NERI research projects:

- 2006-003-K** Development of Crosscutting Materials for the Electrochemical Reduction of Actinide Oxides Used in Advanced Fast Burner Reactors
- 2007-001-K** Experimental Validation of Stratified Flow Phenomena, Graphite Oxidation, and Mitigation Strategies of Air Ingress Accidents
- 2007-002-K** Development of Advanced Voloxidation Process for Treatment of Spent Fuel
- 2007-003-K** Performance Evaluation of TRU-Bearing Metal Fuel for Sodium Fast Reactors to Achieve High Burnup Goal
- 2007-006-K** Development of Computational Models for Pyrochemical Electrorefiners of Nuclear Waste Transmutation Systems
- 2007-007-K** Sodium-Cooled Fast Reactor Structural Design for High Temperatures and Long Core Lifetimes/Refueling Intervals
- 2007-001-F** Advanced Dispersion-Strengthened Ferritic Alloys and Ferritic–Martensitic Steels with Fine Nanoscale Dispersions

Six of these projects fell under the FCR&D work scope. One project team developed state-of-the-art analysis capabilities for SFR structural design. A second also supported SFR research, evaluating the performance of transuranic (TRU)-bearing metal fuel. The team not only contributed to future analysis through benchmarks but also fabricated barrier claddings to address fuel–cladding chemical interaction, as this interaction may limit alloy fuel burnup. Three materials exhibited consistent good performance. A third completed project also researched methods to enhance alloys with potential for not only SFR fuel cladding but also other advanced high-temperature nuclear technologies.

Three completed FCR&D projects addressed aspects of pyroprocessing, a non-aqueous separations technology that could close the fuel cycle. One project developed crosscutting materials for this technology. Another developed 2-D and 3-D models of electrorefiners, which are key components of pyroprocessing. The third project addressed advanced voloxidation for the head-end treatment of used nuclear fuel undergoing pyroprocessing. The researchers used ten criteria to evaluate advanced voloxidation's effect on pyroprocessing of used oxide fuel, and they confirmed positive results. They also determined optimal operating conditions for the process.

Continuing FCR&D projects include one team researching high-level waste forms and another analyzing uncertainties in neutron cross-section data to improve safeguards. Two project teams are improving characteristics of candidate alloys for Generation IV fuel cladding.

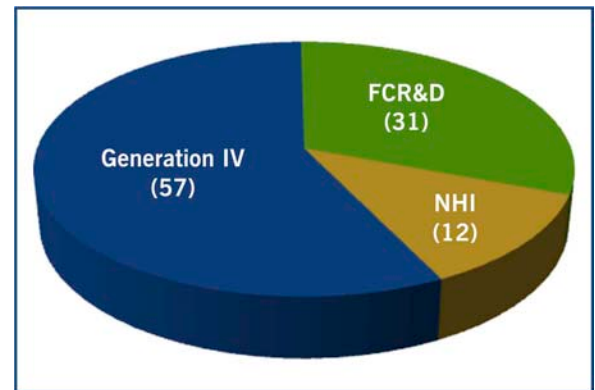


Figure 5. Project distribution by program area (FY 2001 to FY 2009).

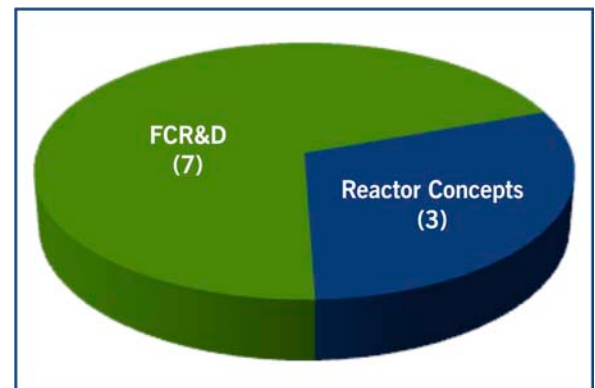


Figure 6. Project distribution by program area in FY 2010.

In the Generation IV program, one team completed an investigation into air ingress-related phenomena in VHTRs to understand consequences of a loss-of-coolant accident. Researchers developed advanced codes, models, and algorithms. Multiple findings include the importance of multi-dimensional simulations for accurate air ingress analyses and the suggestion of two methods to mitigate air ingress in the event of an accident.

Ongoing Generation IV projects include a team investigating advanced multi-physics simulation methods and codes to analyze coupled neutronics and thermofluid behavior of prismatic VHTRs. Another team is developing models to study TRU burner physics and validate design features specific to a typical TRU burner core. One team is examining ceramic composites for use as VHTR and GFR components, while another is working to control VHTR core bypass flow. One ongoing project, originally funded through Nuclear Hydrogen Initiative (NHI), is developing a preliminary design for an integrated complex consisting of a nuclear reactor, electrolytic hydrogen plant, and bitumen up-grader. NHI was terminated as an independent program in FY 2009 and consolidated with the NGNP.

Three FY 2010 projects are funded through Reactor Concepts RD&D. One is looking into a new alloy for next-generation reactor components, one is investigating behavior characteristics of proposed nuclear fuel forms, and the third is developing the framework for an advanced materials test data repository.

Section 4 provides detailed summaries of each of these projects.

3.4 FY 2010 Programmatic Accomplishments

I-NERI accomplishments include not only the completion of seven collaborative research projects but also the initiation of ten new projects: six with Euratom and four with the Republic of Korea. In addition, DOE conducted annual project performance reviews and bilateral program planning meetings with Euratom, France, and the Republic of Korea.

DOE plans the following international activities for FY 2011:

- Initiate new cooperative projects under existing agreements.
- Conduct annual project review/bilateral meetings with international partners.
- Continue pursuing new cooperative agreements with prospective partner countries.

These international collaborations have forged lasting ties that will continue promoting the strong infrastructure necessary to overcome future challenges to the expanded use of nuclear energy. The resulting technological and scientific advances are responding to the need for economical and environmentally conscious sources of energy. I-NERI's goals and objectives continue to be satisfied.





4. Project Summaries and Abstracts

Section 4 provides brief project status reports for active I-NERI R&D projects, as well as summary information about the U.S. partnerships sponsoring those projects: Canada, the European Union, France, and the Republic of Korea.



4.1 U.S.–Canada Collaboration

Director William D. Magwood IV of DOE-NE signed a bilateral agreement on June 17, 2003, with the Assistant Deputy Minister of the Department of Natural Resources Canada, Ric Cameron, and the Senior Vice President Technology of Atomic Energy of Canada Limited, David F. Torgerson. The first U.S.–Canada collaborative research projects were awarded in FY 2004.

Active Projects

During FY 2010, work continued on one U.S.–Canada collaborative project, noted below. Scientists are developing an integrated complex consisting of a nuclear reactor, electrolytic hydrogen plant, and bitumen upgrader. The complex aims to produce hydrogen and, ultimately, synthetic crude oil, gasoline, and diesel fuel. Following is a summary of FY 2010 accomplishments for this project.

2008-001-C Upgrading of the Athabasca Oil Sands for the Production of Diesel and Gasoline

Upgrading of the Athabasca Oil Sands for the Production of Diesel and Gasoline

Research Objectives

The objective of this project is to develop a preliminary design for an integrated complex consisting of a nuclear reactor, electrolytic hydrogen plant, and bitumen upgrader. The complex will provide steam for bitumen extraction and electricity for the electrolytic hydrogen plant. The hydrogen produced will be sent to the bitumen upgrader to produce synthetic crude oil, gasoline, and diesel fuel.

The project team will optimize the integrated plant to maximize thermal efficiency and minimize water usage. Researchers will define requirements, develop a model, and use a commercial process simulator to optimize the integrated complex.

This project comprises three overall tasks:

- Task 1.** Define requirements for the integrated complex.
- Task 2.** Develop an integrated model of a nuclear reactor, electrolytic hydrogen plant, and bitumen upgrader.
- Task 3.** Optimize the integrated plant to maximize thermal management and minimize water usage.

Research Progress

High-temperature electrolysis (HTE) has been identified as a promising and robust technology for greenhouse gas (GHG)-free hydrogen production. The process allows production of both electricity and hydrogen using the same equipment, and HTE's inherent flexibility permits the electrolysis of both steam or a steam/carbon dioxide mixture. HTE also generates an oxygen stream as a product.

Project Number: 2008-001-C

PI (U.S.): J. Stephen Herring, Idaho National Laboratory

PI (Canada): Sam Suppiah, Atomic Energy of Canada, Limited

Collaborators: Canadian Light Source, Saskatchewan Research Council, University of Saskatchewan

Program Area: NHI

Project Start Date: June 2008

Project End Date: May 2011

The project team is investigating HTE, utilizing the excess electricity generated to produce raw materials without GHG production and with reduced natural gas usage. This work has also led to studies on splitting water and carbon dioxide to produce syngas. The workscope includes bench scale testing, computational fluid dynamics (CFD) simulations, system modeling, and scale-up. The largest system, the Integrated Laboratory Scale experiment, consisted of 720 cells (15 kW) that ran for 1080 hours (see Figure 1).

Solid oxide electrolysis cells (SOECs) are very similar in composition to solid oxide fuel cells (SOFCs). Both have oxygen ion conductive electrolyte and porous electrical conductivity electrodes. However, there are some significant differences between SOECs and SOFCs. The direction of the mass fluxes is different, as are the heat requirements. The result of these differences is that SOEC performance degrades faster than SOFC. In the latest 2500-hour test of a cell stack, the degradation seen was 8.15% per 1000 hours. This was great performance for an SOEC, but the typical degradation seen in an SOFC is 1% per 1000 hours.

In October 2009, a number of SOEC experts from around the world attended a workshop hosted by Idaho National Laboratory. The workshop explored ideas on why there was such high performance degradation, such as:

- Oxygen electrode delamination
- Morphology change (e.g., phase change in electrolyte)
- Deactivation due to contaminant transport (chromium, silicon)
- Corrosion of interconnects

The research team plans to continue exploring these possible causes, although some of the research will have to be included in a follow-on project, as this project concludes in a few months.

The team is investigating tools at the Canadian Light Source that can be used to detect the oxidation state of materials in the electrolysis cell. The first stage may be to develop the analysis methodology with button cells because they are the simplest to handle and have the least proprietary technology. When the methods are developed, the team can move on to cell stacks. It may be possible to look at the properties of new cells and compare these with cells that have operated for a period of time.

Once the degradation problem is solved, scientists can prepare a proposal to build a 200 kW pilot plant or a 1–5 MW commercial-scale facility.



Figure 1. HTE modules in the Integrated Laboratory Scale Experiment.

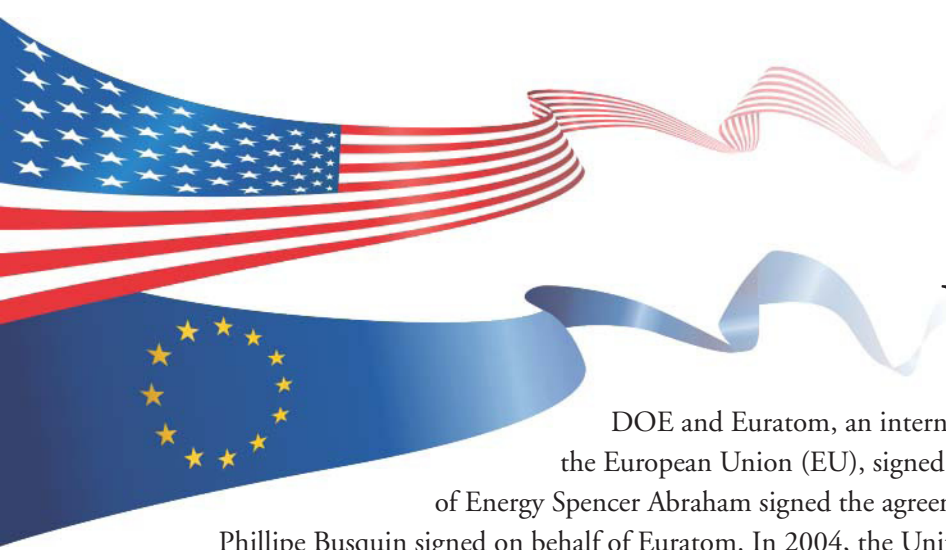


Figure 2. Wide-angle view of the Canadian Light Source.

Project researchers have also studied co-electrolysis of water and carbon dioxide as a route to produce methane or synthetic liquid fuel products. When combined with methanation, the product stream contained 40% methane. Methanol and dimethyl ether can also be produced.

Planned Activities

The project team will continue research into the high performance degradation of SOECs. Discussions are under way regarding use of tools at the Canadian Light Source to assist with this investigation.



4.2 U.S.–European Union Collaboration

DOE and Euratom, an international organization composed of the members of the European Union (EU), signed a bilateral agreement on March 6, 2003. Secretary of Energy Spencer Abraham signed the agreement for DOE, and Commissioner for Research Phillipe Busquin signed on behalf of Euratom. In 2004, the United States and Euratom selected the first ten projects for collaboration.

Active Projects

No U.S.–EU projects were initiated between FY 2007 and FY 2009; therefore, no summary of research progress from FY 2010 is provided here. However, six new collaborations with Euratom were initiated in FY 2010. A listing of these projects follows, along with project abstracts.

- 2010-001-E** Measurements of Fission Fragment Mass Distributions and Prompt Neutron Emission as a Function of Incident Neutron Energy for Major and Minor Actinides
- 2010-002-E** Spherical Particle Technology Research for Advanced Nuclear Fuel/Target Applications
- 2010-003-E** Irradiation and Testing of Advanced Oxide Dispersion-Strengthened and Ferritic–Martensitic Steels
- 2010-004-E** Development of a Standard Neutron Detector for the Energy Range up to 20 MeV and its Application
- 2010-005-E** Interoperability of Material Databases
- 2010-006-E** State-of-the-Art Post-Irradiation Examination of Advanced Nuclear Fuels

Measurements of Fission Fragment Mass Distributions and Prompt Neutron Emission as a Function of Incident Neutron Energy for Major and Minor Actinides

Project Abstract

The project aims to produce new and essential experimental data on fission fragment mass distributions and prompt neutron emission as a function of incident neutron energy for major and minor actinides. Improved fission fragment mass distributions, prompt fission neutron multiplicity, and spectral data are needed to optimize the design and safety assessment of fast reactors, accelerator-driven systems, and waste management scenarios. Researchers will measure fission fragment mass distributions and produce accurate data files for the relevant isotopes as a function of incident neutron energy. Results will contribute to the ENDF and JEFF libraries. The work will be performed by personnel at the Los Alamos National Laboratory (LANL), the Institute for Reference Materials and Measurements (IRMM), and Commissariat à l'énergie Atomique Bruyeres-le-Chatel (CEA); researchers will use neutron facilities at LANL and IRMM together with advanced detectors being developed in these laboratories and at the CEA/DAM laboratory.

Project Number: 2010-001-E

PI (U.S.): Robert C. Haight, Los Alamos National Laboratory

PI (Euratom): Franz-Josef Hamsch, Joint Research Centre–Institute for Reference Materials and Measurements

Collaborators: Commissariat à l'énergie atomique–Centre DAM Bruyeres-le-Chatel

Program Area: FCR&D

Project Start Date: November 2009

Project End Date: October 2012

Spherical Particle Technology Research for Advanced Nuclear Fuel/Target Applications

Project Abstract

This project will advance the state of understanding of particle fuel technology by addressing technical questions related to fuel/target fabrication and performance. Researchers will enhance microsphere fabrication technology by establishing fundamental relationships between process parameters (such as temperature and atmosphere) and key microsphere characteristics (such as porosity, surface area, texture, and second-phase loading). The team will develop a meso-scale model of oxide particle sintering/microstructural evolution to investigate washout and restructuring, among other fuel performance issues. The project consists of three primary tasks:

Sol-Gel Technology. Solution-based routes for the production of spherical particle fuels have demonstrated the ability to form oxide microspheres of controlled size and shape. While previous work has focused on high-density microspheres of a single composition (e.g., UO_2), this project will investigate microspheres with controlled open and interconnected porosity that allow a second oxide phase to infiltrate the pores. Studies will be performed with uranium oxide as the host phase and a rare earth or actinide such as americium as the infiltrated second phase. The task objective is a fundamental understanding of the sol-gel microsphere calcination and infiltration process and an assessment of the range of second-phase loading.

Resin Loading Technology. The resin loading method is a desirable means of minor actinide particle fabrication due to its simplicity for remote operations and minimal waste generated. Although this technology has been successfully used to produce ^{244}Cm targets, the relationships between the loading and resin removal process parameters and particle characteristics such as surface area, morphology, porosity, and residual impurity levels are not fully understood. Using oxide materials as a surrogate, followed by actinides during later stages, researchers will develop a fundamental understanding of these relationships and assess the technology's suitability for nuclear fuel/target applications.

Meso-Scale Modeling of Fuel/Target Fabrication and Performance. For this task the project team will develop a first-generation sintering/microstructural evolution model for oxides to answer outstanding questions related to fuel performance. Researchers will measure fundamental physical properties of pure oxides (heat capacity, crystal structure, toughness, etc.), particle properties (surface area, size, texture, etc.), and bulk powder/particle properties (interparticle cohesive forces, shear data, etc.). Tomographic information on real samples coupled with mathematical expressions for particle flow and mass transport will be integrated into code to computationally simulate sintering/microstructural evolution in oxides.

Project Number: 2010-002-E

PI (U.S.): Stewart Voit, Oak Ridge National Laboratory

PI (Euratom): Mariano Menna, Joint Research Center–Institute for Transuranium Elements

Collaborators: Los Alamos National Laboratory, Sandia National Laboratories

Program Area: FCR&D

Project Start Date: February 2010

Project End Date: January 2013

Irradiation and Testing of Advanced Oxide Dispersion-Strengthened and Ferritic–Martensitic Steels

Project Abstract

This project will further the state of knowledge on irradiation and corrosion effects in materials used for advanced nuclear reactor systems and transmutation test programs. The objective is to share collaborative research results on materials development and characterisation for sodium-cooled fast reactors and gas reactors, as well as transmutation systems using heavy liquid metal coolant and a fast spectrum spallation neutron flux. Modeling and post-irradiation analysis are essential elements of the project.

The research consists of four primary tasks: 1) development and fabrication of advanced oxide dispersion-strengthened (ODS) and ferritic–martensitic (F/M) steels, qualification of these materials at high temperatures (creep, tensile testing and fracture toughness testing), and investigation of welding techniques; 2) examination of corrosion effects of ODS and F/M steels in sodium coolant; 3) investigation of irradiation behavior of ODS steels using programs such as MEGAPIE, Fast Flux Test Facility (FFTF), MATRIX, and the Swiss Spallation Neutron Source (SINQ) Target Irradiation Program (STIP); and 4) multiscale modeling and experimental validation of iron–chromium (FeCr) alloys.

Project Number: 2010-003-E

PI (U.S.): Stuart Maloy, Los Alamos National Laboratory

PI (Euratom): Concetta Fazio, Karlsruhe Institute of Technology

Collaborators: Oak Ridge National Laboratory, Paul Scherrer Institute, SCK•CEN (Belgian Nuclear Research Centre)

Program Area: FCR&D

Project Start Date: December 2009

Project End Date: November 2013

Development of a Standard Neutron Detector for the Energy Range up to 20 MeV and its Application

Project Abstract

The objective of this project is to develop a new type of standard neutron detector (SND) for the energy range up to 20 MeV, with the goal of improving both prompt fission neutron multiplicity and the neutron spectra. The detector will be based on the newly available p-terphenyl scintillator and digital signal treatment technique. The SND will have an accurately measured response function and Monte Carlo (MC) modeling, which will be applied to verify the (n,p) angular distribution. After developing a prototype detector, the project team will apply response function analysis to explore techniques of verifying the (n,p) angular distribution with an accuracy of approximately 1–2%. Researchers will then apply the SND to measure prompt fission neutron spectra in the energy range 0.5–20.0 MeV.

Project Number: 2010-004-E

PI (U.S.): Nikolay Kornilov, Ohio University

PI (Euratom): Franz-Josef Hamsch, Joint Research Centre–Institute for Reference Materials and Measurements

Collaborators: Idaho State University, Los Alamos National Laboratory, National Institute of Standards and Technology

Program Area: FCR&D

Project Start Date: November 2010

Project End Date: October 2013

Interoperability of Material Databases

Project Abstract

Extended materials qualification testing of Generation IV system components that are exposed to high temperatures, neutron fluences, and corrosive environments is necessary to guarantee safe and economic system operations. However, materials test data currently differ in format and associated semantics and are stored in both heterogeneous and distributed database repositories with a variety of working environments and software tools used to access the data, all of which are in a constant state of change. This project will investigate the viability of using standards-compliant schemas and ontologies to address database interoperability, facilitating data exchange between research partners.

Database interoperability will reduce costs associated with redundant materials testing programs, promote long-term data preservation, enable improved auditing traceability, and support the reuse of data.

Although there have been efforts to develop an ontology, systems interoperability of materials databases remained largely unaddressed until very recently. This project will build on the MatML schema for materials properties using results of a recently completed CEN workshop to examine the economics and logistics of standards-compliant schemas and ontologies for interoperability of engineering materials data, including a tensile test schema in correlation with current technology standards and a guide for using and developing data formats for engineering materials test data. The present project will use these results as a starting point. The introduction and adoption of standards-compliant data formats (schemas and ontologies that are a faithful representation of procedural standards for mechanical testing) will allow researchers to leverage established and emerging web-based technologies for data storage and retrieval.

Project Number: 2010-005-E

PI (U.S.): Weiju Ren, Oak Ridge National Laboratory

PI (Euratom): Peter Hähner, Joint Research Centre–Institute for Energy

Collaborators: None

Program Area: Reactor Concepts RD&D

Project Start Date: January 2011

Project End Date: December 2013

State-of-the-Art Post-Irradiation Examination of Advanced Nuclear Fuels

Project Abstract

This project will investigate behavior characteristics of proposed advanced nuclear fuel forms using state-of-the-art experimental techniques. The project has three overall objectives and associated workscopes.

To extend the available knowledge of advanced fuel properties and irradiation behavior. Researchers will investigate properties and behavior of advanced fuels, with particular emphasis on high burnup, fast reactor irradiation behavior, and effects associated with the presence of minor actinides. The fuel systems to be considered include minor actinide (MA) transmutation fuel types, such as advanced mixed oxides (MOX); advanced metal alloys; inert matrix fuel (IMF); and other ceramic fuels, such as nitrides and carbides.

To establish a synergy between multiscale modeling and code development. Experimental data on fuel irradiation behavior will be properly conveyed for the upgrade/development of advanced modeling tools. Establishing viable and effective ways to exchange irradiated fuel samples among participating facilities is essential to this objective's success. The project team will share experimental data and expertise on fuel behavior for joint modeling exercises. The aim is to establish effective synergies between the experimental and modeling groups for a unified and deeper understanding of the behavior of advanced nuclear fuels.

To exchange fuel characterization data among leading experimental facilities. The collaboration will promote effective use of international resources. A key element will be the definition and implementation of a joint characterization program. By sharing results and best practices, research teams will develop and optimize state-of-the-art techniques and facilities for fresh fuel characterization and post-irradiation examination. Specific techniques for study include microprobe analysis, focused ion beam installation and application, micro-focus x-ray diffraction, micro-indentation, and high-resolution thermal properties measurement.

Project Number: 2010-006-E

PI (U.S.): J. Rory Kennedy, Idaho National Laboratory

PI (Euratom): Vincenzo V. Rondinella, Joint Research Center–Institute for Transuranium Elements

Collaborators: None

Program Area: Reactor Concepts RD&D

Project Start Date: January 2011

Project End Date: December 2014



4.3 U.S.–France Collaboration

U.S. Secretary of Energy Spencer Abraham and CEA Chairman Pascal Colombani signed a bilateral agreement on July 9, 2001, to jointly fund innovative U.S.–French research in advanced reactors and fuel cycle development. The U.S.–France collaboration was the first I-NERI agreement to be fully implemented; eighteen U.S.–France collaborative research projects have been awarded since FY 2001.

Active Projects

In FY 2010, U.S.–France researchers contributed to knowledge of candidate materials for advanced high-temperature nuclear systems. One team investigated strengthening ferritic alloys for use in advanced nuclear technologies such as cladding for SFRs. The method involves dispersion of nano-sized particles, and the study achieved fundamental knowledge of the processing and fabrication methods and resulting properties. The other team researched a ceramic composite for use in gas-cooled reactor components: silicon carbide fiber-reinforced silicon carbide matrix (SiC/SiC). The project addressed critical design and qualification issues. A listing of ongoing I-NERI U.S.–France projects follows, along with summaries of the accomplishments achieved in FY 2010.

2007-001-F* Advanced Dispersion-Strengthened Ferritic Alloys and Ferritic–Martensitic Steels with Fine Nanoscale Dispersions

2008-001-F SiC/SiC Composites for Generation IV Reactors

*Completed in FY 2010

Advanced Dispersion-Strengthened Ferritic Alloys and Ferritic–Martensitic Steels with Fine Nanoscale Dispersions

Project Number: 2007-001-F

PI (U.S.): Dave Hoelzer, Oak Ridge National Laboratory, and Stuart Maloy, Los Alamos National Laboratory

PI (France): Yann de Carlan, Commissariat à l'énergie atomique, Saclay

Collaborators: None

Program Area: FCR&D

Project Start Date: June 2008

Project End Date: June 2010

Research Objectives

The objective of this project was to develop high-performance ferritic alloys that are strengthened by a dispersion of nanosized particles. The high-performance alloys resulting from this project are applicable to advanced high-temperature nuclear technologies, such as cladding for sodium fast reactors. Enhanced material performance economizes advanced nuclear reactor requirements by lengthening lifetimes, increasing burnup, and allowing higher operating temperatures with enhanced thermal efficiency and power output. To develop these alloys, the project team focused on:

- Fundamental knowledge of the processing and fabrication methods for achieving the nanosized particle dispersions in the microstructure
- The relationship between the microstructure and deformation and fracture properties
- Stability of the microstructure and mechanical properties during neutron irradiation

This project considered two ferritic alloy systems:

- Tempered martensitic steel (TMS) alloys containing 9% chromium (9Cr) and strengthened by dispersion of nanosized nitride, or nitrocarbide, particles
- Advanced oxide dispersion-strengthened (ODS) ferritic alloys containing 13% to 18% chromium and a dispersion of nanosized oxide particles

The team expanded upon knowledge obtained at Oak Ridge National Laboratory through development of the 14YWT ferritic alloy, which contains a high concentration of titanium-, yttrium-, and oxygen-enriched nanoclusters.

Research Progress

The researchers on this project accomplished the following activities in FY 2010:

- Alloy composition adjustments coupled with optimized thermomechanical treatment (TMT) of the ferritic–martensitic (F/M) steels showed significant increase in strength that was comparable or superior to the commercial ODS PM2000 ferritic alloy. The increased strength was primarily attributable to the increased dislocation subgrain structure combined with the dispersion of nanosized precipitates.

- Results of tests conducted on 14YWT showed a sudden decrease in fracture toughness above 200°C, accompanied by a change from quasi-ductile fracture behavior at room temperature to brittle fracture behavior at 700°C.
- Using transmission electron microscopy (TEM), specimens of 14YWT were subjected to 250 keV Fe⁺ ion irradiation *in situ* to a dose of ~8.0 dpa at room temperature and ~2.2 dpa at 500°C.
- Energy-filtered TEM methods (EFTEM) were used to image the nanocluster and precipitate populations in 14YWT. Results indicated that large precipitates (10–20 nm) became diffuse and dissolved with increasing dose; the research team proposed ballistic cascade mixing to explain this apparent dissolution. Results for the small precipitates (5–10 nm) and nanoclusters (~2 nm) were more ambiguous.

The following provides more detail about the project's achievements.

9Cr TMS fabrication procedures. To achieve optimum microstructures for improved strength at elevated temperatures, researchers developed four heats of 9Cr F-M steel using computational thermodynamics to promote secondary phase strengthening. The heats had a base nominal composition of Fe-9Cr-0.25V-0.25Si-0.07N (wt%) with different concentrations of molybdenum, tungsten, manganese, tantalum, and carbon as shown in Table 1.

Table 1. Nominal composition of the four 9Cr F-M steels.

Heat	Cr	Mn	Mo	W	V	Si	Ta	C	N
1536	9.0	1.0	0.5	–	0.25	0.25	–	0.02	0.07
1537	9.0	0.5	–	1.0	0.25	0.25	–	0.02	0.07
1538	9.0	0.5	–	1.0	0.25	0.25	0.1	0.02	0.07
1539	9.0	0.5	–	1.0	0.25	0.25	0.1	0.08	0.07

The research team optimized the TMT treatments to control the microstructure of the 9Cr F-M steels, considering prior austenite grain size, martensitic packet and lath density, dislocation density, and precipitate size and density. They investigated several TMT methods, including 1) normalization at 1100°C followed by tempering at 760°C and 2) normalization at 1100°C, followed by a series of hot rolling steps, and a final tempering at 760°C. Figures 1 and 2 illustrate the effects of different compositions and treatments on the microstructure. The low-carbon heats (1536–1538) showed similar lath microstructures (Figures 1a and 1b), as opposed to the denser lath structures observed in the high-carbon heat 1539 (Figures 1c and 1d). The lath structures were also slightly more dense when the TMT included hot rolling (Figures 1b and 1d) instead of only of normalizing and tempering (Figures 1a and 1c).

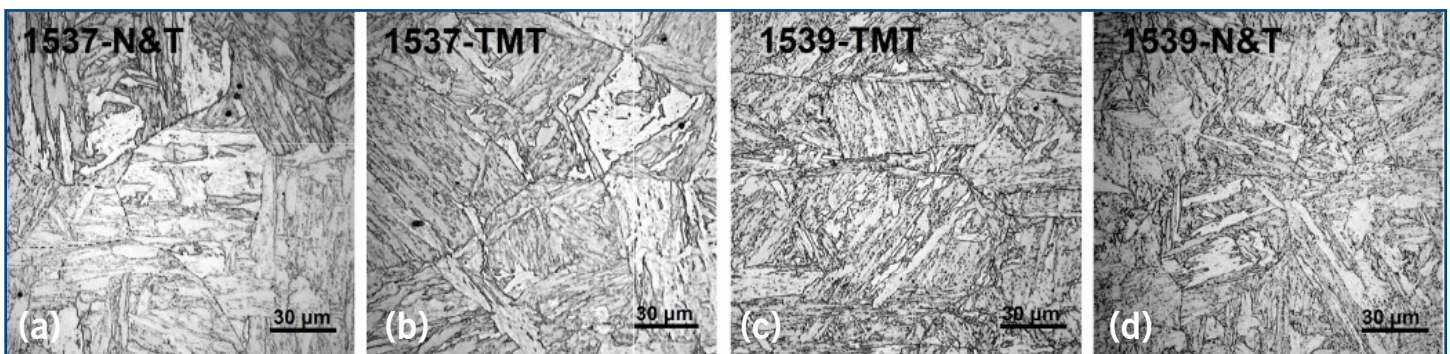


Figure 1. The representative microstructures observed in the experimental 9Cr F-M steels.

Figure 2 shows the precipitate phases calculated for the four 9Cr heats at the tempering temperature of 760°C. Results indicated that similar precipitate phases and content were favored in 1536 and 1537 heats. Tantalum was added to heats 1538 and 1539, which was predicted to result in the additional (Ta,V)C carbide phase. Increased carbon content in the 1539 heat significantly increased the M₂₃C₆ carbide phase with some increase of the (Ta,V)C carbide phase. The TEM microstructural analysis showed precipitate structures that were in reasonable agreement with the calculated phases.

Tensile tests conducted on the four heats over a temperature range of 25°C to 650°C assessed the effects of varied compositions and TMTs. The results showed heats 1536 and 1537 as having similar strengths, consistent with reports on W = 2Mo alloying effect on strength. However, heats 1538 and 1539 showed a significant increase in strength, attributed to the tantalum precipitates. All four heats showed greater strength than NF616 with no significant impairment in ductility. Interestingly, the TMT with the hot rolling step significantly increased strength; these heats had strengths comparable (e.g., 1537-TMT) or superior (e.g., 1538-TMT) to PM2000 at temperatures up to 650°C. The yield strengths are shown in Figure 3, along with values from tensile tests on ODS alloys (PM2000 and MA957) and the NF616 9Cr F-M steel.

Nanocluster-strengthened 14YWT ferritic alloy. The project team studied 14YWT ferritic alloy, focusing on fracture toughness behavior at elevated temperatures and ion irradiation's effects on the nanoclusters' stability. Previous low-temperature tests (<200°C) revealed that the 14YWT ferritic alloy's fracture properties were superior to those of the predecessor 12YWT alloy. The 14YWT (SM6 heat) had a transition temperature (T_0) of around -150°C and upper shelf fracture toughness of about 175 MPa√m. The high fracture toughness below room temperature is extraordinary considering that typical 14YWT tensile yield strength is very high: >1.5 GPa at those temperatures. To ascertain whether 14YWT's high cracking resistance would be retained at higher temperatures, the team carried out static fracture toughness tests in the temperature range of 22°C–700°C using 12.5-mm-diameter disk compact tension specimens and examined the fracture surfaces using scanning electron microscopy (SEM).

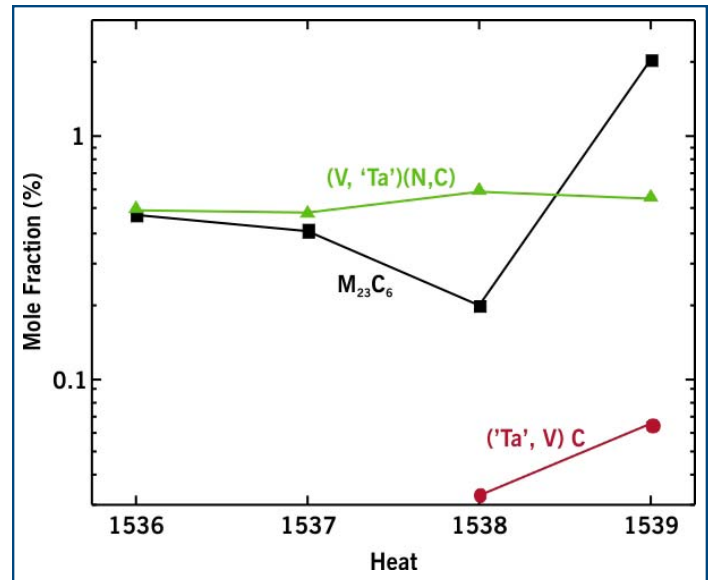


Figure 2. Calculated equilibrium mole fraction of precipitates in the four experimental 9Cr F-M heats after tempering at 760°C.

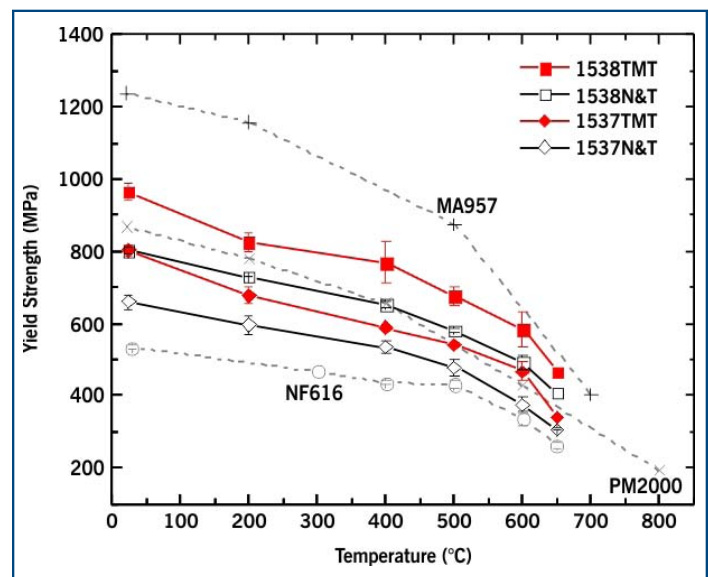


Figure 3. Comparison of the yield strengths between the experimental 9Cr F-M heats, the ODS PM2000 and MA957 alloys, and the NF616 9Cr F-M steel.

Figure 4 compares 14YWT fracture toughness to HT-9 steel at room temperature to 700°C. The fracture toughness values of 14YWT at room temperature and 200°C were 143 MPa√m and 144 MPa√m, respectively. Above 200°C the toughness decreased significantly (52–82 MPa√m). The value at 200°C is believed to be the upper shelf fracture toughness since the ductile-to-brittle fracture transition temperature of 14YWT is below room temperature. Although its upper shelf toughness is much lower than HT-9's ($K_{JQ} > 210$ MPa√m), 14YWT's peak fracture toughness is acceptable thanks to extraordinarily high strength in the temperature range ($\rho 1.5$ GPa).

14YWT shows an abrupt decrease in fracture toughness between 200°C and 300°C, especially when compared to the more gradual decrease observed for HT-9, suggesting a sudden change in fracture mechanism in this temperature region. The team used SEM to compare fracture surfaces after stable crack growth at room temperature and 700°C. The fracture surface at room temperature (Figures 5a and 5b) shows a mixture of numerous nanoscale dimples and cleavage facets over isolated, near-circular areas with diameters of one to several micrometers and decorated with shear lips at their edges. At 700°C (Figures 5c and 5d), the fracture surface appears as a very fine dimpled structure, with dimples of about one micrometer or less. Numerous microcracks formed perpendicular to the fracture surface, with many small dimples on the nearby raised surfaces. The differences in the fracture surfaces suggest that quasi-ductile fracture occurs at room temperature (25°C) and brittle fracture at 700°C. The change to brittle behavior at elevated temperatures was likely caused by shallow nanoscale dimples that formed by decohesion of individual and multiple nanosized grains in the 14YWT microstructure. Since the target application temperature for 14YWT is 500°C or higher, the relatively low fracture toughness above 200°C (82 MPa√m) and change to brittle fracture behavior at elevated temperatures indicate the need for further development of the 14YWT ferritic alloy.

The project team conducted sequential and *in situ* ion irradiation experiments. Specimens of 14YWT were irradiated with 250-keV Fe⁺ ions from the ARAMIS accelerator at room temperature with ion doses up to ~8 dpa and at 500°C with ion doses up to ~2.2 dpa. The team used the EFTEM Fe-M jump ratio technique to image the fine-scale precipitate structures, examining the same areas of the specimens *in situ* after each successive dose of Fe⁺ ions to follow an individual feature over a range of dpa.

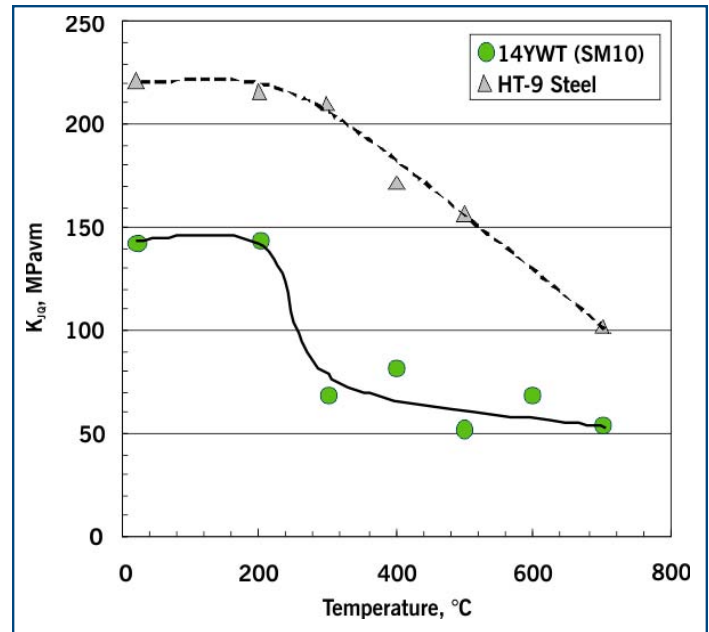


Figure 4. Comparison of fracture toughness for 14YWT and HT-9 as a function of test temperature.

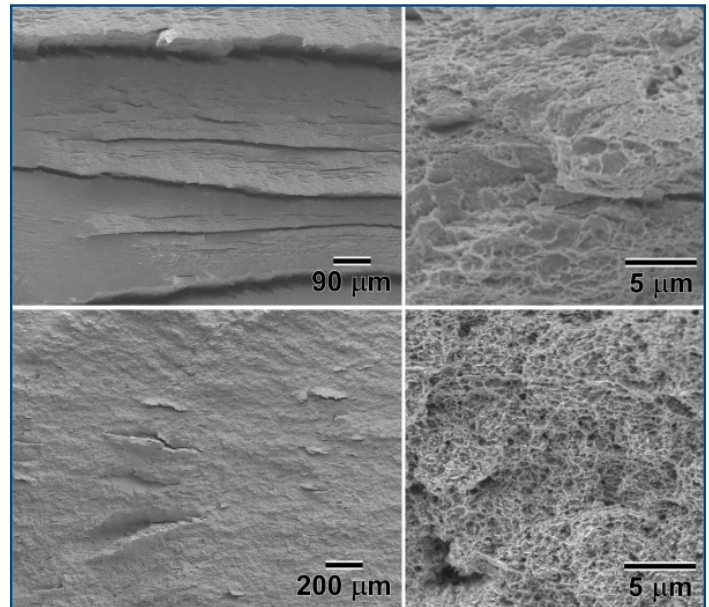


Figure 5. SEM micrographs showing fracture surfaces from tests conducted at (a, b) room temperature and (c, d) 700°C. The crack propagation occurred from right to left.

The results showed that as the 250-keV Fe⁺ irradiation progressed, the precipitate and nanocrystal population changed within the examined areas. In Figure 6a, red arrows identify the locations of precipitate prior to ion irradiation; in the same specimen after an accumulated Fe⁺ dose of ~8 dpa (Figure 6b), the precipitate has disappeared. Most significant was the observation that 250-keV Fe⁺ irradiation slowly destroyed the EFTEM contrast of the particles.

Researchers interpreted this finding as dissolution of the nanosized particles, including the nanoclusters. The ion irradiation experiment at 500°C produced a similar outcome; however, pronounced oxidation of the specimen occurred, which complicated interpretation of the results.

The project team suggests one possible mechanism for explaining the observed phenomena: ballistic cascade mixing with insufficient back diffusion of solutes and vacancies to reform the nanoclusters and other fine-scale precipitates. Dose rate and temperature are known to have coupled effects on microstructural evolution in steels. Limited diffusivity of solute and vacancies is most likely at room temperature; even at 500°C, however, the diffusivity of solute and vacancies may be insufficient for microstructural processes to counteract cascade mixing from the ion irradiation damage in the time available during the irradiation. The foil surface's proximity will have a confounding effect, although the magnitude is unclear. Researchers have not ascertained the temperature range over which the present apparent dissolution effect occurs. Because of the pronounced oxidation that occurred during the 500°C irradiations, determining the temperature range will be very challenging. Such oxidation presents a major barrier to elevated-temperature *in situ* ion irradiation studies of advanced alloys. These issues necessitate further research into the exact mechanism for the observed phenomena from these experiments.

Planned Activities

This project has been completed.

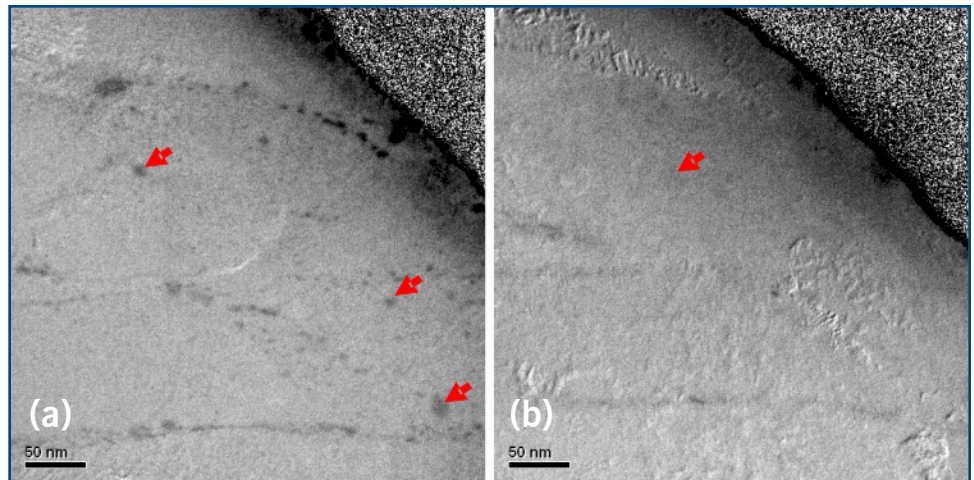


Figure 6. Fe-M jump ratio EFTEM maps of 14YWT in (a) pre-irradiation condition and (b) following successive Fe⁺ ion irradiations at room temperature to a dose of ~8 dpa.

SiC/SiC Composites for Generation IV Reactors

Research Objectives

The objective of this I-NERI collaboration is to address some of the most critical design and qualification issues for silicon carbide fiber-reinforced silicon carbide matrix (SiC/SiC) composite components for use in advanced gas reactors.

In high-temperature reactors, the fuel cladding and the core are subjected to temperatures often far exceeding 1000°C, prohibiting the use of metallic alloys. Ceramic composites are considered advanced materials for use in Generation IV (Generation IV) nuclear systems at temperatures beyond the operating limits for metallic heat-resistant alloys.

Carbon fiber-reinforced carbon matrix (C/C) and SiC/SiC composites are the materials under study. C/C is appropriate for low neutron-loading applications, mostly outside the core in very high-temperature reactors (VHTRs); while SiC/SiC is suitable for high neutron-loading environments, such as VHTR control rods and most core internals of gas-cooled fast reactors (GFRs).

SiC/SiC components are expected to achieve adequate thermomechanical performance, as these composites exhibit a reproducible behavior and adequate strains to rupture. However, because of the complex microstructure, these materials exhibit complex, highly anisotropic, and non-linear behavior. The nuclear community requires a better understanding of the relation between processing, microstructure, damage mechanisms, and mechanical behavior. To achieve this understanding and to improve the behavior laws used for structural calculation, this project team has undertaken a multi-scale approach toward thermomechanical behavior modeling. The project team will:

- Develop a reliable predictive capability of component strength and operational lifetime in a complex environment.
- Analyze relations of the components' mechanical behavior in different geometries.

Research Progress

The macroscopic mechanical behavior of ceramic composites is the consequence of damage mechanisms (matrix cracking, interphase debond, fiber failure) occurring at microscopic to mesoscopic scales. The purpose of a multi-scale approach is to understand the damage mechanisms in various scales in order to develop constitutive models of the macroscopic composite behavior. Therefore, such an approach has to be based on a detailed description of these mechanisms provided by experimental observations. The effort during the current reporting period focused on the correlation between the constitutive properties and the behavior of model composite elements and the *in situ* characterization of damage processes during deformation.

Project Number: 2008-001-F

PI (U.S.): Y. Katoh, Oak Ridge National Laboratory

PI (France): L. Gelebart, Commissariat à l'énergie atomique

Collaborators: Idaho National Laboratory

Program Area: Generation IV

Project Start Date: April 2009

Project End Date: April 2012

The team prepared model uni-directional mini-composite elements using four types of fibers for reinforcement: Hi-Nicalon™ Type-S (HNLS), Tyranno™-SA3 (SA3), experimental Sylramic™ (Syl), and experimental Sylramic™-iBN SiC (Syl-iBN). The fiber/matrix (F/M) interphase was single-layer pyrolytic carbon (PyC) with a nominal thickness of 150 nm.

The mini-composite samples were subjected to tensile tests at room temperature. Strain was measured using a pair of linear variable differential transducers. The team adopted a self-alignment mechanism similar to the one used in single-fiber tensile testing standardized in ASTM C 1557. Cyclic loading with unloading-reloading was incorporated to evaluate interfacial properties. After the tensile tests, researchers examined fracture surfaces using scanning electron microscopy (SEM). They also measured fiber pull-out length and matrix crack spacing to estimate interfacial sliding stress.

Results of the mechanical test are summarized in Table 1. Figure 1 shows representative load-strain evolutions for the HNLS mini-composites, which exhibited typical pseudo-ductile fracture behavior: an initial steep linear region in the load-strain curve, with a second, nearly linear region at higher strains, repeated during tensile loading with multiple unloading-reloading sequences. The initial linear portion corresponds to the mini-composite's linear elastic deformation, whereas the second linear portion corresponds to a process of progressive development and opening of multiple matrix micro-cracks. The HNLS mini-composite strength achieved 77% of the fiber bundle strength.

Figure 2 shows SEM images of the fracture surface of each mini-composite. Syl-iBN had the shortest pull-out lengths (~15 μm) and HNLS the longest (~300 μm); SA3 and Syl-PyC had pull-out lengths of ~100 μm.

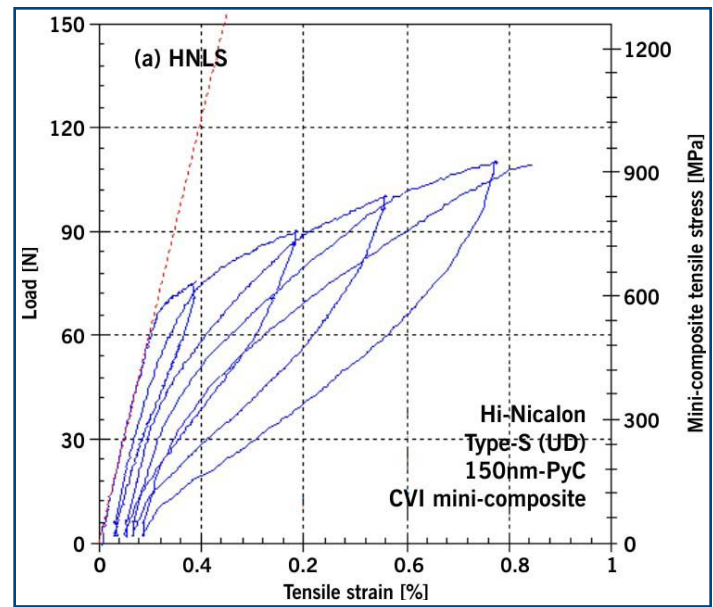


Figure 1. Representative tensile load-strain curves for HNLS mini-composites.

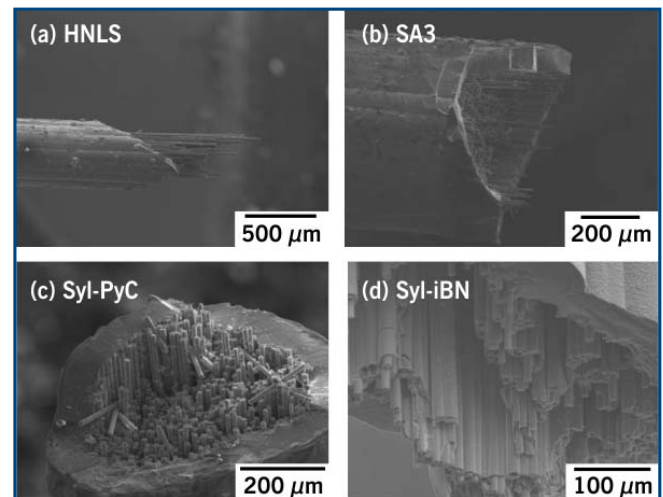


Figure 2. SEM micrographs of the fracture surfaces of the (a) HNLS, (b) SA3, (c) Syl-PyC, and (d) Syl-iBN mini-composites.

Table 1. Tensile test results for the mini-composites.

ID	Fiber	Int.	Matrix	P_r [N]	P_p [N]	ϵ_r [%]	ϵ_p [%]	σ_u [MPa]	σ_p [MPa]	σ^T [MPa]	RS [%]	#
HNLS	Hi-Nicalon Type-S	150 nm PyC	CVI	113 (5)	67 (4)	0.877 (0.029)	0.152 (0.011)	923 (31)	552 (34)	-303 (75)	77 (3)	4
SA3	Tyranno-SA3	150 nm PyC	CVI	105 (6)	80 (8)	0.270 (0.072)	0.114 (0.041)	676 (52)	513 (51)	-110 (121)	53 (3)	4
Syl-PyC	Exp-Sylramic	150 nm PyC	CVI	130 (7)	91 (11)	0.201 (0.044)	0.121 (0.006)	958 (40)	675 (91)	-73 (-)	69 (4)	2
Syl-iBN	Exp-Sylramic-iBN	n/a	CVI	153 (10)	112 (18)	0.174 (0.033)	0.099 (0.012)	1115 (17)	819 (168)	0 (-)	81 (5)	2

P_r denotes the load at fracture, P_p the load at proportional limit (PL), ϵ_r the strain at fracture, ϵ_p the strain at PL, σ_u the ultimate tensile strength, σ_p the PL stress, σ^T the misfit stress, RS the relative strength of the mini-composite to the single fiber strength, and # the number of tests. Numbers in parenthesis show standard deviations.

The investigators estimated F/M interfacial sliding stress, which largely influences the composite fracture properties, using three different methods: tensile hysteresis width analysis, local matrix crack spacing approximated from the fractographic examination, and the fiber pull-out length measurement. Although results exhibited limited agreement with each other, the materials' relative ranking was consistent: the HNLS composite showed the smallest frictional stress, the Syl-iBN composite showed the largest, and the SA3 and Syl-PyC composite values were in the middle. These results could be correlated primarily with the fiber surfaces' topological roughness and secondarily with the clamping stress arising from the thermal expansion differential between the fibers and the matrices. When the interfacial sliding stress was relatively weak, the global load-sharing theory seemed to be the better predictor of mini-composite ultimate tensile stress; whereas with increased interfacial friction, this stress value tended to deviate toward predictions using the local load-sharing theory.

Researchers examined uni-directional composites considered representative of the tows within the woven composites. The test materials consisted of 500 fibers, a PyC interphase, and a matrix fabricated with chemical vapor infiltration (cvi). *In situ* SEM tensile tests were used to determine the spatial distribution of matrix cracks along the mini-composite as a function of the applied load (see Figure 3 for results). Note that after a load of 66 cycles (N), no more cracks appear on the mini-composite: the saturation of matrix crack initiation is achieved. Figure 4 shows the evolution of the matrix crack opening (measured at the mini-composite's surface).

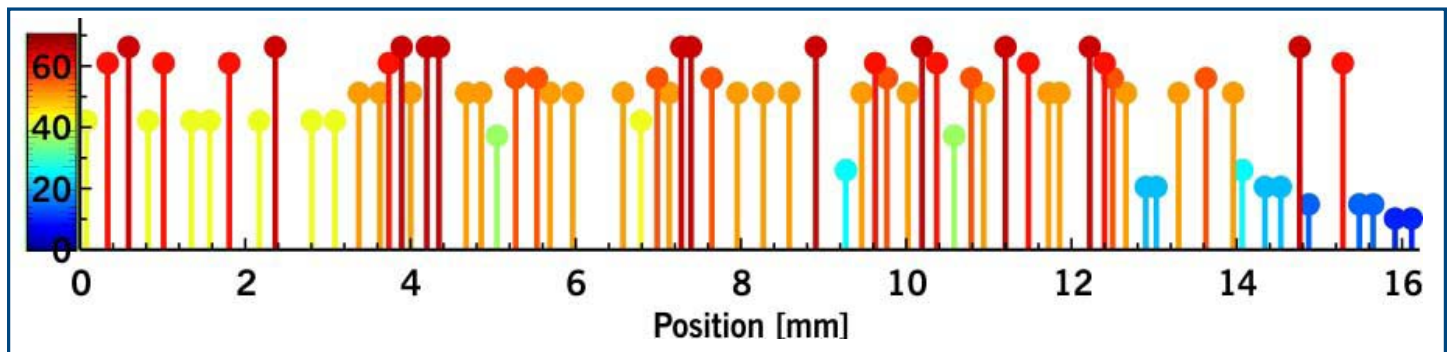


Figure 3. Spatial distribution of matrix cracks along the mini-composite axis, observed for different successive loading levels. The height and color of each "crack" corresponds with the loading level at which the crack is first observed.

However, *in situ* SEM tensile tests are limited to surface observation. They cannot be used to address questions of the matrix crack propagation or initiation and spatial distribution of breaking fibers. Up to now, scientists have been limited to such surface observations, mainly after the ultimate failure (post-mortem). Hence, the project team developed *in situ* tensile tests using x-ray tomography. Tests were conducted on SiC/SiC mini-composites at a high resolution ($0.28 \mu\text{m}$) to detect, for different successive loadings, the matrix cracks and fiber breakings within the sample.

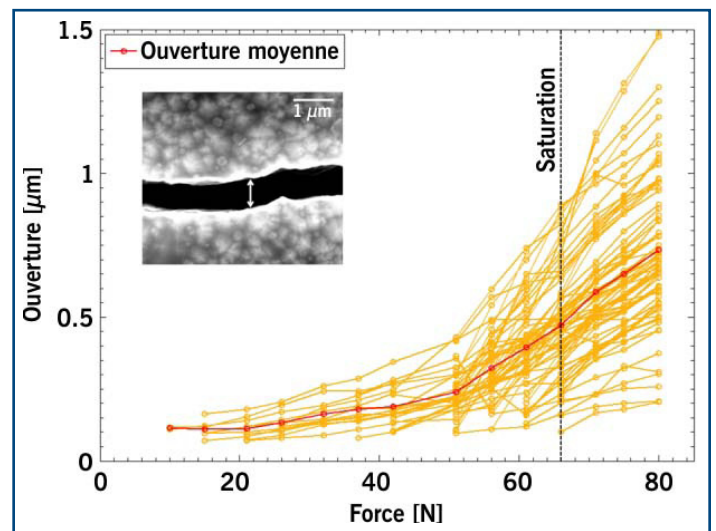


Figure 4. Evolution of the matrix crack openings for all cracks reported in Figure 3. Observations were made at the sample's surface.

The team observed a slow and discontinuous matrix crack propagation: the matrix crack does not propagate instantaneously through the composite and stops between 68 N and 74 N. Initiation occurs at the sample's periphery (50 N), then propagates through the whole periphery (68 N), and finally propagates through the center (80 N). Such a phenomenon is generally not taken into account in 1-D models of mini-composites.

Concerning fiber breakage, the SEM tests indicated low density with a random uniform spatial distribution until 92 N. X-ray tomography, however, revealed high density near the crack and much lower density elsewhere (see Figure 6). These results indicate that ultimate failure is the consequence of a local fiber breakage, which will have to be accounted for when modeling 1-D composites.

Planned Activities

The project confirmed that F/M interfacial debond and sliding are the key properties in constitutive understanding and modeling of the composite mechanical behavior. The team plans continued detailed study, including development of a new experimental method for the explicit determination of these interfacial micro-mechanical properties. They plan to promote these new results through redaction of scientific communications.

In addition, researchers will investigate different 1-D models from the literature to reproduce the mechanical behavior of 1-D SiC/SiC composites. The models are based on various assumptions concerning different damage mechanisms (matrix cracking, interphase debonding, and fiber breakage). However, the lack of experimental data resulted in models that accounted only for macroscopic mechanical behavior. The team will compare and update these models to account for project findings to date. Researchers will use the 1-D models to derive 3-D models, introducing the tow's behavior in 3-D finite element simulations of woven composites (Figure 7).

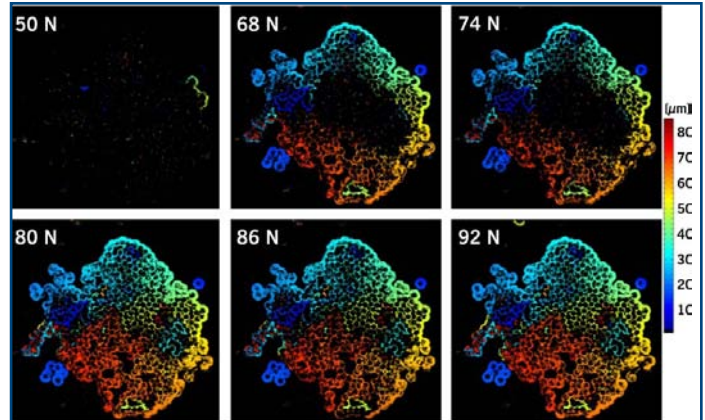


Figure 5. Detection of a matrix crack for six successive loadings. The colors, which indicate the crack's axial position, exhibit the crack's helical shape.

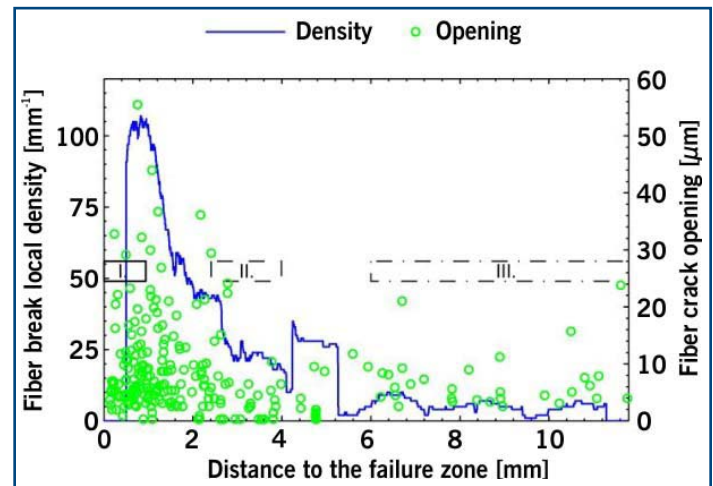


Figure 6. Fiber breakage density as a function of distance to the crack.

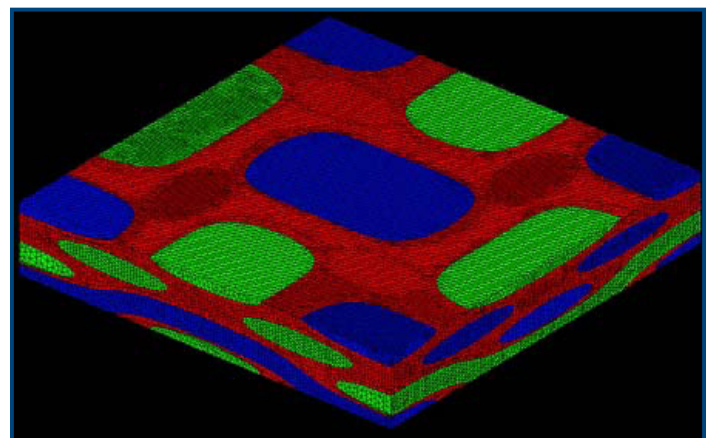
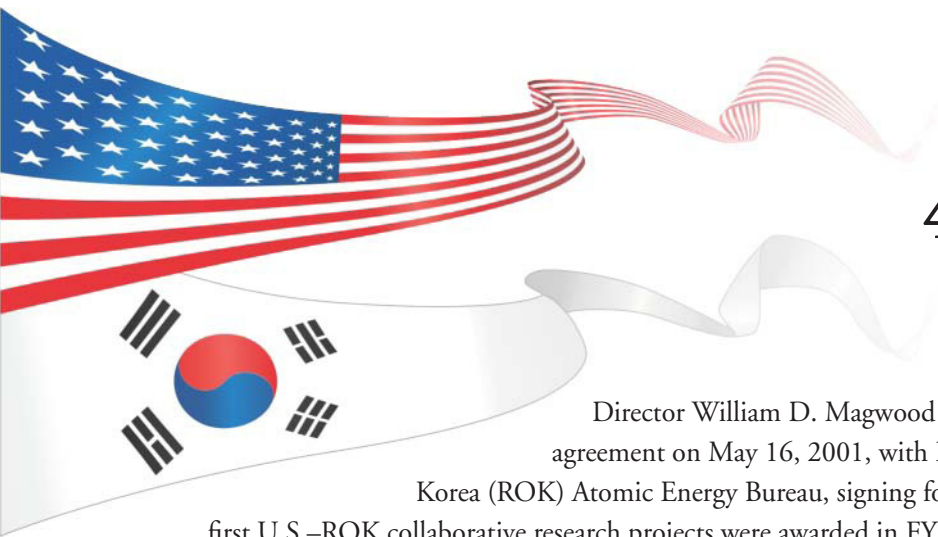


Figure 7. Finite element mesh of a woven composite.



4.4 U.S.–Republic of Korea Collaboration

Director William D. Magwood IV of DOE-NE signed the first bilateral I-NERI agreement on May 16, 2001, with Director General Chung Won Cho of the Republic of Korea (ROK) Atomic Energy Bureau, signing for the ROK Ministry of Science and Technology. The first U.S.–ROK collaborative research projects were awarded in FY 2002, with a total of 41 projects awarded to date.

Active Projects

Five FY 2007 projects were completed during the past fiscal year, as well as one FY 2006 project.⁷ Research continued on six other collaborative projects awarded to ROK partners from FY 2007 through FY 2009. Four new projects were awarded during the past year.

During FY 2010, U.S.–ROK I-NERI research covered a range of topics from early stages of reactor design to systems safety during operation. One team developed four key design analysis capabilities and applied them to SFR pre-conceptual designs. VHTR design was also specifically addressed through development of advanced multi-physics simulation methods and codes for analysis as well as solutions to reduce bypass flow in a VHTR core. One project validated design features specific to a typical transuranic (TRU) burner core, while another evaluated burnup performance of TRU-bearing metal fuel. Other fuel-related research areas included handling used fuel and fission products that result from pyroprocessing, using non-aqueous separations technology to close the fuel cycle, and increasing radiation tolerance in fuel cladding. One project investigated air ingress-related phenomena, suggesting safety-related countermeasures to reduced reactor coolant flow. Adding to and improving available data for research was a specific objective for multiple researchers.

This section provides a listing of FY 2007 through FY 2010 I-NERI U.S.–ROK projects—those that are currently under way, those completed last year, and those newly awarded—along with summaries of FY 2010 accomplishments and abstracts of the new projects.

- 2007-001-K*** Experimental Validation of Stratified Flow Phenomena, Graphite Oxidation, and Mitigation Strategies of Air Ingress Accidents
- 2007-002-K*** Development of an Advanced Voloxidation Process for Treatment of Spent Fuel
- 2007-003-K*** Performance Evaluation of TRU-Bearing Metal Fuel for Sodium Fast Reactors to Achieve High Burnup Goal
- 2007-004-K** Development and Characterization of New High-Level Waste Forms for Achieving Waste Minimization from Pyroprocessing

⁷ The 2010 I-NERI Annual Report provides progress summaries for projects beginning in and after FY 2007. Summaries of earlier I-NERI projects can be found through DOE-NE's website: <http://www.nuclear.gov/INERI/neINERI1.html>.

- 2007-006-K*** Development of Computational Models for Pyrochemical Electrorefiners of Nuclear Waste Transmutation Systems
- 2007-007-K*** Sodium-Cooled Fast Reactor Structural Design for High Temperatures and Long Core Lifetimes/Refueling Intervals
- 2008-001-K** Advanced Multi-Physics Simulation Capability for Very High-Temperature Gas-Cooled Reactors
- 2008-002-K** Experimental and Analytic Study on the Core Bypass Flow in a Very High-Temperature Reactor
- 2008-003-K** Nuclear Data Uncertainty Analyses to Support Advanced Fuel Cycle Development
- 2009-001-K** ZPPR-15 and BFS Critical Experiments Analysis for Generation of Physics Validation Database of Metallic-Fueled Fast Reactor Systems
- 2009-002-K** Enhanced Radiation Resistance Through Interface Modification of Nanostructured Steels for Generation IV In-Core Applications
- 2010-001-K** Investigation of Electrochemical Recovery of Zirconium from Spent Nuclear Fuels
- 2010-002-K** Science-Based Approach to Nickel Alloy Aging and its Effect on Cracking in Pressurized Water Reactors
- 2010-003-K** Low-Loss Advanced Metallic Fuel Casting Evaluation
- 2010-004-K** Development and Characterization of Nanoparticle-Strengthened Dual-Phase Alloys for High-Temperature Nuclear Reactor Applications

* Completed in FY 2010

Experimental Validation of Stratified Flow Phenomena, Graphite Oxidation, and Mitigation Strategies of Air Ingress Accidents

Research Objectives

A loss-of-coolant accident (LOCA), which can cause depressurization conduction cooldown, is considered a critical event for very high-temperature reactor (VHTR) safety. Following helium depressurization, air will likely enter the core through the break, leading to oxidation of the in-core graphite structure—unless countermeasures are taken. Without mitigation features, a LOCA will lead to an air ingress event, which will in turn lead to exothermic chemical reactions of graphite with oxygen, mechanical graphite strength degradation, and toxic gas release, potentially resulting in significant safety problems.

The major objective of this project was to investigate air ingress-related phenomena in VHTRs. The project team performed experiments to better understand accident consequences. Based on the experimental data, current computational methods were validated and evaluated. Finally, this project investigated air ingress mitigation methods, suggesting some promising concepts to avoid potential safety problems.

Research Progress

Task 1. Density difference induced stratified flow analysis. The researchers performed various analyses using computational fluid dynamic (CFD) and analytical methods, focusing on the density gradient-driven stratified flow expected in a VHTR air ingress accident. First, this project team reviewed previous studies on lock exchange phenomena that are physically similar to those in a VHTR air ingress accident. Based on those reviews, they performed a study to identify and compare major air ingress mechanisms (molecular diffusion versus density gradient-driven flow). The results clearly showed that density gradient-driven stratified flow is a dominant air ingress mechanism in the VHTR LOCA. In parallel with the analytical studies, various CFD simulations were conducted using simplified 2-D and detailed 3-D models. The 600 MWth Gas Turbine Modular Helium Reactor (GT-MHR) was selected as the reference reactor. The analytical models agree very well with those of 2-D and 3-D CFD simulations in terms of time scales and the recirculation pattern in the lower plenum. Detailed 3-D calculations also confirm the VHTR air ingress accident, which is based on the density gradient-driven stratified flow.

The team also used CFD analyses to study heterogeneous chemical reaction effects and small break accidents. These analyses showed that the air ingress phenomena are dependent on break size, orientation, and density ratios. In most of the postulated break conditions, the air ingress was dominated by density gradient-driven flow. The results indicate that the density gradient-driven flow is important not only for double-ended guillotine breaks but also for small breaks.

Project Number: 2007-001-K

PI (U.S.): Chang H. Oh, Idaho National Laboratory

PI (ROK): Hee Cheon NO, KAIST

Collaborators: None

Program Area: Generation IV

Project Start Date: October 2007

Project End Date: October 2010

Finally, the team used CFD analyses to investigate patterns in post-onset natural circulation. The objective was to validate the 1-D natural circulation pattern assumed in previous air ingress studies. In this analysis, the 3-D CFD simulation showed very different flow configurations and predicted much faster air ingress speed than the previous 1-D simulations. This difference is due to the temperature gradient between the inside and outside of the reactor, which causes density gradient-driven flow.

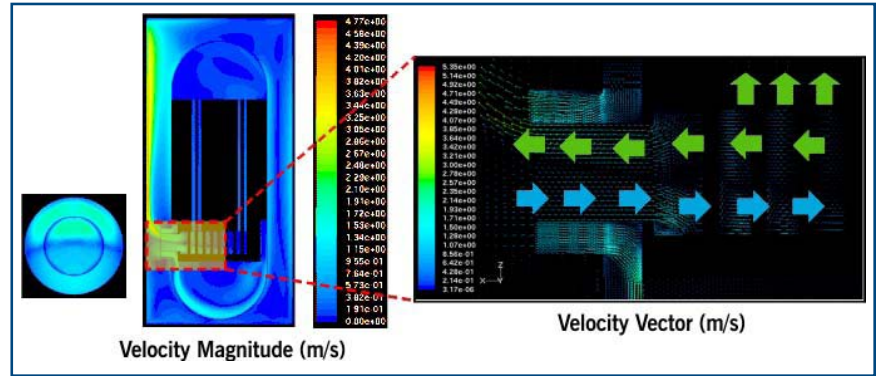


Figure 1. Recirculation pattern after onset natural circulation.

Task 1 results indicate that density gradient-driven flow is a major phenomenon that controls the air ingress process. Therefore, accurate air ingress analyses require multi-D simulations; 1-D modeling cannot represent the correct phenomena.

Task 2. Experimental study on the stratified flow. The project team reviewed previous studies on the density gradient-driven stratified flow and designed air ingress experiments. Researchers also collected previous experimental results and validated some CFD methods using the data.

In FY 2010, the team set up the experimental facility and obtained experimental data to understand stratified flow phenomena in the VHTR and to provide experimental data for validating computational methods. The experiment was focused on the stratified flow in the horizontal pipe and expansion at the pipe and vessel junction. Brine and sucrose were used as heavy fluids, and water was used as the light fluid. The density ratios varied between 0.99 and 0.7. The experiment shows clear stratified flow between heavy and light fluids, even for the low-density differences. The stratified flow experimental data based on the circular pipe was compared with the previous theoretical model based on the rectangular channel. Results are in good agreement with the experimental data within a ten percent deviation. Some blind CFD calculations were carried out for comparison with the experimental data. The simulation result shows very good agreement with the experimental data, indicating that the current CFD code and physical models are appropriate for predicting stratified flow phenomena.

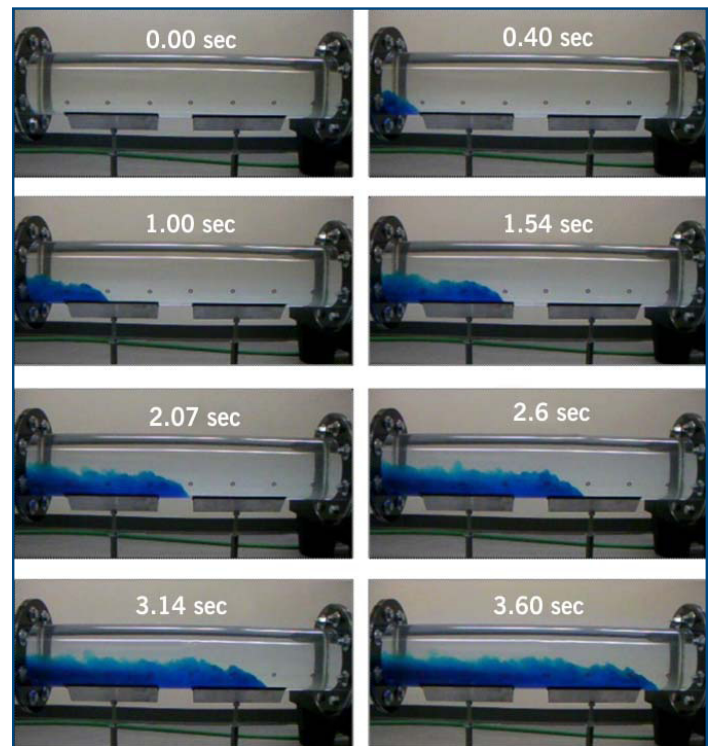


Figure 2. Stratified flow experiment.

Task 3. Advanced graphite oxidation study. Researchers investigated graphite oxidation characteristics in the air ingress accident, considering three main characteristics: (1) effect of oxidation degree on graphite strength, (2) effect of oxidized graphite density on oxidation rate, and (3) surface area density in graphite internal pores. An experimental methodology was developed to validate previous correlations related to oxidized graphite strength, which is essential for analysis of graphite structure fracture. Following the graphite experiment, the team estimated fracture of the graphite structure for the reference VHTR using two computer codes. They predicted graphite oxidation and corrosion using the GAMMA code (a system analysis code), and input this information into the ABAQUS code (a stress analysis code) to estimate fracture time. Further computations were performed using MATLAB to conservatively estimate the maximum allowable burn-off to maintain graphite structural integrity. Finally, the team constructed and implemented advanced graphite oxidation models and algorithms, including tools to study graphite corrosion and fracture, in the GAMMA code.

Task 4. Air ingress mitigation study. As a starting point for this study, the team used root-cause analyses to investigate important factors in air ingress consequences. Based on these analyses, the team developed basic ideas for mitigation methods and proposed some potential candidates. The following two were strongly recommended:

- **In-vessel helium injection in the lower plenum:** Helium is injected into the lower plenum, replacing air in the core and the upper part of the lower plenum by buoyancy force. CFD results show that this method significantly reduces graphite oxidation by reducing oxygen concentration and reaction temperature inside the reactor.
- **Reactor ex-vessel enclosure opened at the bottom:** Cavity design is modified to enclose the reactor in a non-pressure boundary. This enclosure has an opening at the bottom. After depressurization, the air ingress rate is controlled by molecular diffusion through this opening. The opening shifts the air ingress control mechanism from natural convection to molecular diffusion, which slows down air ingress.

The team used CFD methods to validate these air ingress mitigation methods. Results show that both methods effectively mitigate the air ingress process.

Task 5. Experiment on burn-off in the bottom reflector. The project team conducted experiments on nuclear-grade graphite (IG-110 and IG 430) to investigate oxidation characteristics in VHTR core supporting structures. This task was completed in FY 2008–2009.

Task 6. Structure test of burn-off bottom reflector. The team investigated graphite oxidation and mechanical behaviors for selected graphite materials (IG-110, IG-430, and NBG10). Results indicate that graphite mechanical fracture is mainly affected by slenderness ratio and oxidation burn-off. Results suggest the following two correlations for predicting graphite fracture in VHTRs:

$$\sigma_0 = A - B \frac{L}{r} \quad (1)$$

$$\frac{\sigma}{\sigma_0} = \exp(-kd), \quad d = 1 - \frac{M + \{(V_0 - V)\rho_0\}}{M_0} \quad (2)$$

This task also estimated allowable total burn-offs for IG-110, IG-430, and NBG-10 graphite, which can be used for conservative graphite fracture criteria. This estimate showed that the allowable burn-off is predicted when the reaction is dominated by internal pore reactions (f -value = 0).

This task also implemented graphite oxidation models into the GAMMA code and conducted various air ingress analyses using 1-D and 2-D modeling. These analyses showed that core maximum temperature is not affected by onset natural circulation or model type (1-D or 2-D). However, predications of bottom reflector temperature and oxidation patterns were significantly different between 1-D and 2-D modeling because of different flow patterns.

Task 7. Coupling neutronic-thermal hydraulic tools.

For realistic thermal-hydraulics analysis, researchers used COREDAX (a nodal diffusion code) to determine thermal power distributions in the reactor core, which were input into the GAMMA code. Thermal feedback from the GAMMA code affected the cross section, and these effects were reflected in the next COREDAX time-step neutronics calculation. This procedure was included in the coupled GAMMA/COREDAX code and tested on the GT-MHR-600 core with various transient situations.

Task 8. Core neutronic model. This task involved advanced neutronics code development based on the analytic function expansion method. This code provides accurate results compared with the well-known PARCS code. The team completed this task in FY 2008–2009.

Task 9. Coupled core model verification and validation. Homogenized cross sections of GT-MHR-600 assemblies were generated using MCNP calculations and tabulated for representative temperatures. From this data, cross-section values were interpolated for the required temperature and provided to the GAMMA/COREDAX code.

Using this code, the team analyzed an air ingress accident situation. The important parameters were calculated and compared with the results of GAMMA, which used a point kinetics method for power-generation feedback. The GAMMA code and the GAMMA/COREDAX code shows the fuel compact temperature progressing in different directions (see Figure 4).

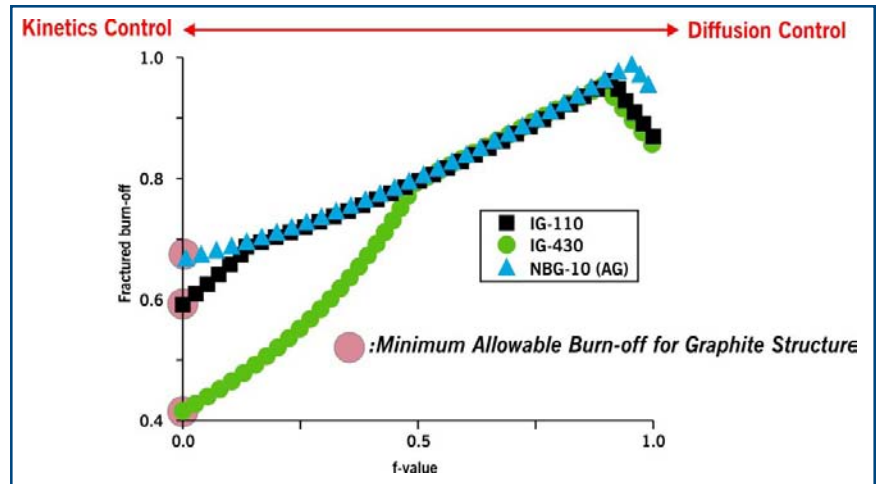


Figure 3. Allowable total burn-off for IG-110, IG-430, and NGB-10.

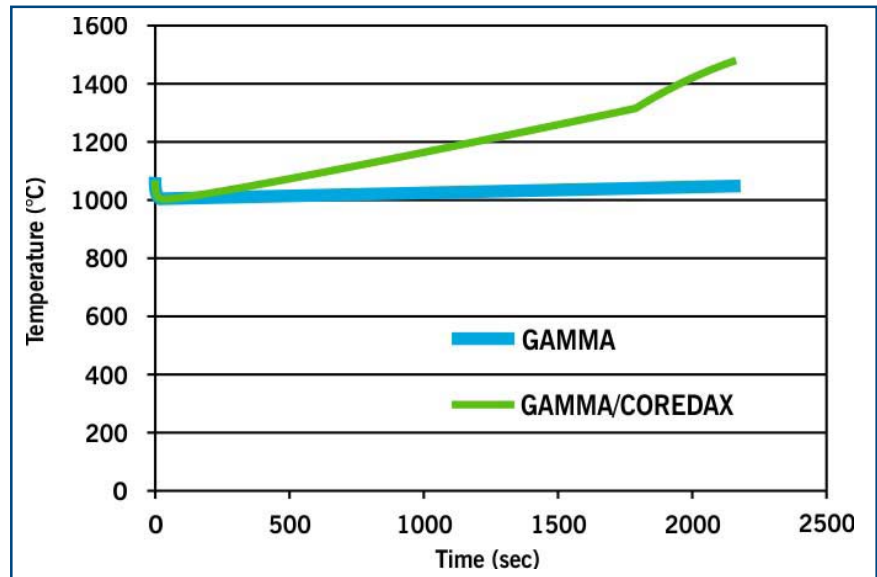


Figure 4. Comparisons of fuel compact temperature.

Planned Activities

FY 2010 was the final year of this project.

Development of Advanced Voloxidation Process for Treatment of Spent Fuel

Research Objectives

This research project addressed advanced voloxidation for the head-end treatment of used nuclear fuel undergoing pyroprocessing. Advanced voloxidation involves oxidizing uranium oxide fuel at high temperature using either air or oxygen, and provides three important advantages as a head-end step for pyrochemical treatment processes of used nuclear fuel. First, it may be used to separate the fuel from the cladding, which would simplify process flow sheets by excluding the cladding constituents from the fuel constituents. Second, advanced voloxidation can supply the electro-reduction process with granule-type fuel particles as a result of high-temperature agglomeration, which may increase the efficiencies of the downstream electro-reduction process. Third, advanced voloxidation can remove problematic constituents from the fuel prior to the downstream pyroprocesses. Gaseous fission products such as cesium, krypton, xenon, technetium, iodine, carbon, and tritium (^3H) may be removed prior to the electro-reduction process, thus simplifying the process flow sheets and yielding more efficient waste treatment operations.

The objective of this work was to develop an advanced voloxidation process that provides a means to recover fuel from the cladding, to prepare fuel for subsequent processing, to simplify downstream processes by removing volatile fission products prior to pyroprocessing, and to safely trap volatile fission products. The work focused on three areas:

- Evaluating the effects of advanced voloxidation on pyroprocessing of used oxide fuel with a determination of a path forward.
- Optimizing off-gas trapping capabilities for fission products with respect to pyroprocessing.
- Developing operational parameters for advanced voloxidation with respect to pyroprocessing.

Research Progress

The project team evaluated the effects of advanced voloxidation on pyroprocessing, considering four representative cases:

- Case 1: chopping and no voloxidation
- Case 2: chopping and low-temperature voloxidation at 500°C

Project Number: 2007-002-K

PI (U.S): B. R. Westphal, Idaho National Laboratory

PI (ROK): J. J. Park, Korea Atomic Energy Research Institute

Collaborators: None

Program Area: FCR&D

Project Start Date: November 2007

Project End Date: October 2010

- Case 3: low-temperature voloxidation taken to 1200°C (advanced voloxidation)
- Case 4: a hybrid of mechanical decladding followed by low-temperature voloxidation

Researchers evaluated these cases against ten criteria, including oxide reduction processing rate, product characteristics (e.g., particle size, density), and interference of cladding in following process steps. Case 3, advanced voloxidation, received the highest grade among the four.

In order to evaluate operational parameters of an advanced voloxidation process, the team used thermodynamic data to investigate oxidation and vaporization behaviors of noble and low-melting-point metals and cesium compounds in terms of thermal treatment atmosphere and temperature. A thermal treatment condition was described for 99% volatilization of metals and cesium compounds. Also, an oxidation and vaporization experiment of noble metal fission products was performed using thermogravimetric analyses and surrogate materials. The test confirmed that most of the molybdenum and ruthenium can be volatilized during the advanced voloxidation process.

To develop granulation operations with surrogate materials, the project designed and manufactured two rotary voloxidizers. The first, with a single roller, exhibited low operational efficiency. The second (Figure 1) was designed with two rollers, allowing higher efficiencies and improved control of particle size. Granules larger than 1 mm were successfully manufactured from U_3O_8 powder by heating the second rotary voloxidizer to 1150°C for 5 hours (see Figure 2). An electro-reduction test was also performed on the U_3O_8 granules wherein the granule shape was retained (Figure 3) and the reduction ratio of uranium was over 99%.

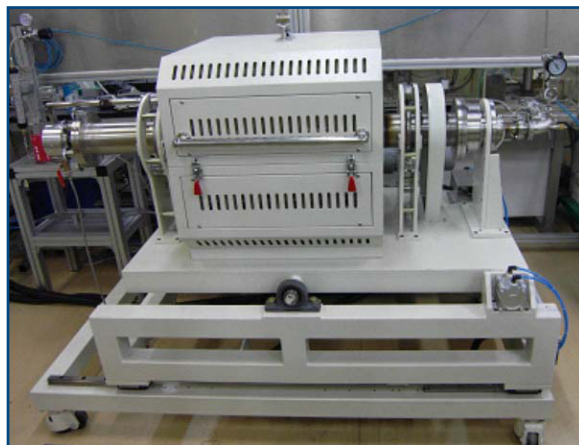


Figure 1. Second rotary voloxidizer.



Figure 2. Photograph of U_3O_8 granules.

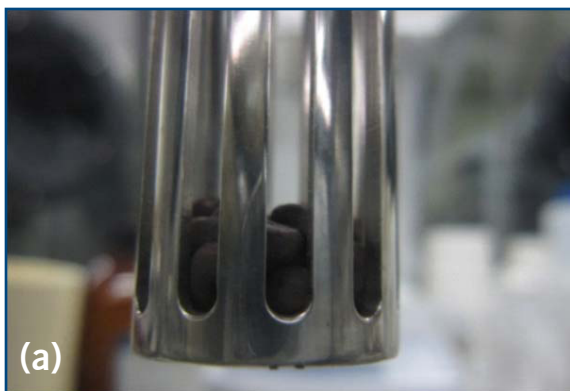


Figure 3. U_3O_8 granules (a) before and (b) after electro-reduction testing.

Based on test results, the project team suggested operating conditions for the advanced voloxidation process, consisting of four process steps:

- Oxidation of UO_2 pellets
- Oxidation of noble metals
- Granulation of U_3O_8 powder
- Reduction of U_3O_8 granules to UO_2 granules

The project team performed inactive cesium trapping experiments on fly ash filters with increasing cesium volatilization quantity (Figure 4). Fly ash filters were durable up to a cesium trapping quantity of 1.4 g-Cs/g-filter. The fly ash filter (70 g) can trap up to ~44 g Cs, equivalent to 12 kg of spent fuel for a pressurized water reactor with a burnup of 45 GWD/MTU. The process successfully trapped inactive molybdenum, tellurium, and mixed species (molybdenum, tellurium, rhenium, antimony) by using a Ca-II filter under a vacuum of 7.6 torr. This filter may also be suitable for trapping elements in gaseous states.

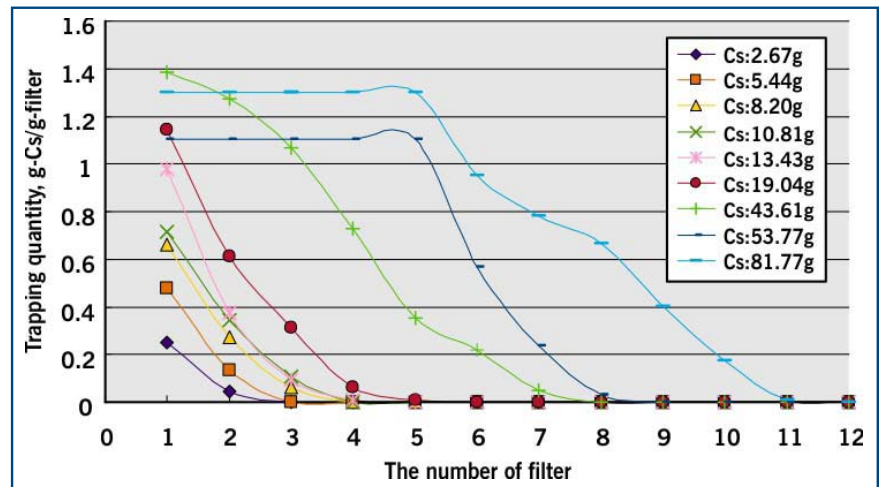


Figure 4. Cesium trapping on fly ash filters with increasing cesium volatilization quantity.

The project team also conducted multiple experiments with radioactive materials in the Hot Fuel Examination Facility to investigate cladding removal, particle size optimization, and off-gas removal/collection with both used mixed oxide (MOX) and light water reactor (LWR) fuels. Three experiments were performed with high burnup MOX fuel from the Experimental Breeder Reactor-II (EBR-II); researchers were investigating oxidation and decladding characteristics while removing and collecting volatile fission products. Successful oxidation and decladding of irradiated MOX fuel was achieved by utilizing a temperature of 600°C for three hours under an oxygen atmosphere. The team also conducted five experiments with irradiated LWR oxide fuel and investigated development of optimal operating conditions for off-gas trapping and particle size control. The project team recognized that fuel handling and sieving affect the determination of true particle size following testing. However, minimizing handling operations resulted in larger particles under static conditions. The formation of a cesium pertechnetate species made the separation of cesium from tellurium on redesigned filters challenging to date. Iodine, on the other hand, was nearly completely removed and collected by the filter media tested.

Planned Activities

This project is complete. However, principal investigators have agreed to pursue joint research on the development of rotary voloxidation technology in FY 2011.

Performance Evaluation of TRU-Bearing Metal Fuel for Sodium Fast Reactors to Achieve High Burnup Goal

Project Number: 2007-003-K

Research Objectives

The objective of this project was to evaluate the high burnup performance of transuranic (TRU)-bearing metal fuel for sodium fast reactors (SFRs). Specific activities included:

- Benchmarking a performance analysis code against test data from Advanced Fuel Cycle test series-1 (AFC-1) and developing suitable models for this analysis, enabling researchers to analyze the fuel's complicated irradiation behavior.
- Fabricating barrier-cladding materials and tubes to address fuel/cladding chemical interaction, as this interaction may limit alloy fuel burnup.
- Conducting diffusion couple testing of metal fuel against barrier cladding to determine whether barrier-cladding material increases fuel burnup performance.

PI (U.S.): J. Rory Kennedy, Idaho National Laboratory

PI (ROK.): Byoung-Oon Lee, Korea Atomic Energy Research Institute

Collaborators: None

Program Area: FCR&D

Project Start Date: November 2007

Project End Date: October 2010

Research Progress

Task 1: Benchmarking of fuel performance codes. The project team jointly decided what part of the fuel performance model to upgrade. Using the AFC-1 technical report, researchers developed a model for helium gas release behavior. AFC-1 fuels contain minor amounts of americium (Am) and neptunium (Np). Neutron capture by ^{241}Am produces helium gas in AFC-1 metallic fuel. This gas is released into the fission gas plenum, so the helium adds to the total gas inventory. Thus, the release of helium gas during ^{241}Am transmutation should be considered in fuel design.

Earlier in this project, researchers experimentally determined the helium generation rate. In the FY 2010 study, this figure was inserted into the FGR routine of the MACSIS code. A helium gas release model was also developed and inserted into the MACSIS code.

Figure 1 presents helium and fission gas release resulting from radiating metallic rodlets in AFC-1 test capsules B and F. The helium release follows the same trend as fission gas release but at a somewhat lower rate (0–15% for helium versus 0–36% for fission gas).

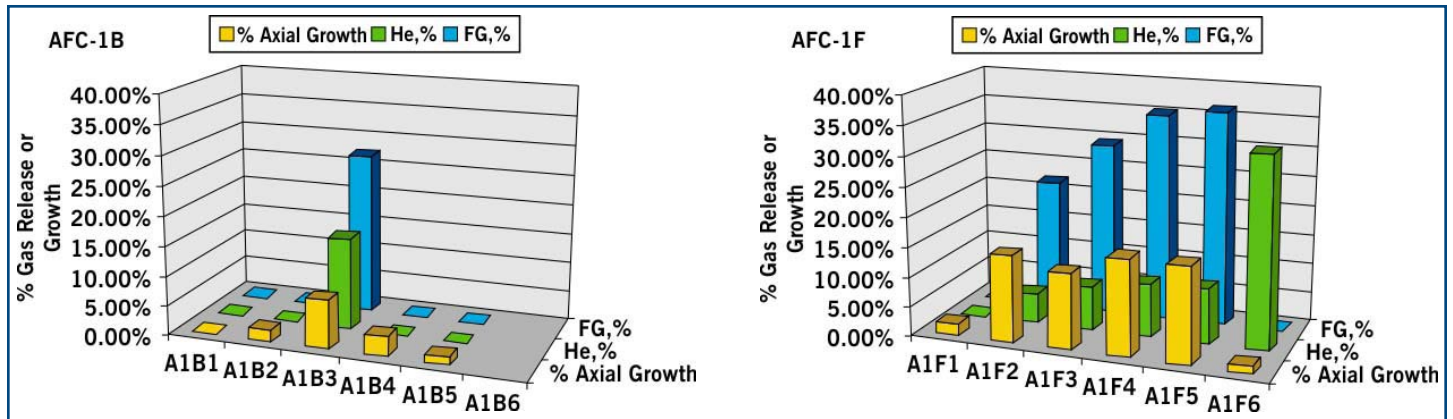


Figure 1. Helium release and fission gas release from metallic alloy transmutation fuel rodlets irradiated in the (a) AFC-1B and (b) AFC-1F capsules.

Using this project’s method to calculate helium release, the project team compared the resulting theoretical amounts with measured release data. The experimental results indicate an incubation period followed by helium gas release that increases with burnup above the burnup threshold of nearly $6E20$ f/cm³.

Task 2: Fabrication of cladding barrier. The research team fabricated coated samples for eight candidate barrier types. Based on FY 2009 project findings, the team produced thicker coatings to enhance barrier performance. Researchers investigated the effect of the nitride morphology and introduced new coating methods, such as cathodic arc ion plating (CAIP). Table 1 provides details of the barrier coating fabrication processed.

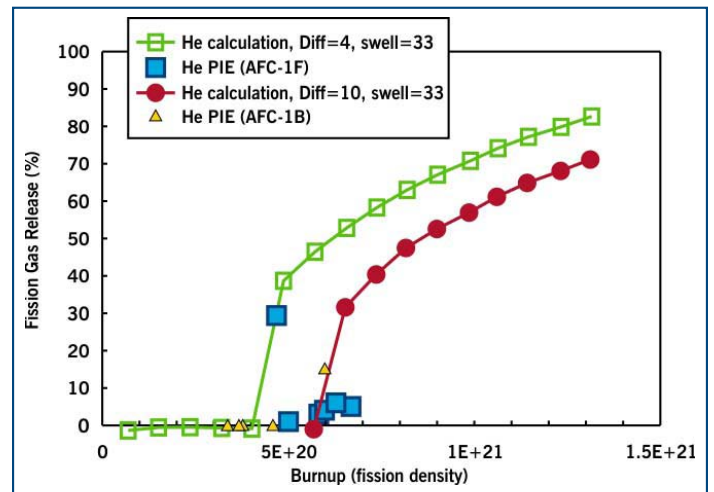


Figure 2. Measured release data versus calculated results.

Table 1. Conditions for barrier fabrication.

Specimen	Zr	V	ZrN _x	VN _x	TiN	CrN
Deposition Condition	RF (Radio Frequency) Sputtering	RF Sputtering	RF Sputtering	RF Sputtering	CAIP	CAIP
Target Material	Zr	V	Zr	V	Ti	Cr
Deposition Power	100W (RF power)	100W (RF power)	100W (RF power)	100W (RF power)	100W 6A/in ²	100W 6A/in ²
Coating Environment	Ar	Ar	Ar:N ₂ (4:1)	Ar:N ₂ (4:1)	N ₂	N ₂
Bias Voltage	–	–	–	–	-50V	-50V
Nominal Thickness	3.8μm	5.2μm	5μm	4μm	12μm	30μm

The project team fabricated cladding tubes from ASTM A182F92, a ferritic-martensitic steel. Each tube had an outside diameter of 5.5 mm, inside diameter of 4.6 mm, and length of 170 mm, electroplated on the inner surface with chromium. Lead wire acted as an anode, and Sargent solution (250 g/l of CrO₃ and 2.5 g/l of H₂SO₄) flowed continuously through the tube. Plating was performed at 24.4 A/dm² for one hour at 80°C. After plating, microstructural observation revealed that a

chromium layer of approximately 20 microns uniformly covered the cladding tube’s entire inner surface. The team conducted a feasibility study on using metal organic chemical vapor deposition to generate a zirconium layer. Researchers effectively coated a disk sample and evaluated the disk coupon’s performance. Finding positive results, they were initiating fabrication of a tube specimen at the writing of this report.

Task 3: Diffusion testing of metal fuel against cladding barrier coatings. Following the diffusion couple testing of TRU metal fuel and rare earth material, the team ranked the performance of the barrier coating candidates. Table 2 summarizes the results. Red indicates that the barrier reacted during the test, resulting in an associated eutectic reaction between the fuel and the clad material. Yellow indicates that although eutectic reaction was prevented, the barrier was degraded through dissolution or cracking after the test. Green indicates that the barrier coating prevented any eutectic reaction or interdiffusion and remained intact after the test. Three barriers exhibited good performance regardless of the TRU metal fuel and rare earth element: vanadium (V) fabricated by physical vapor deposition (PVD) and titanium nitride (TiN) and chrome nitride (CrN) deposited by CAIP.

Table 2. Performance of the cladding barrier coating materials.

Diffusion Couple Test		Metal (PVD, ED for Cr)	Uniform Nitride (PVD)	Gradient Nitride (PVD)	Uniform Nitride (CAIP)
Zr	U-Pu-Zr	Barrier reacts Zr-rich phase	Barrier reacts Zr-rich phase	Barrier reacts Zr-rich phase	
	Ce-La	(Fe, Cr) _x Ce _y eutectic formation	(Fe, Cr) _x Ce _y eutectic formation	(Fe, Cr) _x Ce _y eutectic formation	
	Nd	Barrier intact eutectic prevention	Barrier intact eutectic prevention	Barrier intact eutectic prevention	
V	U-Pu-Zr	Barrier intact eutectic prevention	Cracked barrier eutectic prevention	Cracked barrier eutectic prevention	
	Ce-La	Barrier intact eutectic prevention	Partial dissolution	(Fe, Cr) _x Ce _y eutectic formation	
	Nd	Barrier intact eutectic prevention	Partial dissolution	Barrier intact eutectic prevention	
Ti	U-Pu-Zr				Barrier intact eutectic prevention
	Ce-La				Barrier intact eutectic prevention
	Nd				Barrier intact eutectic prevention
Cr	U-Pu-Zr	Eutectic prevention crack prevention			Barrier intact eutectic prevention
	Ce-La	Barrier intact crack prevention			Barrier intact eutectic prevention
	Nd	Barrier intact crack prevention			Barrier intact eutectic prevention

Planned Activities

This project is complete.

Development and Characterization of New High-Level Waste Forms for Achieving Waste Minimization from Pyroprocessing

Research Objectives

The objective of this project is to develop new high-level waste (HLW) forms and fabrication processes to dispose of active metal fission products that are chemically removed from electrorefiner salts in the pyroprocessing-based fuel cycle. The current technology for disposing of these byproducts involves non-selectively discarding fission-product-loaded salt in a glass-bonded sodalite ceramic waste form (CWF). Selective removal of fission products from the molten salt would minimize the volume of HLW generated. Novel methods, including chemical precipitation, are currently being developed to achieve selective separation of fission products, but an investigation has yet to be performed regarding suitable waste forms for the separated fission products. The precipitates formed are expected to be oxides, sulfates, and/or phosphates that would be incompatible with the sodalite CWF. Thus, a completely novel approach to waste form fabrication is required.

Project Number: 2007-004-K

PI (U.S.): Steven M. Frank, Idaho National Laboratory

PI (ROK.): Yung-Zun Cho, Korea Atomic Energy Research Institute

Collaborators: None

Program Area: FCR&D

Project Start Date: November 2008

Project End Date: October 2011

Research Progress

During the project's first year, researchers established an immobilization method for waste salt and rare earth oxide waste. They investigated the chemical behavior of metal chlorides and the leach resistance of a waste form prototype, using the findings to select possible material systems.

In the past year, the research team adjusted the basic material systems to enhance reactivity and increase waste loading. They also performed a series of consolidation tests to obtain some characteristics of unique waste forms. The results informed a scheme for the waste form immobilization process, which will be established in the project's final year.

Researchers used a series of silicon-aluminum-phosphate (SAP) compositions to perform the dechlorination tests. The LiCl-KCl waste exhibited two distinct dechlorination temperature ranges with midpoints of about 400°C and 700°C (Figure 1). Iodine, as a radionuclide with a long half-life, is vaporized at temperatures below 450°C. Dechlorination yields for 10 hours were 7% at 350°C, 53% at 450°C, 62% at 550°C, and 100% at 650°C. Also, adding Fe₂O₃ to a basic material system (SiO₂-Al₂O₃-P₂O₅-Fe₂O₃, SAP-Fe) enhanced the reactivity between SAP and waste salt, resulting in a high reaction ratio; the SAP-to-salt ratio changed from 3:1 for SAP 1071 to 2:1 for SAP-Fe.

To obtain waste form characteristics for the consolidation tests, researchers varied the waste form's glass composition, glass content, and consolidation temperature. The simulated waste was 89 weight-percent (wt%) LiCl-KCl, 5 wt% CsCl, 5 wt% SrCl₂, and 1 wt% CsI. Researchers determined microstructure, morphology, and leach resistance using x-ray diffraction (XRD), field emission scanning electron microscopy (FE-SEM) and a product consistency test—Method A (PCT-A). When using a silicate glass to consolidate products consisting of silicate and phosphate compounds, a processing temperature above 1050°C was required to obtain appropriate densification. Weight loss (vaporization) was found to be negligible during consolidation at the given temperatures.

SEM analysis indicated that the waste form has a silicon-rich phase and a phosphate-rich phase, but the two phases were not clearly distinct. The analysis showed 10-nm grains attributable to the incompatibility between the silicate and phosphate phases. The grain size indicates phase separation—that is, two phases uniformly distributed in the matrix. The team conducted PCT-A using 20 consolidated samples, obtaining each element's normalized mass loss range (see Figure 2). The test showed a loss of approximately 10⁻²–10⁻³ g/m² for the target radionuclides (Cs/Sr) and 10⁻¹–10⁻³ g/m² for the waste form's main components. Under the given conditions, the glass content and composition did not greatly affect the leach resistance, but increasing the processing temperature slightly enhanced the waste form's durability. In summary, the waste salt was effectively stabilized and solidified in the matrix.

For rare earth oxide waste, a zinc oxide/titanium oxide (ZIT) material composition (ZnO-TiO₂-P₂O₅-SiO₂-B₂O₃-CaO) was changed to increase waste loadings, based on the low heat generation of lanthanide fission products. Researchers fabricated a series of consolidated forms at 1100°C. PCT-A indicated the leaching concentration was below the detection limits of inductively coupled plasma mass spectrometry (ICP-MS) (below 10 parts per billion). The main leachant components were Ca and B.

The project team down selected three candidate waste forms for remote fabrication in Idaho National Laboratory's Hot Fuels Examination Facility (HFEF). The starting material used for fission product immobilization was ER salt that contained

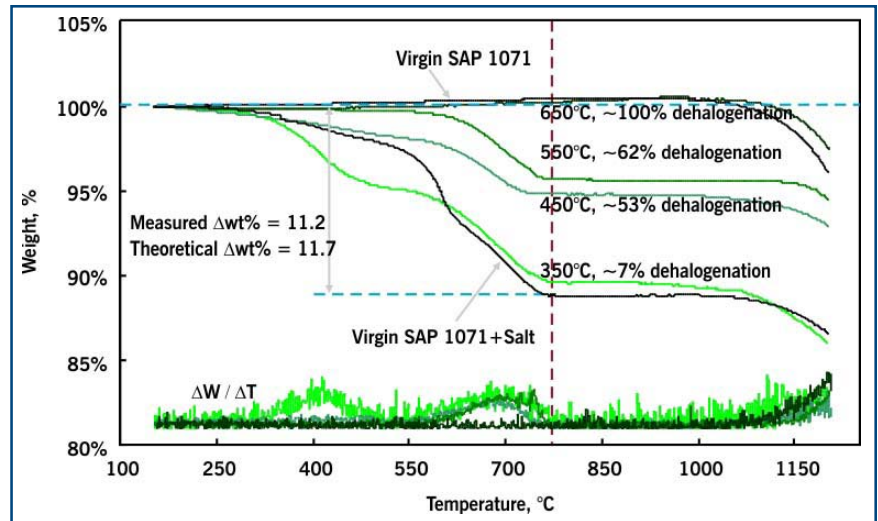


Figure 1. Thermogravimetric analysis of products after dechlorination at four temperatures.

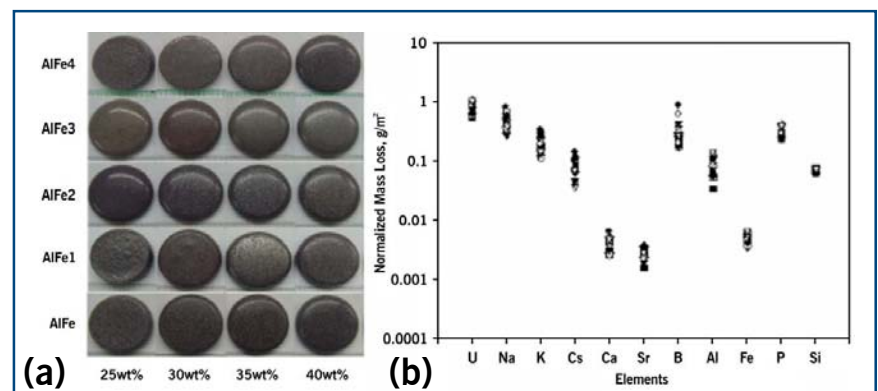


Figure 2. (a) Photograph of a consolidated form prepared at 1050°C by changing glass composition/content, and (b) normalized mass loss of each element by PCT-A test.

actinide chlorides at approximately 5 wt% and surrogate rare earth chloride fission products at approximately 15 wt%. The team demonstrated a chemical reduction method to reduce the ER salt's actinide content to low concentrations. After removing the reduced actinides from the ER salt, researchers performed an oxygen sparging method that reacted with the rare earth elements (REEs) to form precipitates of the REE oxide or oxychlorides. A portion of the ER salt containing the REE precipitates was used to produce the candidate waste forms.

The three candidate waste forms, as described earlier, are a silica-alumina-phosphate/glass (SAP) material, a ZIT material, and a high-loaded CWF composed of glass bonded sodalite. Production of the CWF involved occluding a portion of the ER salt/precipitate mixture into a zeolite matrix; then a glass binder was mixed in and heated to produce a densified ceramic body. The SAP waste form is produced by first dechlorinating the ER salt/precipitate mixture by mixing it with the SAP reagent and allowing the mixture to react in an oxygenated atmosphere at elevated temperature. The reaction product is then solidified into a glass matrix. Dechlorination of the ZIT waste form is accomplished by distilling the ER salt off the REE precipitate. The oxide and oxychloride precipitate is then added to the ZIT reagent and processed at high temperature. The resulting waste form immobilizes the fission product precipitates in a monazite-like matrix. After production, the project team will characterize and test these materials and compare them to other HLW forms.

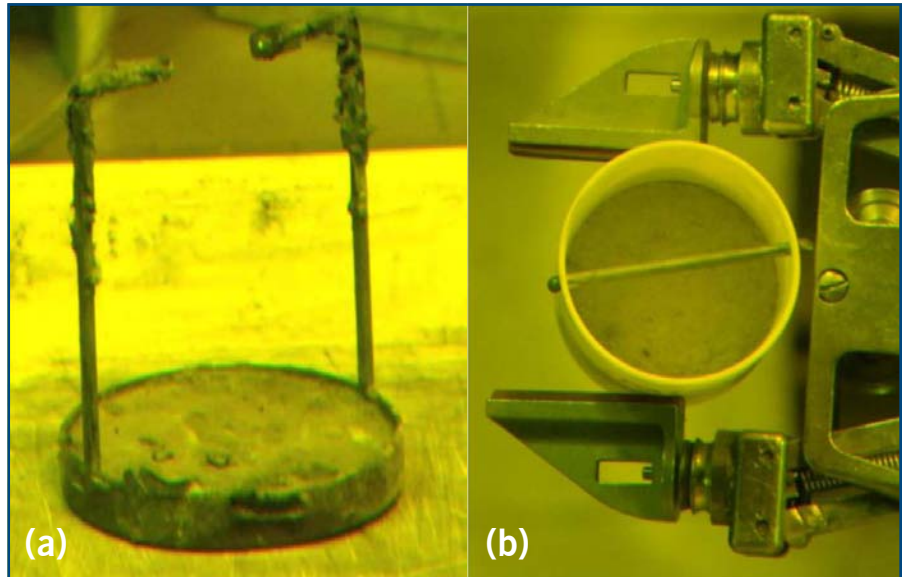


Figure 3. (a) High-fission-product-loaded ER salt used to fabricate in-cell waste forms. (b) High-loaded CWF produced in HFEF in 2010.

Planned Activities

During the final year, the project team will complete fabrication of the SAP and ZIT candidate waste forms in HFEF. The team will prepare samples in the newly renovated sample preparation area in HFEF's main cell. Researchers will then begin characterizing and testing these materials using the following methods:

- Chemical analysis of dissolved samples
- Density measurement
- XRD
- SEM
- Leach/corrosion testing (PCT)

Extensive investigation will determine the waste forms' physical and chemical properties and their chemical durability.

Development of Computational Models for Pyrochemical Electrorefiners of Nuclear Waste Transmutation Systems

Project Number: 2007-006-K

PI (U.S.): Michael F. Simpson, Idaho National Laboratory

PI (ROK): K. R. Kim, Korea Atomic Energy Research Institute

Collaborators: Seoul National University, University of Idaho

Program Area: FCR&D

Project Start Date: November 2007

Project End Date: September 2010

Research Objectives

This project supports closing the nuclear fuel cycle using non-aqueous separations technology. The research team aimed to develop computational models of electrorefiners based on fundamental chemical and physical processes. Electrorefining is a critical component of pyroprocessing, a non-aqueous chemical process which separates spent fuel into four streams:

- Uranium metal
- Uranium/transuranic metal
- Metallic high-level waste containing cladding hulls and noble metal fission products
- Ceramic high-level waste containing sodium and active metal fission products

Having rigorous yet flexible electrorefiner models will facilitate process optimization and assist in troubleshooting as necessary. To attain such models, the project team has worked on approaches to develop both a computationally light and portable two-dimensional (2-D) model and a computationally intensive three-dimensional (3-D) model for detailed and fine-tuned simulation.

Research Summary

Data compilation. Project researchers have been treating spent fuel from the Experimental Breeder Reactor-II (EBR-II) using engineering-scale electrorefiners (Mk-IV and Mk-V) in Idaho National Laboratory's Fuel Conditioning Facility. The research team selected the Mk-IV electrorefiner (see Figure 1) for modeling because of the relative simplicity of its spatial geometry, the vast amount of Mk-IV data available, and accumulated operational experience. For the model reference case, the team selected one of the repeatability runs performed for the EBR-II Spent Fuel Treatment demonstration.

Participating organizations also actively identified and gathered data regarding relevant thermodynamic, physical, and electrochemical properties. Some basic electrochemical properties such as U^{3+}/U couple exchange current density are not readily available in open literature, so the project team arranged experimental projects measuring the exchange current densities, charge transfer coefficients, and diffusion coefficients. Researchers applied a linear polarization resistance technique to measure U^{3+}/U couple exchange current density and charge transfer coefficients in a LiCl-KCl eutectic mixture at 500°C. In addition, the diffusion coefficient of U^{3+} in the molten salt at 500°C was measured via chronopotentiometry (CP) on a tungsten electrode.

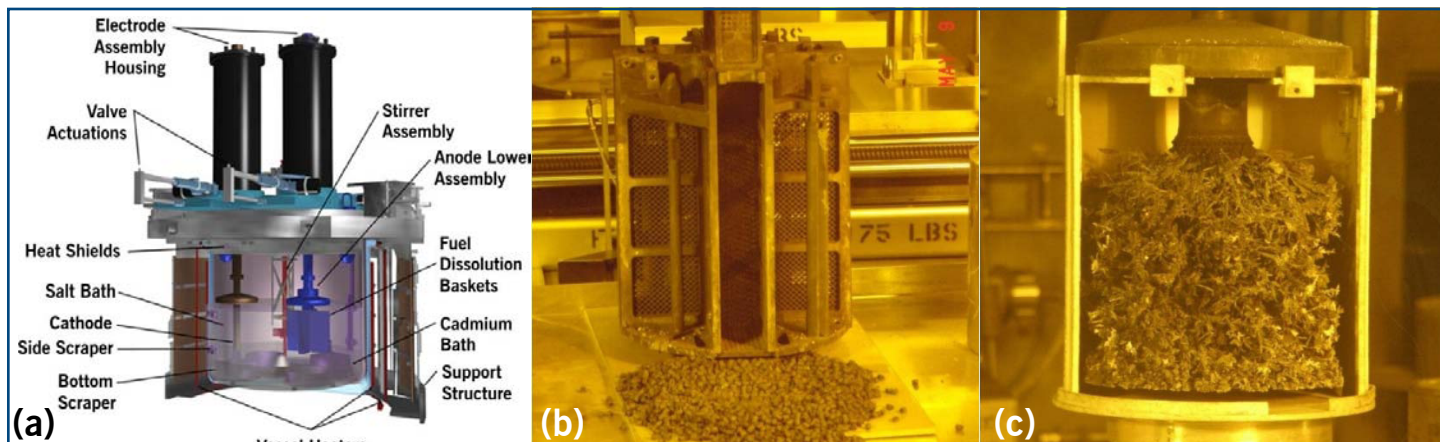


Figure 1. (a) Mk-IV electrorefiner, (b) the anode, and (c) the cathode.

2-D model development. The project team decided to use a general scientific programming language, MatLab, as a development platform. The primary reason for selecting this software tool is flexibility in dealing with time-varying anode and cathode surface electrochemistry, molten salt electrolyte flow, and electric potential distribution in the electrolyte within a single application environment.

The team developed a 1-D model of the Mk-IV electrorefiner. The computations modeled spent nuclear fuel dissolution at the anode taking into account only uranium (U^{3+}), plutonium (Pu^{3+}), and zirconium (Zr^{4+}). Uranium and plutonium are the two elements of highest importance in the system, while zirconium is the most active of the noble metals and is present in the highest concentration (nominally 10% of the fuel mass). Results from the modeling process reveal plutonium is rapidly exhausted from the anode fuel baskets. Throughout the remainder of the electrorefining process, uranium is the main species being both dissolved from the anode and deposited on the cathode. As time progresses, however, zirconium dissolution and deposition start to become important processes. The anodic surface area calculations involved individual exposed surface areas for each species as well as models of the changing surface area as a function of fuel porosity. The total anode potential as calculated by the model has been compared to experimental data sets. The researchers developed an optimization routine for describing anodic oxidization behaviors, and they applied it to the reduction reactions occurring at the electrorefiner cathode within the electrochemical processing of used nuclear fuel.

The team also examined 2-D potential and current distributions within the bulk electrolyte of the Mk-IV electrorefiner. The potential distributions showed that the highest potential gradients exist directly between the anodes and cathode. In general, the uranium, plutonium, and total potential gradients increase throughout the process, while zirconium potential gradients decrease. The result shows that as the electrorefining progresses, more zirconium and less uranium and plutonium are being electrotransported.

3-D model development. In view of the spatial characteristics provided, operational data from the Mk-IV electrorefiner, and model requirements, the research team decided to use a combination of applications weighing on flexibility, long-term sustainability, and upgradeability. The application selected for electrochemistry computation was REFIN-1D, a proprietary code maintained in the FORTRAN language at the NUTRECK of Seoul National University. A commercial software package (ANSYS-CFX) was used to deal with three-dimensional characteristics of molten salt flow and electric potential distribution.

To examine surface electrochemical behaviors, the team developed REFIN code for a one-dimensional time-dependent electrokinetic model. Resulting REFIN predictions showed good agreement with the Mk-IV repeatability test data. ANSYS-CFX was selected to address electrolyte fluid dynamics. In the simulation, the finite volume method was used to solve the conservation equations of mass, momentum, and energy. The concentration boundary layers near the electrode surfaces were effectively calculated from the CFX solver near the anode and cathode surfaces. The prescribed computations gave the diffusion

layer thicknesses effectively and showed that heterogeneous diffusion boundary layers exist owing to the flows incurred by various stirring devices such as the cadmium stirrer and the rotating cathode. The current density distribution patterns were analyzed with respect to various rotating electrode speeds and applied current patterns. The results showed good agreement with the general observations of the electrorefining process.

While using a growing cylinder to model the effective cathode surface area profile, researchers considered five effective anode surface area profiles. Root Mean Square Deviation (RMSD) evaluation revealed that the anode surface area profile with the square root retraction rate gives the best-fitting result among the considered cases.

Alternative validation approaches. To further aid model development and validation, researchers performed experiments on a rotating cylinder hull (RCH) cell with an aqueous electrolyte (see Figure 2). They modeled the RCH cell using both the 2-D and 3-D models. The deposition behavior of uranium to a rotating cathode shares much commonality with the metal (e.g., copper) deposition behavior of the aqueous RCH cell. The aqueous RCH cell enabled examination of a wide range of electrochemical behaviors. The team used the cell to validate the developed models for the molten salt electrorefining system indirectly without needing additional electrorefiner process data. The models calculated the potential and current distributions throughout the cell. The general trends reveal excellent agreement between the models throughout the considered operating conditions, reinforcing the validity of both modeling approaches. Measured potentials also agreed well with the model predictions.

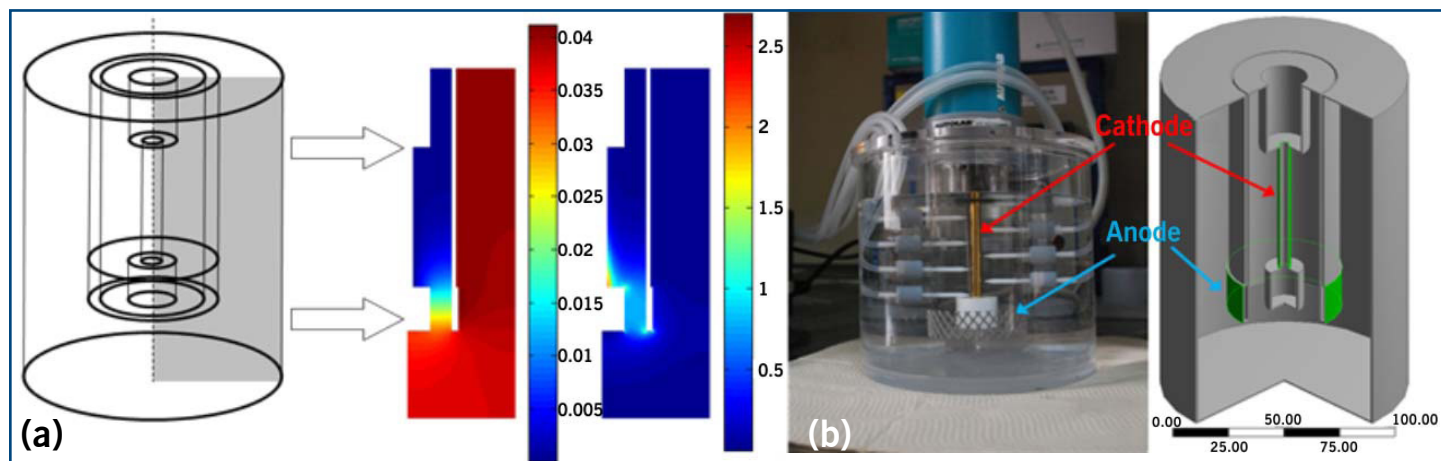


Figure 2. (a) Aqueous RCH cell equipment and (b) the associated model.

In addition to the RCH experiment and modeling comparison, detailed conditions and parameters for a second Mk-IV electrorefiner experiment were compiled and distributed to the participants. Both U.S. and ROK researchers simulated the results of the experiment using their respective models. This allowed for both cross-validation of the models and comparisons to experimental data. The second experiment was similar to the first in terms of the fuel composition, fuel chopping length, and anode/cathode configuration. However, the current profile of the second test was distinct from the previous one. Not all results were available at the time of the writing of this summary, but the model predictions thus far have matched the data quite closely.

Results. This and previous model validation activities showed that the models satisfactorily capture the electrorefining process's key characteristics. The team considers the project models to be good tools for process analysis, optimization, and design.

Planned Activities

This project is complete.

Sodium-Cooled Fast Reactor Structural Design for High Temperatures and Long Core Lifetimes/Refueling Intervals

Research Objectives

The research objectives of this project were to develop new state-of-the-art design analysis capabilities for high-temperature structural design of sodium-cooled fast reactors (SFRs). Through this collaboration, four key design analysis capabilities were developed and applied to SFR pre-conceptual designs:

- Material selection for potential SFR services
- Design loads and load history generations
- Simplified elastic and detailed inelastic structural design
- Seismic and buckling instability evaluations

Research in the final project year focused on the fourth task—developing seismic technologies for SFRs subject to elevated temperatures, enhancing structural design to protect components from long-term thermal creep damage.

Research Progress

The project team carried out six subtasks in FY 2010:

- Development of a seismic analysis model for an advanced burner test reactor (ABTR)
- Seismic time history response analyses
- Seismic integrity evaluations for the reactor vessel
- Buckling instability evaluations for the reactor vessel
- Seismic integrity evaluations for reactor internals
- Seismic integrity evaluations for intermediate heat transport system (IHTS) piping

A brief summary of these tasks follows.

Development of a seismic analysis model for the ABTR. The project team established seismic analysis modeling technology for a SFR—specifically, the pre-conceptual design for the ABTR. This model is to be used for a seismic time history response analysis. Therefore, the team constructed stick models for the reactor building, reactor vessel, reactor internals, upper internal

Project Number: 2007-007-K

PI (U.S.): James J. Sienicki, Argonne National Laboratory

PI (Euratom): Gyeong-Hoi Koo, Korea Atomic Energy Research Institute

Collaborators: None

Program Area: FCR&D

Project Start Date: November 2007

Project End Date: November 2010

structure, core support structure, core assemblies, intermediate heat exchangers, primary pumps and inlet pipes, reactor head, and seismic isolation devices. The completed model comprises 40 nodes and 33 elements.

A key finding is the effect of fluid-added mass on the dynamic characteristics of reactor structures and components submerged in the primary sodium coolant. The project team developed key technologies using a detailed finite element analysis technology with a specific KAERI-developed fluid-added mass and damping (FAMD) computer code.

The modal frequency analyses showed that the dynamic characteristics of a reactor vessel are significantly coupled with the reactor internals, core assemblies, and components through core support structure connected to the reactor vessel bottom head. The fluid-added masses invoked by the fluid gaps between structures result in significantly lower natural frequencies.

Seismic time history response analyses. Two horizontal seismic design loads—the artificially generated Operating Basis Earthquake (OBE), 0.15 g, and the Safe Shutdown Earthquake (SSE), 0.3 g—served to calculate the seismic response of safety-related nuclear structures. The vertical SSE load is 0.2 g. These input motions have enough peaks in synthetic acceleration time histories to meet research needs. The scenarios also meet NRC Regulatory Guide 1.60 criteria for seismic design spectra.

The results show that, for the SSE, most relative horizontal seismic displacements are less than 10 mm, confirming adequacy for that aspect of the functional design. However, horizontal relative deflections between the reactor building and the basemat are as high as 217 mm for the OBE and 400 mm for the SSE. The latter exceeds the specified ABTR seismic deflection limits of 300 mm. The high value is mainly due to a three-second seismic isolation period of only 0.333 hertz (Hz). The design utilizes the multiple friction pendulum system for seismic isolation. Therefore, the seismic isolation frequency should be increased to more than 0.5 Hz.

Using the results of these analyses, the project team calculated floor response spectra at various locations for seismic isolation and non-isolation designs. The spectra were defined in accordance with ASCE standards for nuclear structures.

Seismic integrity evaluations for the reactor vessel. The project team established a procedure using spectrum analysis to evaluate the reactor vessel's seismic integrity. The researchers performed the evaluations using a detailed 3-D finite element analysis model. Since the spectrum analysis is based on the modal analysis, the finite element model had the equivalent dynamic characteristics.

The results showed that the ABTR reactor vessel satisfies ASME acceptance criteria for SSE D-level service. The seismic margins were calculated at 1088% for the seismic isolation design and 510% for the non-seismic isolation design.

Buckling instability of the reactor vessel. The task objective is to evaluate the buckling limit of the ABTR reactor vessel preconceptual design for a horizontal seismic load. In this evaluation, both seismic isolation and non-isolation designs are considered for thin reactor vessels subjected to elevated temperature services. The project team used two methods to calculate the buckling load: a numerical simulation method using finite element analysis and a theoretically based evaluation formula. The team considered the material aging effect caused by a 60-year design lifetime and 510°C normal operating temperature, using an isochronous stress-strain curve corresponding to these conditions for the non-linear elastic-plastic buckling analysis method. The evaluation results showed that plasticity behavior significantly affects buckling strength; however, the initial geometrical imperfections have little effect.

Table 1 presents summary results of the buckling limit evaluations. Results indicate that the non-seismic isolation design does not satisfy ASME buckling limit regulations. The calculated load factor is 1.47 for the non-seismic isolation design, which is less than the 1.5 called for by the design code. The seismic isolation design, however, does satisfy these regulations with sufficient margins. The calculated load factor is 8.86, satisfying the design rule with a margin of about 591%. Thus, for the ABTR to withstand horizontal seismic loads against buckling, seismic isolation design is a key feature for a thin reactor vessel design.

Table 1. Summary of buckling limit evaluations for the reactor vessel.

	Design Load Q_d (MN)	Critical Load Q_{cr} (MN)	Calculated Load Factors ⁽¹⁾	Critical ⁽²⁾ (Level D)	Remarks
Isolation Design	1.14	10.1	8.86	> 1.5	Satisfy
Non-Isolation Design	6.87	10.1	1.47	> 1.5	Not Satisfy

(1) ASME Boiler and Pressure Vessel (BPV) Code, Section III, Division 1, Subsection NH, Appendix T: Load Factor = Q_{cr} / Q_d

(2) ASME BPV Code, Section III, Appendix F

Seismic integrity evaluations for reactor internals. The project team carried out seismic analysis, including fluid structure interaction modeling, for the internal structures submerged in the sodium pool. Researchers evaluated vibration and seismic response characteristics. The floor response spectra at the core support structure were applied to the seismic analysis. Using the calculated results, the team evaluated the internal structure's design integrity.

The researchers considered the combined seismic loads and both the isolated and non-isolated conditions. For the non-isolated conditions, the team found that the primary stress intensity greatly exceeded ASME limits. For the isolated conditions, there were overall decreases in dynamic responses. Thus, the reactor building should be isolated to best preserve internal structural integrity.

Seismic integrity evaluations for IHTS piping. The project team examined stress linearization in sections handling heat transport. During the transient operating and steady state conditions, maximum temperatures in these sections are above 427°C. Researchers evaluated structural integrity of IHTS hot leg piping, considering the seismic load. The team used floor response spectra to perform seismic analyses for both the isolation and non-isolation models.

Early results indicate that the hot leg piping layout cannot satisfy the structural integrity of the service limits, as the seismic load creates excessive primary stress. To ensure structural integrity, energy absorbers (snubbers) could be installed in the hot leg piping layout. Seven energy absorbers can reduce the primary stresses remarkably, but the absorbers cannot satisfy the inelastic strain limit. Conservative precautions call for a modified hot leg piping layout with nine snubbers. This modified layout satisfies the structural integrity parameters.

Planned Activities

This project is complete.

Advanced Multi-Physics Simulation Capability for Very High-Temperature Gas-Cooled Reactors

Research Objectives

The project objective is to develop a suite of advanced multi-physics simulation methods and codes that are applicable to high-fidelity, spatially detailed analyses of the coupled neutronics and thermo-fluid behavior of prismatic, very high-temperature gas-cooled reactors (VHTRs). The research scope includes:

- Developing functions and capabilities for a practical reload core design of the VHTR.
- Generating a multigroup cross-section library specific to VHTR analysis.
- Developing a consistent and optimized coupling strategy of neutronic and thermo-fluid models to obtain highly accurate multi-physics solutions.
- Systematically verifying and validating the codes and models using various numerical benchmark problems and high-temperature reactor experiments.

Project Number: 2008-001-K

PI (U.S.): Changho Lee, Argonne National Laboratory

PI (ROK): Hyun Chul Lee, Korea Atomic Energy Research Institute

Collaborators: Seoul National University

Program Area: Generation IV

Project Start Date: October 2008

Project End Date: September 2011

Research Progress

Task 1: High-performance 3-D whole core transport calculation. Using DeCART, the project team implemented new functions required for the reload core design of the VHTR. Revisions included restart calculation, radial and axial shuffling of fuel blocks, and fuel decay during fuel reloading. The KAERI library processing system was updated to generate cross-section libraries specific to VHTR analysis. For accuracy, researchers adjusted the resonance integral table for U-238 absorption cross sections, in accordance with Monte Carlo solutions.

The team took a first step toward performing transient analysis, which was enacted on a partially inserted control rod. The researchers used the fine-mesh finite-difference method to develop a three-region approach.

To account for thermal feedback, researchers updated the decoupling approach of planar method of characteristics (MOC) and 3-D coarse-mesh finite-difference calculations. To improve convergence, cell-wise cross sections were functionalized in terms of fuel and moderator temperatures.

Task 2: Adaptation of the SHARP modeling and simulation capability. Researchers applied angular domain decomposition in DeCART v1.2anl, enhancing parallel performance by allowing more than one processor per 2-D MOC plane. Gamma transport capability was implemented in the code for the coupled neutron and gamma heating calculation. To support the

capability, gamma libraries were generated using the NJOY code based on ENDF/B-VII data. Gamma production cross sections and neutron heating factors were provided for 261 isotopes in the 238 neutron group and 48 gamma group structures, and photon interaction cross sections were produced for 100 elements in the 48 gamma group structure.

Task 3: Development of thermo-fluid methods. The team developed a computational fluid dynamics model of the prismatic VHTR core, reflector, upper plenum, and lower plenum. The computer-aided design (CAD) models describing each block type were assembled into a single CAD representation of one-sixth of the VHTR core. An axially uniform paved hexahedral mesh was then generated based on the CAD description. The model assumes a uniform vertical three-millimeter gap between all blocks—a preliminary representation of the bypass flow path. The initial mesh, which uses approximately 22 million cells, is coarsened axially. This reduces computational burden and simplifies post-processing during the initial scoping simulations that support development of the coupled multi-physics framework.

To complete baseline simulations with the nominal coarse mesh and the solver options, the team used 128 processors of a commercial-grade cluster with a high-speed interconnect. Fully converged results were obtained after 4252 steady state iterations. Figure 1 shows the outlet velocity profile: 74.1% of the total flow passes through the coolant channels, 10.5% passes through the gap bypass between blocks, and 15.4% passes through the control rod holes. For the simplified upper and lower reflector configuration, the frictional pressure loss within the coolant channels was quite small (~ 25 kPa); therefore, the form losses at the inlet and outlet were substantial contributions to the total pressure loss. Figure 1 shows the predicted temperature profile at the outlet plane for all materials, assuming radially uniform power with a cosine axial distribution.

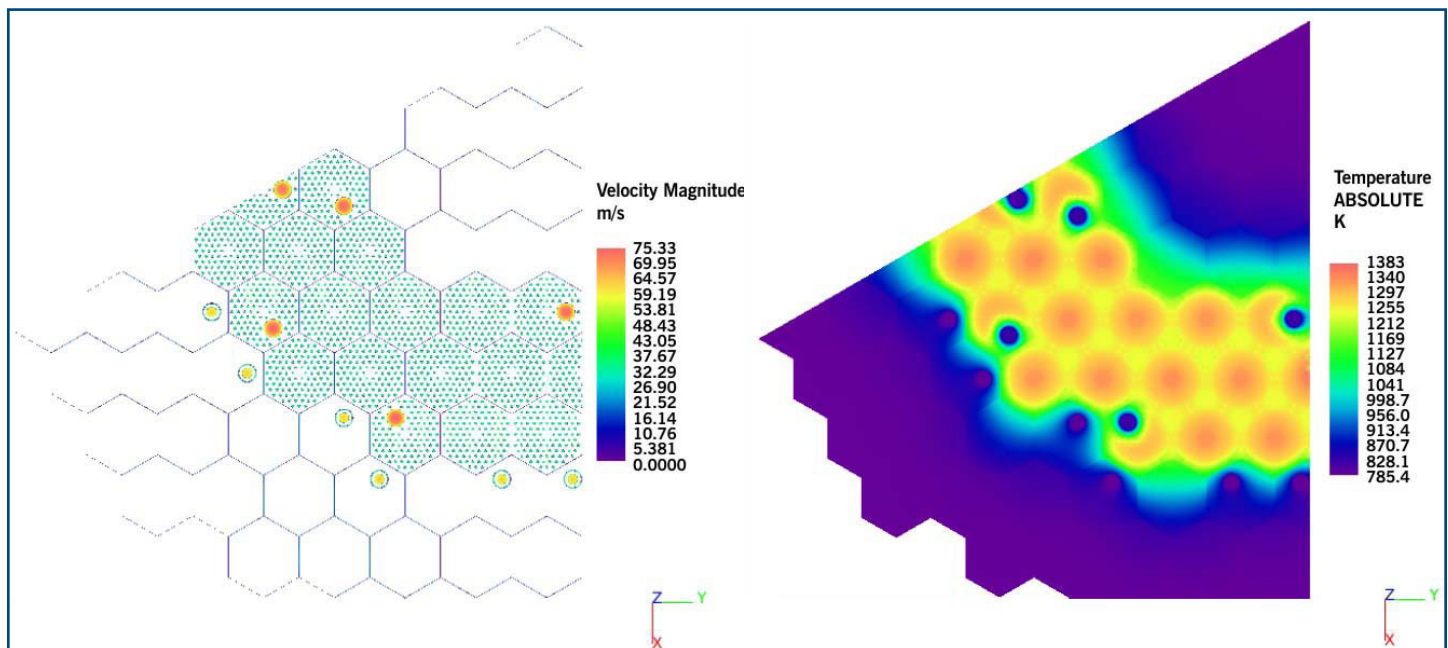


Figure 1. Predicted velocity and temperature distributions at the active core outlet plane.

In order to improve the thermo-fluid capability of DeCART v2.0, researchers developed a new thermo-fluid analysis code specific to the prismatic-type reactor: GAMMA-Core. Because the GAMMA-Core code is able to use the same grids as DeCART, no grid mapping is necessary when coupling the two codes. This year, the team focused on developing the interface module between DeCART and GAMMA-Core using socket programming. Figure 2 shows the geometric configuration of the single-column problem and the preliminary results from the coupled analysis with DeCART/GAMMA-Core. The results appear to be reasonable, but detailed verification is planned in the following year.

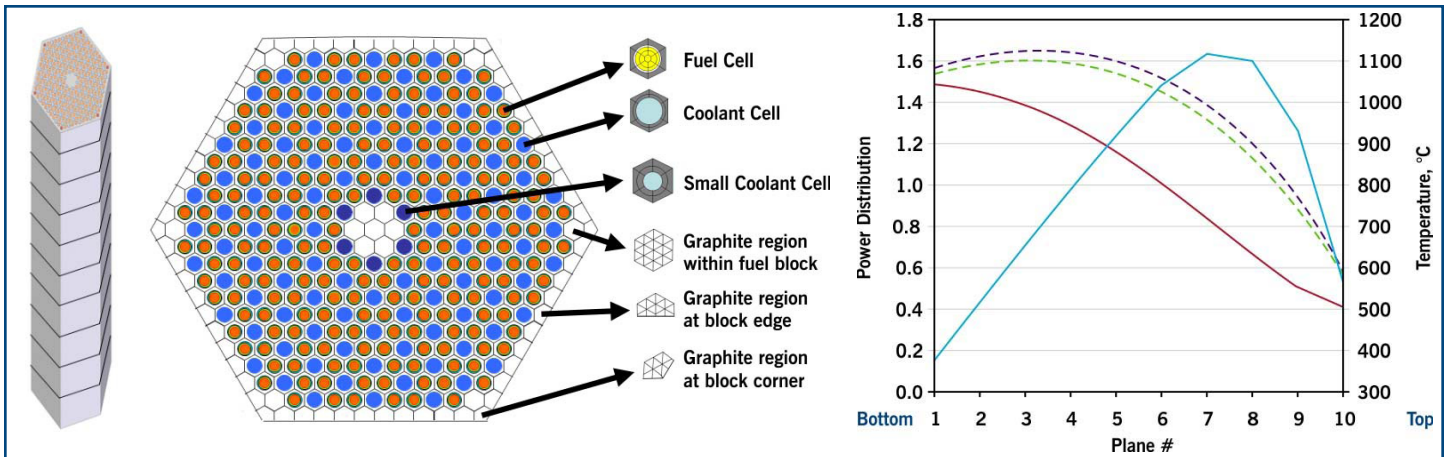


Figure 2. Geometry of a single-column benchmark problem and preliminary results of coupled analysis.

Task 4: Development of the coupling strategy. The research team performed several mesh sensitivity studies for coupled DeCART/STAR-CD simulations. From these analyses, researchers determined that the axial resolution previously used in the DeCART model was too coarse. In particular, the MOC planes were too thick to properly account for the temperature feedback being provided by STAR-CD.

The team made some improvements to the coupling scheme. By using the relatively fine axial mesh in the global CMFD solver in DeCART, the power profile can be computed with the same axial resolution as the STAR-CD mesh. The implementation was tested on the one-sixth VHTR core model. The resulting temperature profiles were more realistic and smoother, and the convergence of the DeCART/STAR-CD simulations was improved. Improvements included capability to monitor changes in temperature distribution during the STAR-CD iterations. This implementation provided a criterion to determine when to alternate between DeCART and STAR-CD. The updated criterion provided a more physical evaluation of the convergence monitoring and reduced the computational burden of coupled calculations.

Task 5: Verification and validation. The project team developed several numerical benchmark problems for depletion and coupled neutronic and thermo-fluid calculations. Researchers based a two-dimensional core depletion benchmark problem on the PMR200 core. Preliminary results from DeCART for the 2-D core depletion problem showed overestimation of k_{eff} over the entire burnup compared to the McCARD Monte Carlo solution. However, the overestimation was likely attributed to the poor accuracy of the 47-group HELIOS library. Therefore, the project team plans to conduct the same calculation with the new 190-group library in FY 2011.

Single-column and seven-column benchmark problems were prepared for coupled analysis. Figure 3 shows the seven-column benchmark problem. Both U.S. and ROK researchers plan to simulate and analyze those problems,

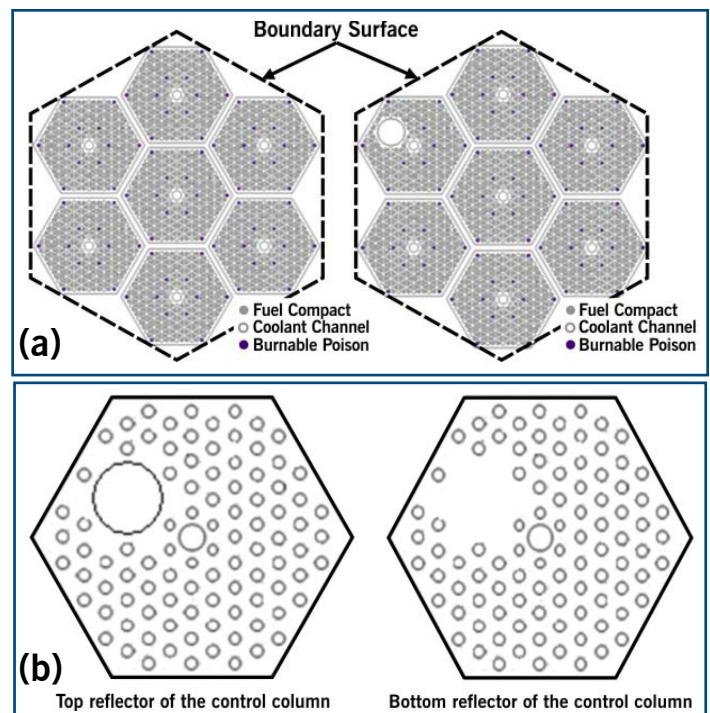


Figure 3. Geometry of seven-column benchmark problem for coupled calculation: (a) seven-column configuration; (b) top/bottom reflector of the control column.

thus testing both coupled systems. For validation, the project team used DeCART to analyze two HTR experiments, HTTR and VHTRC. The predicted core multiplication factors with progressive fuel loadings in HTTR were overestimated by up to 1900 per cent mille (pcm) compared to those measured. For VHTRC, DeCART's predicted core multiplication factors with different temperatures were also up to 1100 pcm larger than those measured. VHTRC isothermal temperature coefficients (ITCs) differed from the measurements by up to 22%. For both experiments, however, the DeCART solutions agreed well with the Monte Carlo solutions. Further investigation will be made for conclusions.

Planned Activities

For Task 1, the team will further verify new functions implemented in DeCART for a practical reload design of the VHTR. The KAERI cross-section libraries developed for the VHTR will be tested with the benchmark problems. Researchers will add capabilities required for transient calculations and conduct preliminary tests.

Task 2 is complete, but the 238-group cross-section library will be regenerated to take into account the wider-spectrum range of VHTR cores.

For Tasks 3, 4, and 5, the team will continue coupled simulations of DeCART/STAR-CD and DeCART/GAMMA-CORE for various numerical benchmark problems, making detailed comparisons between the two system solutions.

Experimental and Analytic Study on the Core Bypass Flow in a Very High-Temperature Reactor

Research Objectives

The main purpose of this project is to develop an improved understanding of the core bypass flow phenomenon in a very high-temperature reactor (VHTR). Specific objectives are to generate experimental data to validate the software used for calculating bypass flow in a prismatic VHTR core, to validate thermo fluid analysis tools and their model improvements, and to identify and assess measures for the reduction of bypass flow.

To achieve these objectives, the project team has defined the following five tasks:

- Design and construct experiments to generate validation data for software analysis tools.
- Determine experimental conditions and define measurement requirements and techniques.
- Generate and analyze experimental data.
- Validate and improve the thermofluid analysis tools.
- Identify measures to control bypass flow and assess their performance.

Researchers accomplished the following activities during FY 2010:

- Completed construction of two separate experimental facilities for air tests and matched index of refraction (MIR) tests.
- Determined the experimental condition and test matrix using thermo fluid analyses.
- Developed a measurement technique.
- Generated first experimental data.
- Performed benchmark calculations to validate the analysis model adopted in the thermofluid analysis codes.
- Identified measures to reduce the bypass flow.

Project Number: 2008-002-K

PI (U.S.): Richard R. Schultz, Idaho National Laboratory

PI (ROK): Min-Hwan Kim, Korea Atomic Energy Research Institute

Collaborators: Argonne National Laboratory, Seoul National University, Texas A&M University

Program Area: Generation IV

Project Start Date: November 2008

Project End Date: October 2011

Research Progress

Design and construction of experimental facilities. In FY 2010, the project team completed construction of the multi-block air test facility and the MIR test facility, based on the designs generated earlier in this project (see Figures 1, 2, and 3).

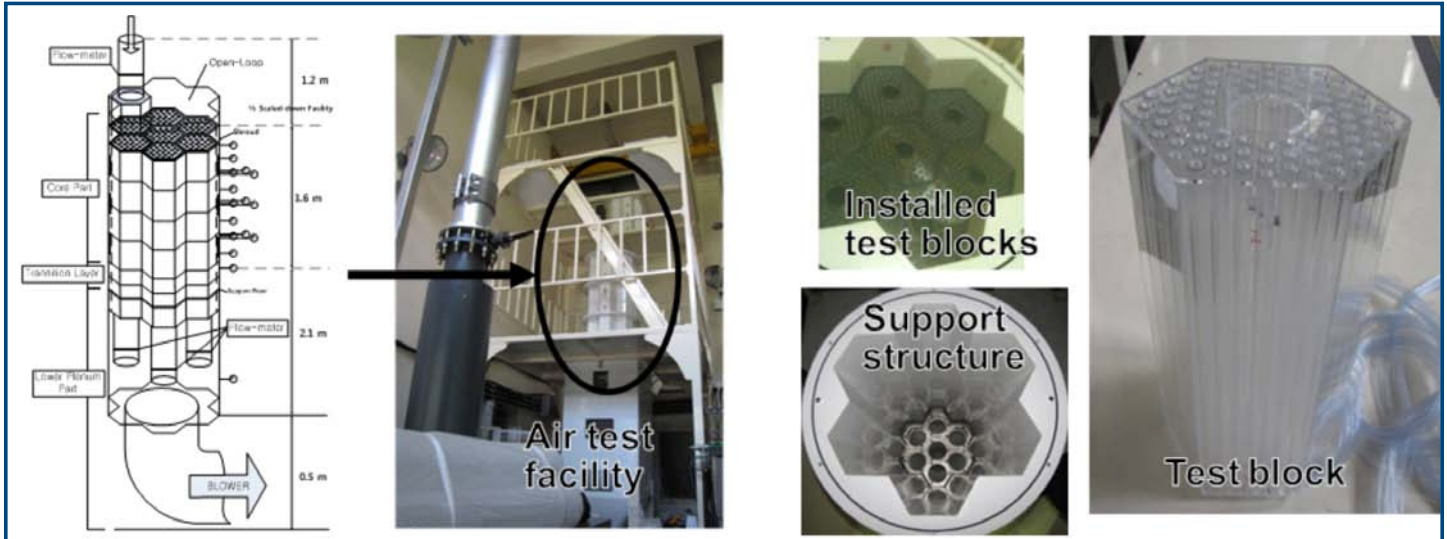


Figure 1. Multi-block air test facility at Seoul National University.

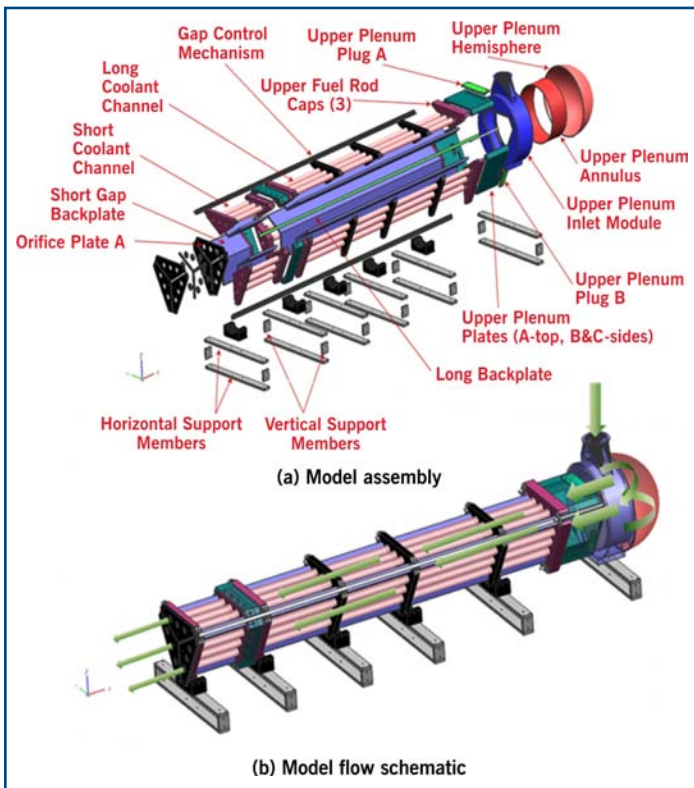


Figure 2. MIR bypass model at Idaho National Laboratory.

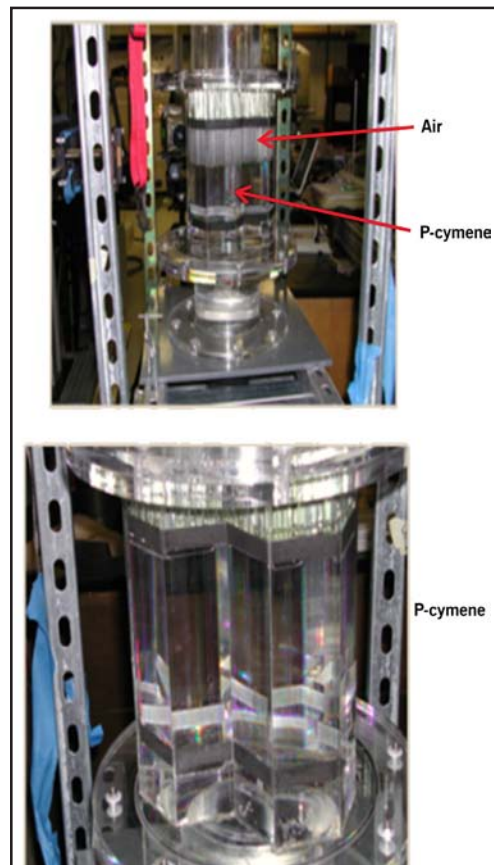


Figure 3. MIR test facility and model at Texas A&M University.

Determination of experimental conditions. The team performed preliminary analyses of the multi-block air test facility to investigate major phenomena, using both the GAMMA+ and the CFD codes. The analytic cases were selected after considering a combination of block arrangements, bypass-gap size, and cross-gap size. A comparison of the two outcomes resulted in these major findings:

- The bypass flow depends highly on bypass gap size and decreases at the outlet.
- The presence of a reflector region results in bypass flow increase.
- Change of cross-gap size has little effect on the bypass flow distribution.
- Variant gap distributions give rise to a local variant bypass flow distribution.
- Flow rate at each block column is almost uniformly distributed.

The team performed pre-test calculations to predict MIR experiment results at both locations and to identify the diagnostic instrumentation measurement protocol. Researchers constructed computational fluid dynamics (CFD) models (each in excess of five million nodes). In addition to the above, these CFD calculations indicate:

- The bypass-gap fluid tends to flow down the bypass's vertex region since this region has the least frictional resistance to flow.
- Minimal gap widths, e.g., ~1 mm, lead to laminar flow in the gap and cross-flow regions, whereas larger bypass gaps lead to either transition or turbulent flow.
- The bypass region clearly has greater frictional resistance than the cooling channels.

Development of measurement techniques. The team conceptualized and designed the special test block shown in Figure 4. A total of 16 pressure taps measure the static pressure of coolant holes within the fuel block and bypass gaps of the block periphery. A guide pipe secures the space for the pressure tubes connecting the pressure taps.

Experimental data. The team performed two experiments to validate the experimental concept and measurement techniques: R2-BG2-CG2 and R2-BG2-CG0. R2 indicates the two reflector columns were installed with five fuel columns. The BG2 and CG2 represent the two-millimeter bypass gap and two-millimeter cross gap, respectively. The present air test setup and techniques assured reasonable pressure distributions (see Figure 5).

The team also conducted experiments to quantify flow and pressure distribution within the model. Researchers are still evaluating the pressure data. The flow data indicate equal distribution between the prismatic blocks and compare well with the CFD calculations performed to date.

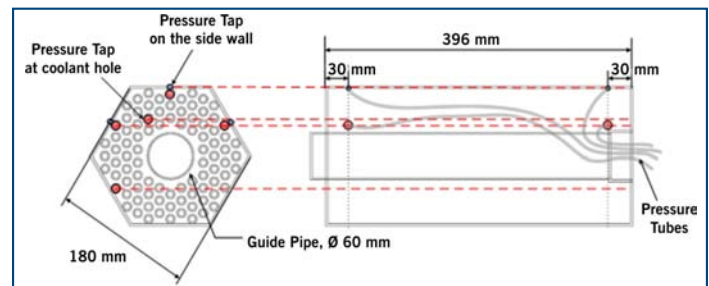


Figure 4. Schematic diagram of the fuel block.

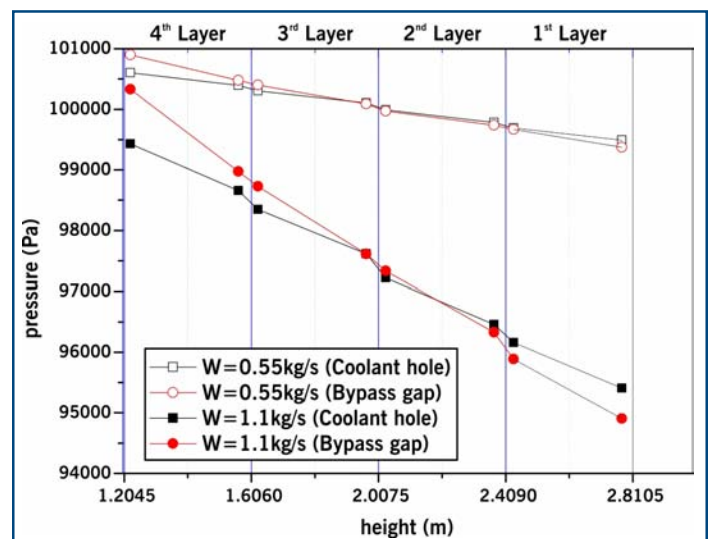


Figure 5. Pressure distribution within the test section (R2-BG2-CG2).

Benchmark calculations using GAMMA+ and CFX.

The team performed benchmark calculations to investigate the performance of system code GAMMA+ for a simple multi-block experiment. Conducting CFD analyses using the CFX code compensated for a lack of comparison data. The team compared CFD and GAMMA+ results in detail (Figure 6). Findings suggest that, for accurate bypass flow predictions, researchers using GAMMA+ allow for a blockage effect at the region of merging flow.

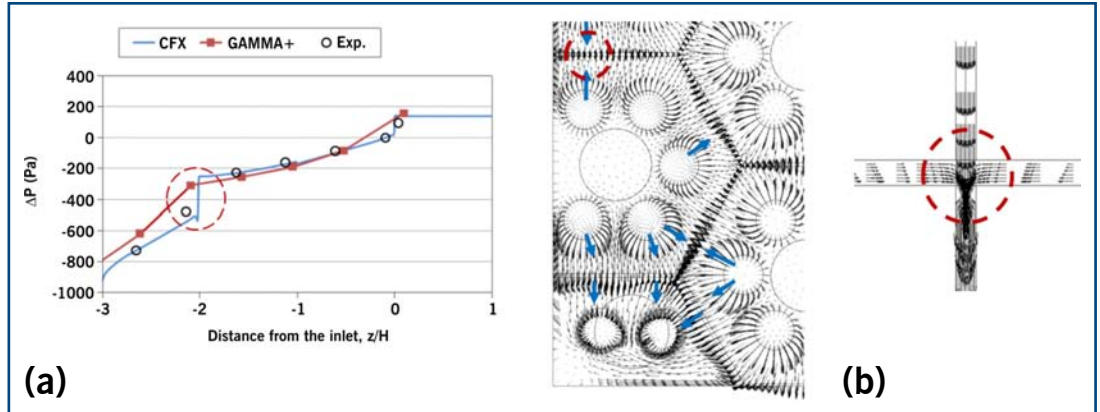


Figure 6. (a) Comparison of benchmark calculations and (b) description of flow region where an additional model is required in the GAMMA+ code.

Validation calculations using GAS-NET. The team conducted validation studies of GAS-NET using data from a set of experiments performed at the Seoul National University Multi-Block Test Facility. The data permitted individual study of GAS-NET axial and cross-flow pressure drop estimates. The analysis was complicated by several factors, including test assembly entrance and exit losses in excess of coolant-hole losses, as well as a dearth of pressure measurements for precisely allocating overall pressure loss amongst these individual losses. Despite these weaknesses, it appears gap pressure loss is predicted to within ten percent. The team also determined that neither the Groehn nor Kaburaki cross-flow correlations do an acceptable job in predicting the loss for the experiment-specific geometry. The results indicate that the cross-flow leakage loss is highly dependent on dimensions and geometry.

Identification of measures for bypass flow reduction. The team identified three measures for bypass flow reduction (see Figure 7):

- According to the literature survey, seal elements on the bottom core blocks were the only devices for bypass flow reduction, making seal elements the first option.
- Transition blocks could be staggered such that the top surface of one transition block obstructs bypass flow from the other.
- As analyses suggest that reflector blocks increase the bypass flow, using reflector blocks with grooved surfaces would increase flow resistance, reducing bypass flow.

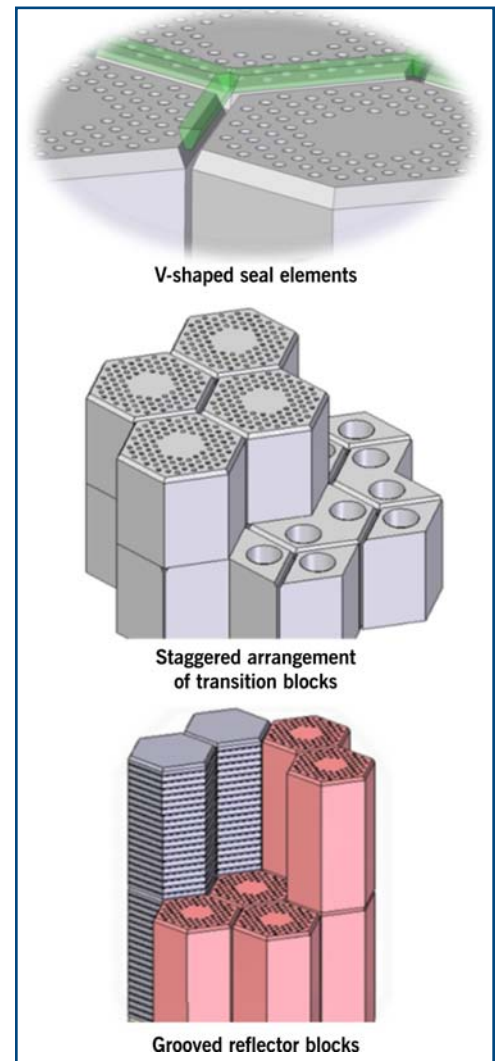


Figure 7. Identified measures for the bypass flow reduction.

Planned Activities

Major tasks for FY 2011 are divided into three areas, as shown below.

Final experimental data from the air and MIR tests. The project team will use the first round of experimental data to modify the air test facility's test section for more reliable results. In the MIR experiments, researchers will analyze flow behavior within the bypass gap and cross-flow passages for bypass gaps ranging from one to five millimeters. The team will investigate flow structure; the flow's tendency to move in the vertex region; and how laminar, transition, and turbulent gap flows influence overall flow distribution in the core region.

Final thermofluid analysis. The team will carry out analyses for the air test experiment using GAMMA+ and GAS-NET to verify the improved model. Additional GAMMA+ calculations will support hot-spot analysis for a reference VHTR. In addition, the project will provide a detailed comparison of velocity distribution after performing a CFD benchmark calculation for the MIR test.

Performance assessment of selected measures for bypass flow reduction. The team expects modifications to the air test facility will be needed to carry out this task.

Nuclear Data Uncertainty Analysis to Support Advanced Fuel Cycle Development

Research Objectives

This project aims to provide improved neutron cross-section data with uncertainty or covariance data for isotopes important for advanced fuel cycle and nuclear safeguards applications. An additional objective is to assess nuclear integral parameter uncertainties due to the cross-section data. The goal is to improve safety validation and reduce capital cost through system design optimization for advanced fuel cycle development.

Research Progress

During this year, the project team:

- Completed a preliminary resonance-region cross-section evaluation with covariance data for ^{240}Pu .
- Initiated resonance evaluation efforts for ^{237}Np and ^{244}Cm .
- Completed evaluations of corresponding high-energy cross-section data (i.e., above the resonance region) for all three isotopes.

Figure 1 shows the new total, elastic, fission, and capture cross sections of ^{240}Pu . The team will test the new data through benchmarks and use the findings to enhance the next set of evaluations.

To evaluate the new ^{240}Pu data, researchers replaced the ENDF/B-VII.0 resonance parameters with the new parameters and added the resonance parameter covariance matrices (RPCMs). The team then combined the new resonance parameters and RPCMs and the high-energy cross-section and covariance data, generating a complete ENDF-format file. Figure 2(a) shows the ^{240}Pu neutron capture cross section and correlation matrix.

The objective of the ^{244}Cm evaluation effort is to provide resonance parameter covariance data while preserving the existing data—the “retroactive” feature of SAMMY R-Matrix software. For JENDL-4, a Japanese nuclear data center, the ^{244}Cm RPCMs were generated using SAMMY in the energy range from 10^{-5} eV to 1 keV. The current project used the retroactive method to generate the RPCM for ^{244}Cm .

Project Number: 2008-003-K

PI (U.S.): Michael E. Dunn, Oak Ridge National Laboratory

PI (ROK): Choong-Sup Gil, Korea Atomic Energy Research Institute

Collaborators: None

Program Area: FCR&D

Project Start Date: November 2008

Project End Date: September 2011

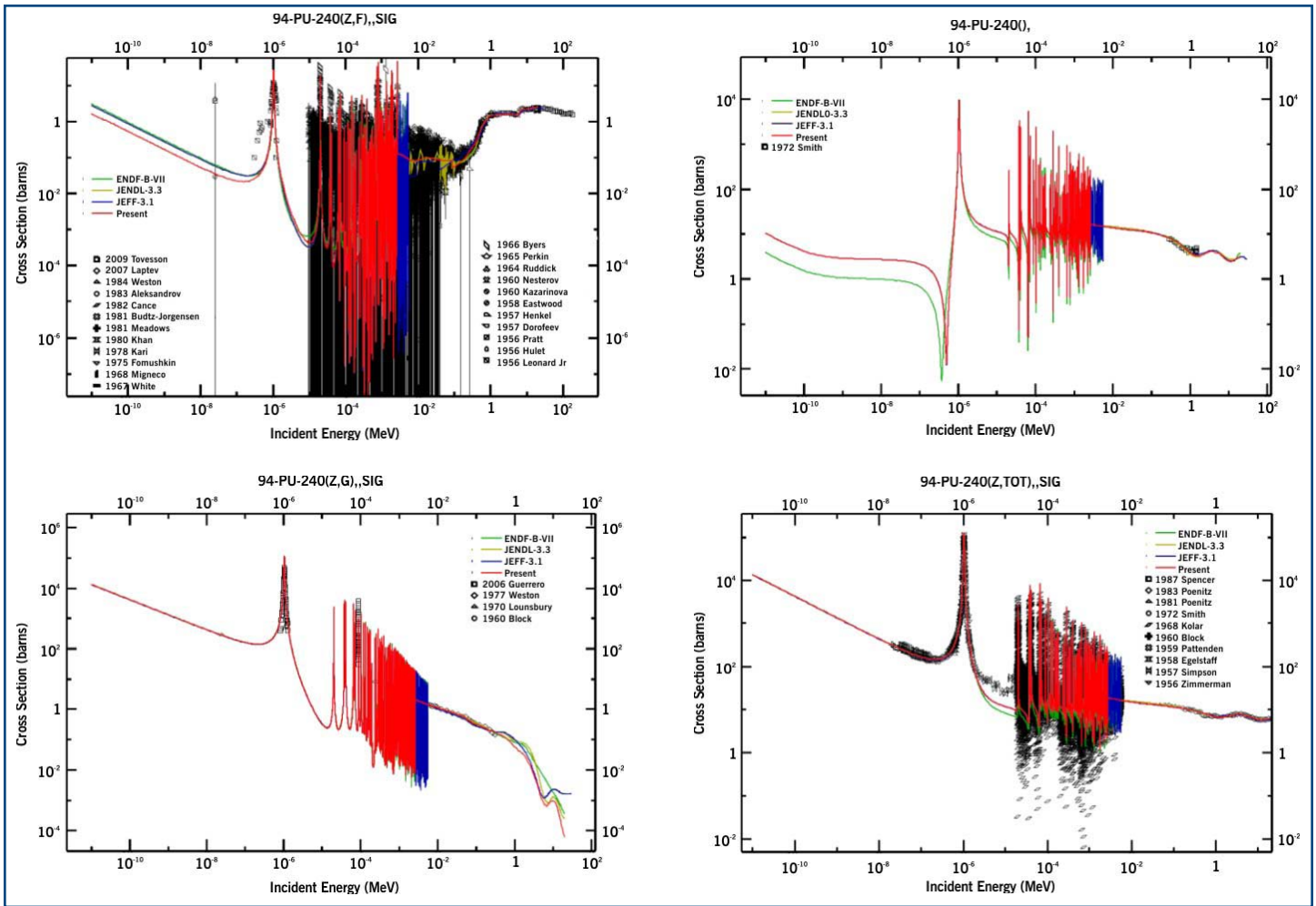


Figure 1. New ²⁴⁰Pu cross-section data compared with measurements and existing libraries. Clockwise from upper left: total, elastic, fission, and capture cross section.

These activities complement ongoing high-energy cross-section and covariance analysis of the Cm isotopes. The project team has completely re-evaluated the cross-section data and covariance matrix above resonance energy for ²⁴⁴Cm with EMPIRE/KALMAN software. Figure 2(b) shows the fission cross section and correlation matrix for the new ²⁴⁴Cm data.

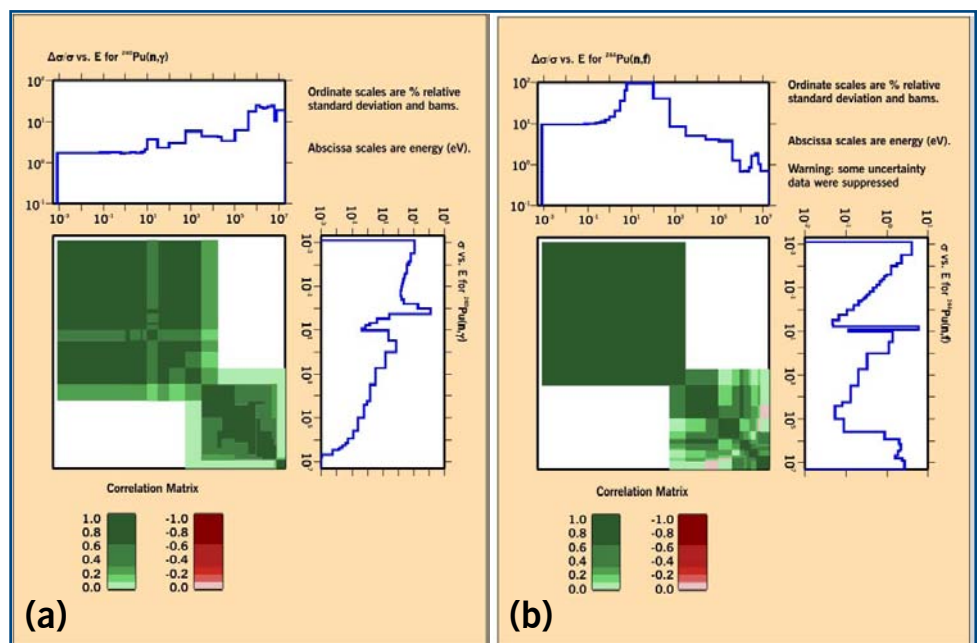


Figure 2. The new (a) ²⁴⁰Pu capture and (b) ²⁴⁴Cm fission cross sections and correlation matrices.

To prepare for demonstration and testing of the improved cross-section files, researchers carried out sensitivity and uncertainty calculations for various benchmark experiments and compared the results with existing data. The tests included not only data validation but also assessments of uncertainty due to uncertainties in k-effective (k_{eff}) nuclear cross-section data. Five benchmarks were collected from the International Criticality Safety Benchmark Evaluation Project (ICSBEP). For those benchmarks, Table 1 provides JENDL-3.3 k_{eff} values and associated total uncertainties with covariance data from JENDL-3.3, a low-fidelity project (Lo-Fi), JENDL-4, and this project. The new covariance data of ^{237}Np , ^{240}Pu and ^{244}Cm from this work were substituted for those of JENDL-3.3. Unfortunately, the resulting uncertainties are not significantly lower because the amounts of the noted isotopes in the benchmarks are very small, except for Pu240-JEZEBEL.

Table 1. Total uncertainties of k_{eff} for criticality safety benchmark problems.

Isotope	Benchmark Problem	k_{eff} by DANTSYS with JENDL-3.3	Total Uncertainty (%)			
			JENDL-3.3	Lo-Fi	JENDL-4.0	This Work
^{237}Np	FLATTOP-Np237-1	0.98883	0.402	0.403	0.402	0.401
	FLATTOP-Np237-3	1.00365	0.291	0.292	0.291	0.291
^{240}Pu	Pu239-JEZEBEL	0.99634	0.467	0.473	0.462	0.462
	Pu240-JEZEBEL	0.99927	0.511	0.619	0.402	0.402
^{244}Cm	Cm244-JEZEBEL	0.99921	0.598	0.598	0.598	0.598

The team has tested the new ^{240}Pu data for nine benchmarks. Figure 3 shows the comparison between the MCNP-reported k_{eff} for the nine models and the results reported in the International Handbook of Evaluated Criticality Safety Benchmark Experiments (IHECSBE).

In general, the nuclides' small contribution to the k_{eff} estimation hinders identification of appropriate benchmark problems for testing covariance data of minor actinides. In conventional benchmark problems, changes due to revised covariance data are nearly undetectable. The team therefore introduced three fictitious critical systems, each composed of 100% of a nuclide, and used them to test the new ^{237}Np , ^{240}Pu , and ^{244}Cm covariance data. The fictitious critical systems clarify the new data's effects.

The fictitious critical system was assumed to be a bare sphere, as a sphere has minimal critical mass and the smallest physical dimensions of any shape. The sphere's critical radius was determined by DANTSYS calculation with the JENDL-3.3-based 44-group cross-section library. All the DANTSYS calculations were conducted in P_3 - S_{16} approximation. Table 2 describes key parameters of the fictitious critical systems.

Table 2. Fictitious critical systems determined by DANTSYS calculation based on JENDL-3.3.

Actinide	Critical Radius (cm)	Atom Density (atoms/barn-cm)
93-Np-237	9.200	5.144E-02
94-Pu-240	7.235	4.977E-02
96-Cm-244	8.046	3.333E-02

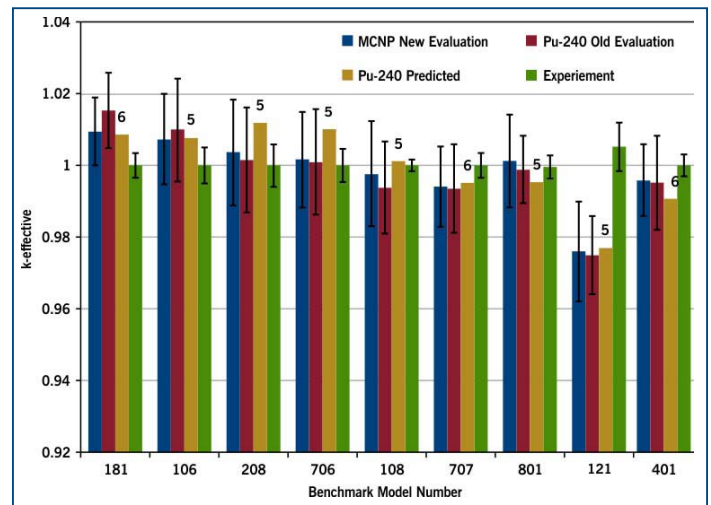


Figure 3. A comparison of MCNP5 k_{eff} simulations for this study versus IHECSBE results. "Pu-240 Predicted" refers to results of the evaluated benchmark experiments using the ENDF/B-5 or 6 library, as shown above the respective bars in the graph.

Figure 4 shows the reaction covariance data's uncertainty contributions for the fictitious systems, comparing results from JENDL-3.3, Lo-Fi, JENDL-4, and this project (KAERI/ORNL). The uncertainty of total k_{eff} with the low-fidelity ^{237}Np covariance data was estimated to be 4.90%, which is very large compared with those of JENDL-3.3 (1.45%), JENDL-4 (1.93%), and this project (1.85%). The uncertainty of the Lo-Fi ^{237}Np fission covariance data is up to four times greater than the others.

The k_{eff} of total uncertainty with Lo-Fi and JENDL-3.3 ^{240}Pu covariance data were estimated to be 3.27% and 2.47%, respectively. Compared with the total uncertainties of 1.07% and 1.08% with JENDL-4.0 and this project's covariance data, the Lo-Fi and JENDL-3.3 ^{240}Pu covariance data had considerable impact. As with the ^{237}Np fictitious critical system, the Lo-Fi ^{240}Pu fission covariance data increase the uncertainty. The total ν covariance data also generate large uncertainties in the k_{eff} with Lo-Fi and JENDL-3.3.

The uncertainty of ^{244}Cm total k_{eff} with the Lo-Fi was estimated to be 27.57%. The extremely large uncertainty is mainly due to overestimation of the total fission covariance data. This project underestimated the fission uncertainty for both the ^{244}Cm and ^{237}Np covariance data.

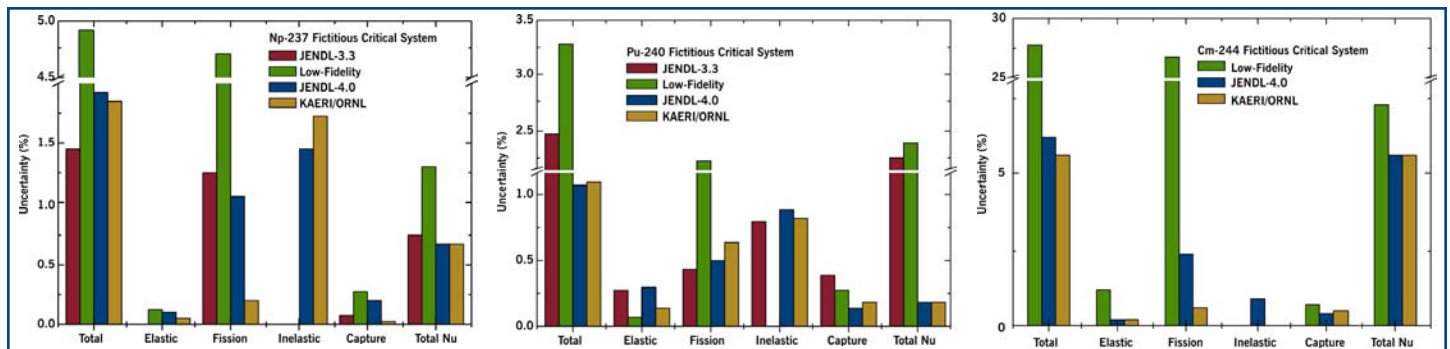


Figure 4. Total k_{eff} uncertainty variations for fictitious critical systems of 100% ^{237}Np , ^{240}Pu and ^{244}Cm , as determined using covariance data from JENDL-3.3, Lo-Fi, JENDL-4.0, and this project (KAERI/ORNL).

Planned Activities

For the upcoming year, the project team will finalize evaluations of ^{237}Np , ^{240}Pu , and $^{240-250}\text{Cm}$ and test the new data in benchmark calculations. Researchers will document the evaluation process in detail and submit the complete ENDF-format files of the noted isotopes for inclusion in the U.S. ENDF/B system.

ZPPR-15 and BFS Critical Experiments Analysis for Generation of Physics Validation Database of Metallic-Fueled Fast Reactor Systems

Research Objectives

This collaborative research program comprises two related research areas. First, the project team will archive the Zero Power Plutonium Reactor (ZPPR)-15 physics experiment database, specifically loading records for Phases A, B, C, and D. Researchers will use this data to generate high-fidelity as-built Monte Carlo models that allow these valuable metallic fuel measurements to contribute fully to reducing uncertainties in validating advanced methods and design analysis methods.

Second, the team will set up an experimental plan and develop models to study the physics of a transuranic (TRU) burner reactor. The last 20 years have seen a considerable evolution in the fast reactor core concept. Physics experiments will validate design features specific to a typical TRU burner core and produce valuable high-fidelity models. The experimental plan will cover the physics areas that the ZPPR-15 physics experiment did not, while considering licensing requirements for a commercial reactor.

Research Progress

Task 1: Generation of the ZPPR-15A experimental database. The complete loading records for all ZPPR-15 Phase A configurations have been captured, verified, and entered into a database. The researchers reviewed all ZPPR-15A drawer master identifications and logbooks. These activities represent a significant part of the effort to generate the detailed as-built models.

The team has completed and analyzed five as-built models, including the reference critical configuration and control rod worth measurements as a function of position. Researchers analyzed these experiments with continuous-energy Monte Carlo using both ENDF/B-V.2 and ENDF/B-VII.0. Results with ENDF/B-VII.0 data are excellent, although they show a slight underestimation of k_{eff} by approximately 100 pcm.

Task 2. Compilation of physics experiments at the Big Physical Stand (BFS-2) facility. The team used archived information from Task 1 to set up an as-built Monte Carlo model of the BFS-73-1 experiment conducted at the BFS-2 facility at the Institute of Physics and Power Engineering (IPPE) in Russia. Researchers analyzed the as-built Monte-Carlo model with three evaluated nuclear data files (ENDF/B-VII.0, JEFF-3.1, and ENDF/B-VI.6).

Project Number: 2009-001-K

PI (U.S.): Richard McKnight and Won Sik Yang, Argonne National Laboratory

PI (ROK): Sang Ji Kim, Korea Atomic Energy Research Institute

Collaborators: Korea Advanced Institute of Science and Technology

Program Area: Generation IV

Project Start Date: November 2009

Project End Date: October 2012

The BFS-2 facility is the site of an ongoing TRU burner physics experiment; the reference configuration for this experiment went critical on August 12, 2010. This project team has already determined the most desirable experimental configuration for the ongoing experiment, and team members continue to discuss further measurements and exchange information.

Task 3: Analysis of ZPPR-15 experiments. Using the as-built Monte Carlo models from Task 1, the project team has analyzed the five associated configurations. Team members investigated change in the multiplication factor, which varies with the modeling method for the drawer masters and with the cross-section library's origin, and evaluated the sensitivity of the multiplication factor to the multigroup cross section. Using the resulting cross-section uncertainty, they estimated uncertainty in the criticality prediction. They also used deterministic neutronics analysis tools to carry out a preliminary analysis of ZPPR-15 Loading 15.

The ZPPR-15 experimental information is relatively new to the ROK researchers. Therefore, the team developed examination tools for the as-built Monte Carlo input to the VIM code, facilitating an enhanced understanding of the experimental configuration. Four deliverable utility codes were produced: COVIM, AEVIS, HOVIC, and PVIM. The table below lists their functions.

Table 1. Brief description of tools for ZPPR-15 analysis.

Name	Function
COVIM	Automatic conversion of VIM input file into MCNP input. Supports hexagonal, rectangular, plate geometries of VIM.
AEVIS	Analysis and summary of cell-by-cell description of a VIM input file. Summarizes each drawer cell's material discontinuity along with macro body lists used to construct the cell, plate location in a drawer, and material distribution within a drawer.
HOVIC	Homogenization tool for a drawer master. Provides several ways to homogenize a plate in a drawer master.
PVIM	Drawing tool of each drawer master. Provides the 2-D drawing of a drawer master in x-y, y-z, z-x planes. Each plate can be filled by material number, edit region number, body number, etc.

PVIM output allows a user to visualize the detailed plate-by-plate geometry in a versatile domain (see Figure 1). This task cannot be performed adequately by hand.

Through an additional sub-task to Task 3, researchers developed a transport theory-based one-dimensional neutron flux solver equipped with flux-volume homogenization routine. This model will address the current design code's insufficient treatment of cell heterogeneity effects, particularly to accurately account for the slab-cell heterogeneity effect characteristic of the ZPPR subassemblies.

Planned Activities

The team generated detailed as-built Monte Carlo models for five of the twelve planned configurations of ZPPR-15 Phase A experiments, and has analyzed these five configurations. In FY 2011, the team plans to complete models for the remaining sodium void configurations and analyze them. Additional effort on the ZPPR-15A database will also be required to identify the remaining experimental measurements and their uncertainties. The TRU burner physics experiments at the BFS-2 facility will be completed, making available the reference as-built Monte Carlo model. Finally, the team plans to develop a two-dimensional neutron transport solver, as described above.

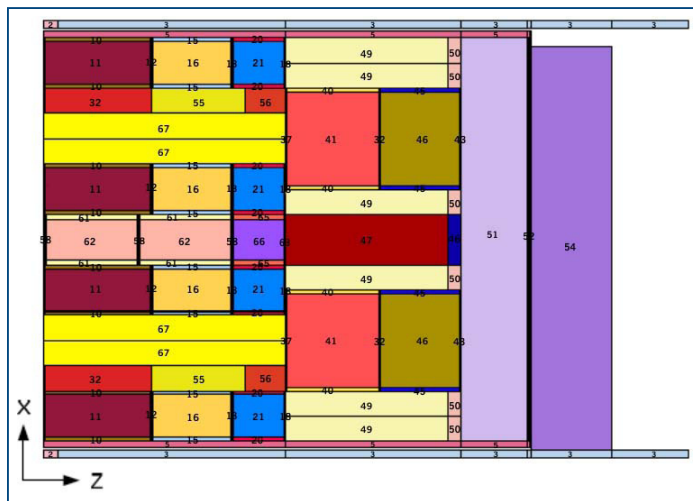


Figure 1. Layout of drawer master 103 in z-x plane (z:x=15:1).

Enhanced Radiation Resistance through Interface Modification of Nanostructured Steels for Generation IV In-Core Applications

Research Objectives

The objective of this project is to increase radiation tolerance in candidate alloys for advanced reactor fuel cladding through optimization of grain size and grain boundary characteristics. The focus is on nanocrystalline metal alloys with a face-centered cubic (fcc) crystal structure. The long-term goal is to design and develop, via grain boundary engineering, bulk nanostructured austenitic steels with enhanced void swelling resistance, substantial ductility, and enhanced creep resistance at elevated temperatures. The combination of grain refinement and grain boundary engineering approaches allows researchers to tailor the material strength, ductility, and resistance to swelling by 1) changing the sink strength for point defects, 2) increasing the nucleation barriers for bubble formation at grain boundaries, and 3) changing the precipitate distributions at boundaries.

At elevated temperatures, austenitic steels possess good creep and fatigue properties compared to those of ferritic/martensitic steels; at low temperatures, austenitic steels exhibit better toughness. However, austenitic steels have a major disadvantage in that they are vulnerable to significant void swelling in nuclear reactors, especially at the higher temperatures and radiation doses anticipated in Generation IV (Generation IV) reactors. This lack of resistance to void swelling led to ferritic/martensitic steels being considered the preferred material for fast reactor cladding applications.

Recently, researchers at Oak Ridge National Laboratory developed a new type of austenitic stainless steel, HT-UPS (high-temperature ultrafine precipitate-strengthened), that is expected to show enhanced void swelling resistance through the trapping of point defects at nanometer-sized carbides. Reducing the grain size and increasing the fraction of low-energy grain boundaries are expected to reduce the available radiation-induced point defects (owing to the increased sink area of the grain boundaries), make bubble nucleation at the boundaries less likely (by reducing the fraction of high-energy boundaries), and improve strength and ductility under radiation (by producing a higher density of nanometer-sized carbides on the boundaries). This project will focus on void swelling, but advances in processing of austenitic steels are likely also to improve the radiation response of the mechanical properties.

Project Number: 2009-002-K

PI (U.S.): Todd R. Allen, University of Wisconsin–Madison

PI (ROK): Jinsung Jang, Korea Atomic Energy Research Institute

Collaborators: Seoul National University Texas A&M University

Program Area: FCR&D

Project Start Date: October 2009

Project End Date: September 2012

Research Progress

In FY 2010, the project team processed a series of Fe-14Cr-16Ni alloys and 304 and 316L stainless steels using equal channel angular processing (ECAP), reducing the average grain sizes by two orders of magnitude—from hundreds of microns down to a few hundred nanometers. After eight ECAP processing passes, researchers examined the model alloy's grain structure in the transverse and flow planes (see Figure 1). The grains in the transverse plane were equiaxed, with no observable texture and an average grain size of 360 nm.

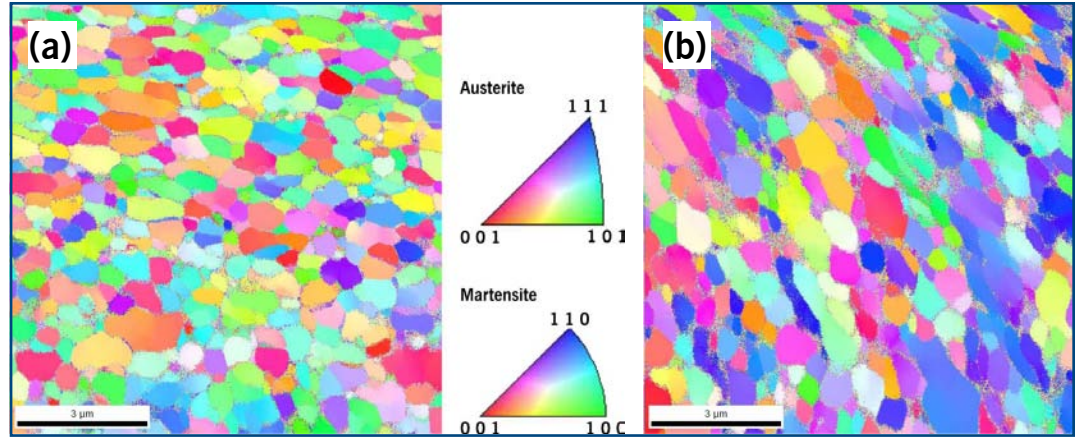


Figure 1. Inverse-pole-figure images of post-ECAP Fe-14Cr-16Ni alloys (eight passes, 500°C): (a) transverse plane; (b) flow plane.

Researchers also performed systematic examinations on the ultrafine grains' thermal stability at several elevated temperatures for various annealing times ranging from two minutes to one hour. They also used an *in situ* annealing transmission electron microscopy (TEM) experiment to observe the abnormal grain growth of the model alloy directly. For the ultrafine grain (UFG) (post-ECAP) model alloy, grain growth begins between 500°C and 600°C; higher temperatures cause significant coarsening due to the high driving force from material deformations. Furthermore, the UFG alloy has a particularly low carbon concentration, and hence no carbide precipitates are present to hinder grain boundary motion during coarsening.

The team evaluated mechanical properties of the ECAP-processed alloys using nanoindentation and tensile testing at elevated temperatures. The sample that underwent eight passes at 500°C showed nearly a 60% increase in strengthening, which mainly originates from grain refinement, martensite formation, and dislocation density increase. Results of tensile tests performed on UFG alloys and coarse grain (CG) as-received alloys at room and elevated temperatures indicated that the UFG FeCrNi alloy's ductility decreases with increased temperature (see Figure 2). Two hypotheses could explain the degradation of ductility at higher temperatures. First, deformation twinning is an important mechanism that may enhance ductility of austenitic stainless steels. At higher temperatures, however, deformation twinning is suppressed, effecting lower ductility. Second, martensitic phase transformation could induce plasticity at lower temperatures, a reaction that could also be suppressed at elevated temperatures.

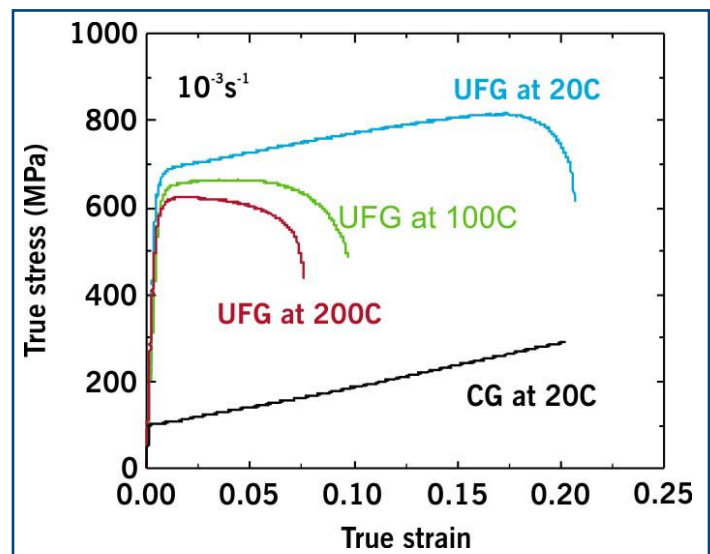


Figure 2. True stress–true strain curves of UFG and CG Fe-14Cr-16Ni.

To further improve the grain boundary character distribution of ECAP-processed alloys, the team performed a systematic grain boundary engineering experiment and evaluated the processed samples using the electron backscatter diffraction (EBSD) technique. They found that the fraction of coincident site lattice (CSL) boundary evolutions decreases with increased annealing time (see Figure 3). A transient high-temperature annealing can effectively reduce the fraction of high-angle random grain boundaries while moderately increasing grain size.

Finally, the researchers initiated a proton irradiation experiment with a newly-designed sample stage that can effectively eliminate indium leakage during high-temperature irradiation.

Planned Activities

For the upcoming year, research on austenitic steel will continue. Researchers will process oxide dispersion-strengthened steel using ECAP and will study the response of nanocrystalline steel to both proton irradiation and *in situ* krypton ion irradiation. Specifically, the research team will:

- Further optimize alloy grain boundary character distribution by promoting a higher portion of low Σ grain boundaries while retaining grain size at a sub-micron scale.
- Use ECAP to refine the grain structures of the oxide dispersion-strengthened alloy.
- Perform proton irradiation on post-ECAP and as-received specimens and complete the post-irradiation examination.
- Perform *in situ* TEM on post-ECAP alloys.

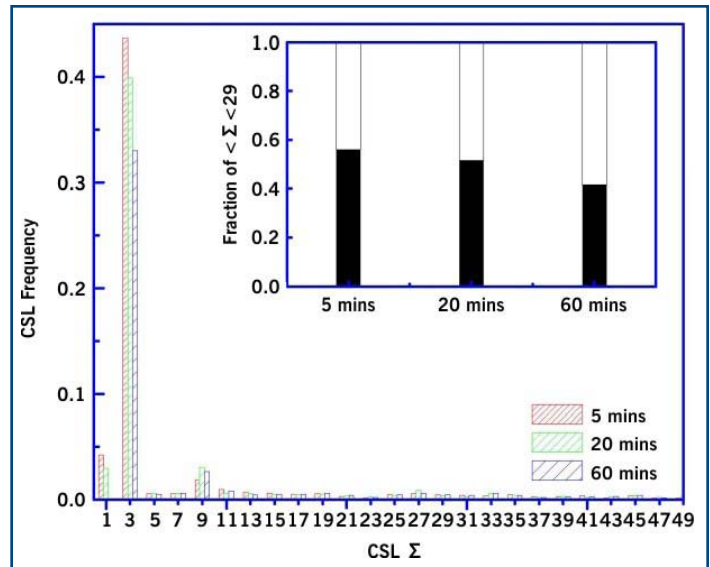


Figure 3. Fraction of CSL boundaries versus annealing time at 700°C.

Investigation of Electrochemical Recovery of Zirconium from Spent Nuclear Fuels

Project Abstract

The project is developing an electrochemical model that can be applied to recovery of zirconium from a variety of spent nuclear fuel types. Metallic fuel from a fast reactor, such as the Experimental Breeder Reactor-II, is alloyed with zirconium that partially partitions into the molten salt electrolyte during standard operations. Recovery of this zirconium is currently accomplished only via co-deposition with uranium, which results in significant product-processing challenges. With the assistance of a detailed, three-dimensional multi-species model, it should be possible to design a process by which pure zirconium can be recovered from electrorefiners and effectively managed as waste. Similarly, spent oxide fuel from water-cooled reactors contains significant amounts of zirconium in the form of zircaloy cladding material. If this zirconium can be efficiently separated from actinides and fission products, it can be inexpensively disposed of in low- and intermediate-level waste sites. Electrorefining can, hypothetically, be used to achieve this separation. However, this process has not been tested owing to restrictions on performing separations processes on spent fuel in the ROK. The ability to model the zirconium electrorefining process is, thus, viewed as critical for development of this technology. The aforementioned three-dimensional, multi-species model could be used for this application. This project utilizes both modeling and experimental studies to provide significant waste management benefits to both the U.S. and the ROK. It also effectively builds on progress from a previous I-NERI project on electrorefiner modeling (2007-006-K).

Project Number: 2010-001-K

PI (U.S.): Michael Simpson, Idaho National Laboratory

PI (ROK): Il-Soon Hwang, Seoul National University

Collaborators: Korea Atomic Energy Research Institute, University of Idaho

Program Area: FCR&D

Project Start Date: December 2010

Project End Date: September 2013

Science-Based Approach to Nickel Alloy Aging and its Effect on Cracking in Pressurized Water Reactors

Project Abstract

Aging of structural materials in pressurized water reactors (PWRs) has been one of the major issues for plant safety and life extension. A new alloy (Alloy 690) has been introduced for nozzles in reactor pressure vessel heads and tubing in steam generators (SGs). Alloy 690 has shown acceptable resistance to environmental degradation and aging phenomena, but some concerns remain unresolved. Two major challenges require investigation: 1) possible deterioration of a dissimilar metal weld, such as Alloy 690/low alloy steel (LAS), over long-term service, and 2) susceptibility of the new alloy to corrosion based on the lab test data, especially in lead (Pb)-contaminated SG water.

Issues regarding dissimilar metal weld aging include the interface between the LAS and weld sides, the weld itself, and the Alloy 690 heat-affected zone. Using a mock-up system, the project team will investigate how aging affects chromium (Cr) dilution in Alloy 152, examining the weld side of the Alloy 152–LAS interface. Cr dilution decreases the alloy's resistance to stress corrosion cracking (SCC). Microstructural properties of the weld specimen will be characterized as a function of aging time. Researchers will characterize the nanostructure of aged weld samples, such as Cr profiles across the interface between the weld and LAS. The team will use conventional methods (SIMS and TEM) combined with a state-of-the-art method, such as an “atom probe.” Using SCC crack growth rate (CGR) testing, researchers can quantitatively evaluate resistance to SCC at the LAS–weld interface. Since the SCC of structural alloys is related to properties of native oxide layers, surface oxides on the aged weld specimens will need to be characterized. It is essential to overcome the current limitation of typical *ex situ* methods and pursue an *in situ* approach. Therefore, researchers will develop a hydrothermal cell for the *in situ* surface oxide analysis using Raman spectroscopy. Based on these characterizations, the project team can evaluate the effect of aging on the dissimilar metal weld, especially at the LAS–weld interface.

Regarding the SG tube aging, earlier studies suggest that the presence of Pb ions can dramatically alter the oxide chemical compositions and phases, but this degradation mechanism is poorly understood at the fundamental level. Synchrotron x-ray reflectivity (XR) combined with resonant anomalous x-ray reflectivity (RAXR) will be applied to obtain the molecular-scale details of Pb distribution and the chemical states at the metal oxide–liquid interface. The results will provide direct insight into how the oxide adsorbs and incorporates Pb ions. Findings will be compared with those of typical *ex situ* oxide film analysis and *in situ* electrochemical spectroscopy.

Project Number: 2010-002-K

PI (U.S.): Chi Bum Bahn and Ken Natesan, Argonne National Laboratory

PI (ROK): Ji Hyun Kim, Ulsan National Institute of Science and Technology

Collaborators: None

Program Area: Reactor Concepts RD&D

Project Start Date: December 2010

Project End Date: September 2013

Low-Loss Advanced Metallic Fuel Casting Evaluation

Project Abstract

A metallic alloy serves as the reference fuel for the sodium-cooled fast reactor (SFR) being developed by the Korea Atomic Energy Research Institute (KAERI). Metallic fuel has been studied and is considered a leading candidate for advanced driver and transmutation fuels. The steps in the fabrication process for metallic SFR fuel are 1) casting the fuel pins, 2) fabricating the fuel rods and loading them with sodium and fuel pins, and 3) fabricating the fuel assemblies. Fuel pin casting is the dominant source of fuel losses and recycle streams in the fabrication process. Losses occur in mold and crucible interactions, crucible coating infiltration, fuel particle adherence to the mold material and, in the case of americium-bearing alloys, volatilization. These losses and waste streams lower productivity and economic efficiency of fuel production. Waste streams must therefore be minimized and fuel losses quantified and reduced.

The scope of this project consists of three major tasks: 1) casting development and mold loss comparison, 2) coating development and characterization, and 3) continuous casting development. In the first task, the project team will cast numerous fuel pins, evaluating fuel losses in the melting chamber, the crucible, and the mold. Researchers will then identify and implement efforts to reduce those losses. A related task is the development of improved crucible coatings, as porous coatings are a source of fuel loss (as well as potential fuel contamination in the event of a coating reaction). The third task involves the continuous casting of uranium–zirconium alloys. Continuous casting saves time, energy, and labor and reduces waste streams. However, there has been no large-scale uranium production using this process, so this task will provide valuable data on the process's feasibility.

The project team seeks to minimize losses and waste streams in the fuel fabrication process, further enhancing the technology readiness level of metallic fuel.

Project Number: 2010-003-K

PI (U.S.): Randall Fielding, Idaho National Laboratory

PI (ROK): Ki-Hwan Kim, Korea Atomic Energy Research Institute

Collaborators: None

Program Area: FCR&D

Project Start Date: December 2010

Project End Date: October 2013

Development and Characterization of Nanoparticle-Strengthened Dual-Phase Alloys for High-Temperature Nuclear Reactor Applications

Project Abstract

Metallic materials in future fast reactors will have to maintain their integrity in harsh environments: radiation doses up to 400 dpa and temperatures up to 700°C. This project aims to develop a new high-performance reactor core material by combining the best materials development ideas. In the past decade, nanostructured ferritic alloys (NFAs) have been developed to improve high-temperature strength and radiation resistance. These NFAs have been base alloys for various fundamental studies. Also, ferrite–martensite dual-phase steels have been developed to increase ductility and fracture toughness and are used to produce high-toughness components for automobiles. In this project, researchers will attempt to combine the former strengthening mechanism with the latter composite mechanism to produce high-strength, high-toughness NFAs.

In processing, nanoclusters (or nano-oxide particles) will be introduced to selected Fe-Cr steels by mechanical alloying, and then the material produced will be thermally treated to yield two phases—nanocluster-strengthened ferrite and martensite—with different chemistries. The final product will be a nanostructured dual-phase alloy. The project team will characterize both the preliminary materials and one optimized material. The detailed characterization for the optimized material will focus on its high-temperature mechanical behaviors. In addition, the project team will study thermal stability of nanoparticles and constituent phases using both computational and experimental tools.

Project Number: 2010-004-K

PI (U.S.): Thak Sang Byun, Oak Ridge National Laboratory

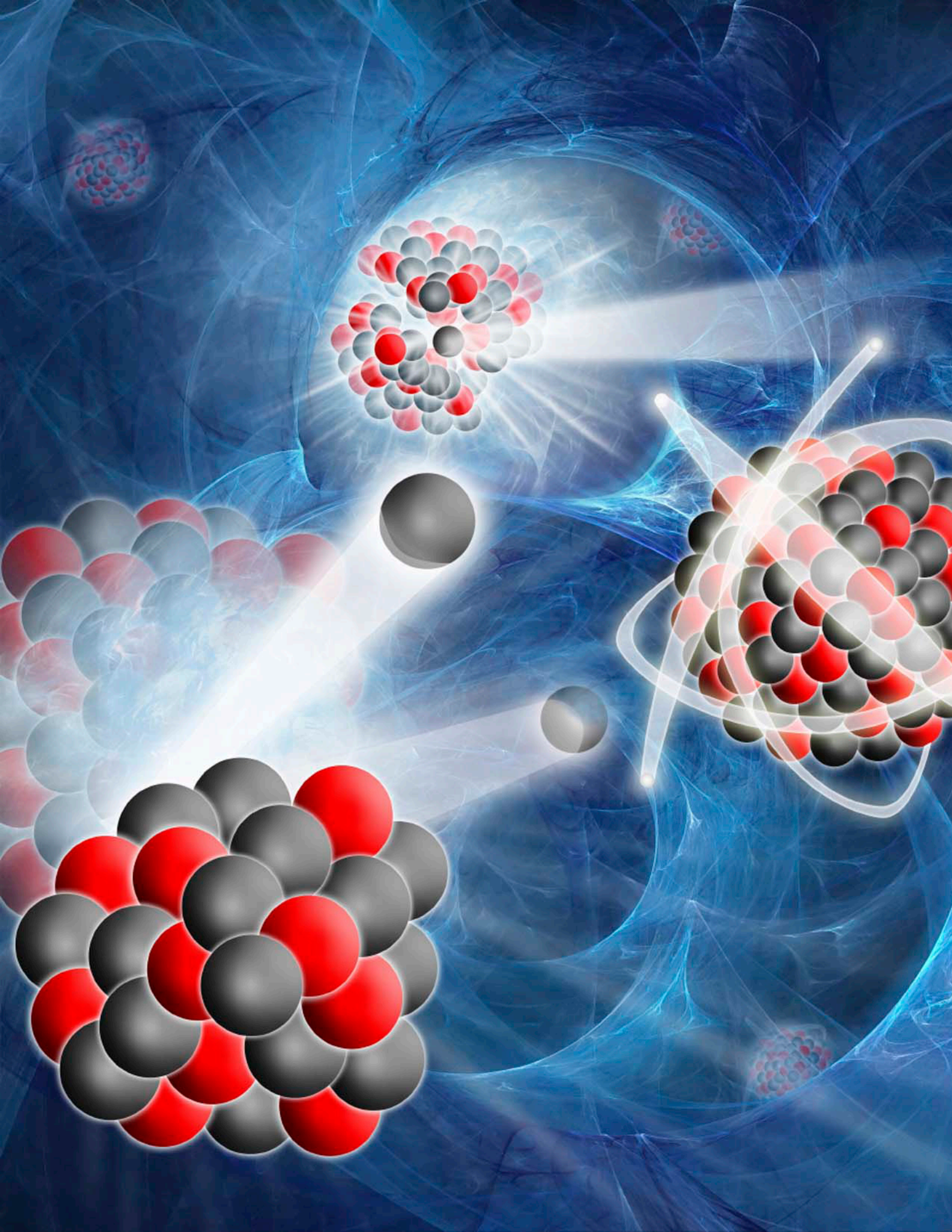
PI (ROK): Ji Hyun Yoon, Korea Atomic Energy Research Institute

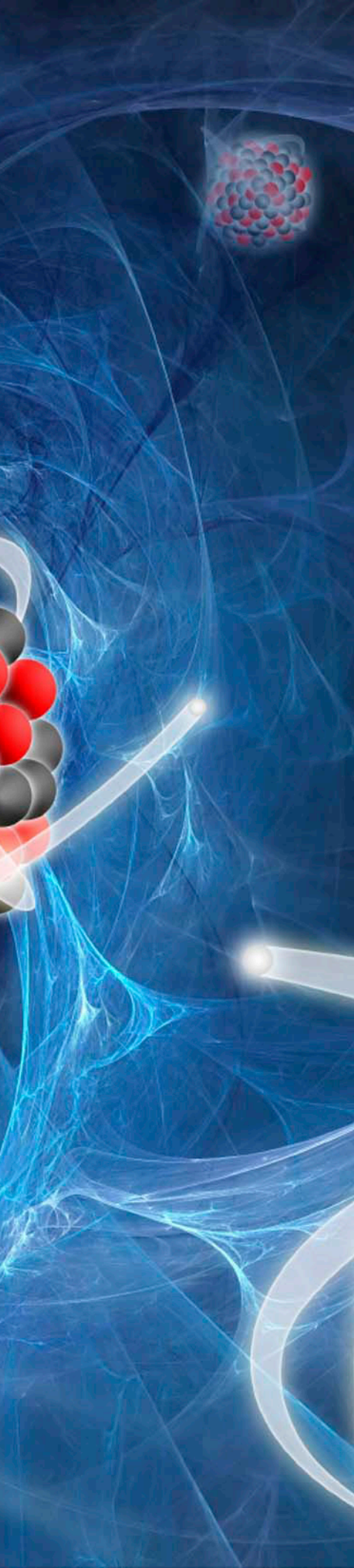
Collaborators: None

Program Area: FCR&D

Project Start Date: December 2010

Project End Date: September 2013





Appendix I: Index of I-NERI Projects

FY 2007 Projects

- 2007-001-F*** Advanced Dispersion-Strengthened Ferritic Alloys and Ferretic–Martensitic Steels with Fine Nanoscale Dispersions
- 2007-001-K*** Experimental Validation of Stratified Flow Phenomena, Graphite Oxidation, and Mitigation Strategies of Air Ingress Accidents
- 2007-002-K*** Development of an Advanced Voloxidation Process for Treatment of Spent Fuel
- 2007-003-K*** Performance Evaluation of TRU-Bearing Metal Fuel for Sodium Fast Reactors to Achieve High Burnup Goal
- 2007-004-K*** Development and Characterization of New High-Level Waste Forms for Achieving Waste Minimization from Pyroprocessing
- 2007-006-K*** Development of Computational Models for Pyrochemical Electrorefiners of Nuclear Waste Transmutation Systems
- 2007-007-K*** Sodium-Cooled Fast Reactor Structural Design for High Temperatures and Long Core Lifetimes/Refueling Intervals

FY 2008 Projects

- 2008-001-C*** Upgrading of the Athabasca Oil Sands for the Production of Diesel and Gasoline
- 2008-001-F*** SiC/SiC Composites for Generation IV Reactors
- 2008-001-K*** Advanced Multi-Physics Simulation Capability for Very High-Temperature Gas-Cooled Reactors
- 2008-002-K*** Experimental and Analytic Study on the Core Bypass Flow in a Very High-Temperature Reactor
- 2008-003-K*** Nuclear Data Uncertainty Analyses to Support Advanced Fuel Cycle Development

FY 2009 Projects

- 2009-001-K*** ZPPR-15 and BFS Critical Experiments Analysis for Generation of Physics Validation Database of Metallic-Fueled Fast Reactor Systems
- 2009-002-K*** Enhanced Radiation Resistance through Interface Modification of Nanostructured Steels for Generation IV In-Core Applications

FY 2010 Projects

- 2010-001-E** Measurements of Fission Fragment Mass Distributions and Prompt Neutron Emission as a Function of Incident Neutron Energy for Major and Minor Actinides
- 2010-002-E** Spherical Particle Technology Research for Advanced Nuclear Fuel/Target Applications
- 2010-003-E** Irradiation and Testing of Advanced Oxide Dispersion-Strengthened and Ferritic–Martensitic Steels
- 2010-004-E** Development of a Standard Neutron Detector for the Energy Range up to 20 MeV and its Application
- 2010-005-E** Interoperability of Material Databases
- 2010-006-E** State-of-the-Art Post-Irradiation Examination of Advanced Nuclear Fuels
- 2010-001-K** Investigation of Electrochemical Recovery of Zirconium from Spent Nuclear Fuels
- 2010-002-K** Science-Based Approach to Nickel Alloy Aging and its Effect on Cracking in Pressurized Water Reactors
- 2010-003-K** Low-Loss Advanced Metallic Fuel Casting Evaluation
- 2010-004-K** Development and Characterization of Nanoparticle-Strengthened Dual-Phase Alloys for High-Temperature Nuclear Reactor Applications



Appendix II: Acronyms and Initialisms

μm	Micrometer	Cm	Curium
1-D	One-Dimensional	CMFD	Computational Multi-phase Fluid Dynamics (code)
2-D	Two-Dimensional	CPU	Central Processing Unit
3-D	Three-Dimensional	Cr	Chromium
3H	Tritium	CrN	Chrome Nitride
9Cr	Nine Percent Chromium	Cs	Cesium
A	Ampere	CSL	Coincident Site Lattice
Å	Angström	CVI	Chemical Vapor Infiltration
ABTR	Advanced Burner Test Reactor	CWF	Ceramic Waste Form
AFC-1	Advanced Fuel Cycle test series-1	dm	Decimeter(s)
Am	Americium	DOE	Department of Energy
ANL	Argonne National Laboratory	dpa	Displacement Per Atom
Ar	Argon	EBR-II	Experimental Breeder Reactor-II
ASCE	American Society of Civil Engineers	EBS	Electron Backscatter Diffraction
ASME	American Society of Mechanical Engineers	ECAP	Equal Channel Angular Processing
ASTM	American Society for Testing and Materials	EFTEM	Energy-Filtered Transmission Electron Microscopy
B	Boron	ENDF	Evaluated Nuclear Data File
BFS	Big Physical Stand (facility)	ER	Electrorefiner
BNL	Brookhaven National Laboratory	EU	European Union
C	Carbon	Euratom	European Atomic Energy Community
°C	Celsius	eV	Electron Volts
Ca	Calcium	FAMD	Fluid-Added Mass and Damping
CAD	Computer-Aided Design	fcc	Face-Centered Cubic
CAIP	Cathodic Arc Ion Plating	FCR&D	Fuel Cycle Research and Development
C/C	Carbon Fiber-Reinforced Carbon Matrix	Fe	Iron
CFD	Computational Fluid Dynamics	FE-SEM	Field Emission Scanning Electron Microscope/Microscopy
CG	Coarse Grain	FFTF	Fast Flux Test Facility
CGR	Crack Growth Rate		
Cl	Chlorine		

FGR	Fission Gas Release	in	Inch(es)
F-M	Ferretic–Martensitic	I-NERI	International Nuclear Energy Research Initiative
F/M	Fiber–Matrix		
FY	Fiscal Year	INL	Idaho National Laboratory
g	Gram(s)	IPPE	Institute of Physics and Power Engineering
GBE	Grain Boundary Engineering	IRMM	Institute for Reference Materials and Measurements
GFR	Gas-Cooled Fast Reactor	ITC	Isothermal Temperature Coefficient
GHG	Greenhouse Gas	JEFF	Joint Evaluated Fission and Fusion
GPa	Gigapascal(s)	JENDL	Japanese Evaluated Nuclear Data Library
GT-MHR	Gas Turbine–Modular Helium Reactor	K	Potassium
H	Hydrogen	KAERI	Korea Atomic Energy Research Institute
HFEF	Hot Fuels Examination Facility	KAIST	Korea Advanced Institute of Science and Technology (formerly)
HLW	High-Level Waste		
HNLS	Hi-Nicalon™ Type-S	keff	k-effective (neutron multiplication factor)
HTE	High-Temperature Electrolysis	keV	Kiloelectron Volts
HTR	High-Temperature Reactor	kg	Kilogram(s)
HT-UPS	High-Temperature Ultrafine Precipitate-Strengthened	kPa	Kilopascal(s)
		kW	Kilowatt
Hz	Hertz	La	Lanthanum
I	Iodine	LANL	Los Alamos National Laboratory
ICP-MS	Inductively Coupled Plasma Mass Spectrometry	LAS	Low-Alloy Steel
ICSBEP	International Criticality Safety Benchmark Evaluation Project	LFR	Lead-Cooled Fast Reactor
		Li	Lithium
IHECSBE	International Handbook of Evaluated Criticality Safety Benchmark Experiments	LLNL	Lawrence Livermore National Laboratory
		LOCA	Loss-of-Coolant Accident
IHTS	Intermediate Heat Transport System	LWR	Light Water Reactor
IAEA	International Atomic Energy Agency	m	Meter(s)
IFNEC	International Framework for Nuclear Energy Cooperation	MA	Minor Actinide
IMF	Inert Matrix Fuel	MC	Monte Carlo

MeV	Mega-electron Volt	ORNL	Oak Ridge National Laboratory
MIR	Matched Index of Refraction	Pa	Pascal(s)
mm	Millimeter(s)	Pb	Lead
Mn	Manganese	pcm	Per Cent Mille
Mo	Molybdenum	PCT-A	Product Consistency Test – Method A
MOC	Method of Characteristics	PL	Proportional Limit
MOC	Models of Computation	PNNL	Pacific Northwest National Laboratory
MOX	Mixed Oxide	Pu	Plutonium
MPa√m	Megapascal Square Root Meter (measure of fracture toughness)	PVD	Physical Vapor Deposition
MSR	Molten Salt Reactor	PWR	Pressurized Water Reactor
MWth	MegaWatt thermal	PyC	Pyrolytic Carbon
N	Nitrogen	R&D	Research and Development
N	Number of Cycles	RAXR	Resonant Anomalous X-ray Reflectivity
Nd	Neodymium	RCH	Rotating Cylinder Hull
NE	Office of Nuclear Energy	RD&D	Research, Development and Demonstration
NFA	Nanostructured Ferritic Alloy	REE	Rare Earth Element
NIST	National Institute of Standards and Technology	RF	Radio Frequency
nm	Nanometer(s)	RMSD	Root Mean Square Deviation
Np	Neptunium	ROK	Republic of Korea
NRC	Nuclear Regulatory Commission	RPCM	Resonance Parameter Covariance Matrix
NUTRECK	Nuclear Transmutation Energy Research Center of Korea	s	Second(s)
O	Oxygen	S	Sulfur
OBE	Operating Basis Earthquake	SA3	Tyranno™-SA3
ODS	Oxide Dispersion-Strengthened	SAP	Silicon-Aluminum-Phosphate
OECD	Organisation for Economic Co-operation and Development	SCC	Stress Corrosion Cracking
ONC	Onset Natural Circulation	SCWR	Supercritical Water-Cooled Reactor
		SEM	Scanning Electron Microscope/Microscopy
		SFR	Sodium-Cooled Fast Reactor

SG	Steam Generator	TiN	Titanium Nitride
Si	Silicon	TMS	Tempered Martensitic Steels
SiC/SiC	Silicon Carbide Fiber-Reinforced Silicon Carbide Matrix	TMT	Thermomechanical Treatment
SIMS	Secondary Ion Mass Spectrometry	TRU	Transuranic
SINQ	Swiss Spallation Neutron Source	U	Uranium
SND	Standard Neutron Detector	UFG	Ultrafine Grain
SNF	Spent Nuclear Fuel	V	Vanadium
SNL	Sandia National Laboratory	V	Volt
SOEC	Solid Oxide Electrolysis Cell	VHTR	Very High-Temperature (Gas-Cooled) Reactor
SOFC	Solid Oxide Fuel Cell	W	Tungsten
Sr	Strontium	W	Watt
SSE	Safe Shutdown Earthquake	wt. %	Weight Percent
STIP	Swiss Spallation Neutron Source Target Irradiation Program	XR	X-ray Reflectivity
Syl	Sylramic™ (fiber)	XRD	X-ray Diffraction
Syl-iBN	Sylramic™-iBN (fiber)	Zi	Zirconium
Ta	Tantalum	ZIT	Zinc Oxide/Titanium Oxide
TEM	Transmission Electron Microscope/ Microscopy	ZPPR	Zero Power Plutonium Reactor
		Zr	Zirconium

